Functional insights into the role of a bacterial virulence factor and a host factor in *Neisseria gonorrhoeae* infection

Funktionelle Einblicke in die Rolle eines bakteriellen Virulenzfaktors und eines Wirtsfaktors bei der Infektion mit *Neisseria gonorrhoeae*

Doctoral thesis for a doctoral degree
at the Graduate School of Life Sciences,
Julius-Maximilians-Universität Würzburg,
Section infection and immunity
submitted by

Tao Yang

from

Hunan China

Würzburg 2020

Submitted on: ……..……..

Office stamp

Members of the Thesis Committee

Chairperson: Prof. Dr. Thomas Dandekar

Primary Supervisor: Prof. Dr. Thomas Rudel

Supervisor (Second): PD Dr. Vera Kozjak-Pavlovic

Supervisor (Third): Prof. Dr. Alexandra Schubert-Unkmeir

Supervisor (Fourth): Dr. Brandon Kim

Date of Public Defence: ……..……

Date of Receipt of Certificates: ……

Table of contents

Table of contents

Table of contents

Table of contents

Abstract

Neisseria gonorrhoeae (GC) is a human specific pathogenic bacterium. Currently, *N. gonorrhoeae* developed resistance to virtually all the available antibiotics used for treatment. *N. gonorrhoeae* starts infection by colonizing the cell surface, followed by invasion of the host cell, intracellular persistence, transcytosis and exit into the subepithelial space. Subepithelial bacteria can reach the bloodstream and disseminate to other tissues causing systemic infections, which leads to serious conditions such as arthritis and pneumonia. A number of studies have well established the host-pathogen interactions during the initial adherence and invasion steps. However, the mechanism of intracellular survival and traversal is poorly understood so far. Hence, identification of novel bacterial virulence factors and host factors involved in the host-pathogen interaction is a crucial step in understanding disease development and uncovering novel therapeutic approaches. Besides, most of the previous studies about *N. gonorrhoeae* were performed in the conventional cell culture. Although they have provided insights into host-pathogen interactions, much information about the native infection microenvironment, such as cell polarization and barrier function, is still missing.

This work focused on determining the function of novel bacterial virulence factor NGFG_01605 and host factor (FLCN) in gonococcal infection. NGFG_01605 was identified by Tn5 transposon library screening. It is a putative U32 protease. Unlike other proteins in this family, it is not secreted and has no *ex vivo* protease activity. NGFG_01605 knockout decreases gonococcal survival in the epithelial cell. 3D models based on T84 cell was developed for the bacterial transmigration assay. NGFG_01605 knockout does not affect gonococcal transmigration.

The novel host factor FLCN was identified by shRNA library screening in search for factors that affected gonococcal adherence and/or internalization. We discovered that FLCN did not affect *N. gonorrhoeae* adherence and invasion but was essential for bacterial survival. Since programmed cell death is a host defence mechanism against intracellular pathogens, we further explored apoptosis and autophagy upon gonococcal infection and determined that FLCN did not affect apoptosis but inhibited autophagy. Moreover, we found that FLCN inhibited the expression of E-cadherin. Knockdown of E-cadherin decreased the autophagy flux and supported *N. gonorrhoeae* survival. Both non-polarized and polarized cells are present in the cervix, and additionally, E-cadherin represents different polarization properties on these different cells. Therefore, we established 3-D models to better understand the functions of FLCN. We discovered that FLCN was critical for *N. gonorrhoeae* survival in the 3-D environment as well, but not through inhibiting autophagy. Furthermore, FLCN inhibits the E-cadherin expression

and disturbs its polarization in the 3-D models. Since *N. gonorrhoeae* can cross the epithelial cell barriers through both cell-cell junctions and transcellular migration, we further explored the roles FLCN and E-cadherin played in transmigration. FLCN delayed *N. gonorrhoeae* transmigration, whereas the knockdown of E-cadherin increased *N. gonorrhoeae* transmigration.

In summary, we revealed roles of the NGFG_01605 and FLCN-E-cadherin axis play in *N. gonorrhoeae* infection, particularly in relation to intracellular survival and transmigration. This is also the first study that connects FLCN and human-specific pathogen infection.

Zusammenfassung

Neisseria gonorrhoeae (GC) ist ein humanpathogenes Bakterium. Gegen jedes kommerziell erhältliche Antibiotikum konnten bereits Resistenzen entdeckt werden. Die Infektion von Neisserien startet mit der Kolonisierung der Zelloberfläche, gefolgt von der Invasion in die Zelle, intrazellulärer Persistenz, Transzytose und Verlassen des subepithelen Raums. Subepithele Bakterien können den Blutfluss erreichen und sich somit auf andere Gewebe verbreiten und dadurch schwerwiegende Erkrankungen wie Arthritis und Lungenentzündungen verursachen. Zahlreiche Studien haben die Interaktion zwischen Wirtszelle und Pathogen zwischen Adhärenz und Invasion gut charakterisiert. Allerdings ist der Mechanismus des intrazellulären Überlebens und der Transmigration weitestgehend unbekannt. Um neue therapeutische Ansätze zu definieren ist es deshalb wichtig weitere bakterielle und zelluläre Faktoren verantwortlich für Interaktionen zwischen Wirt und Pathogen zu identifizieren. Außerdem wurden Studien über *N. gonorrhoeae* bisher in konventioneller Zellkultur durchgeführt. Auch wenn diese weitere Einsichten in Wirt-Pathogen Interaktionen geben, ist viel Information in der nativen Infektionsumgebung, wie Zellpolarisierung oder Barrierefunktionen, bisher nicht bekannt.

Diese Arbeit fokussiert sich auf die Bestimmung eines neuen bakteriellen Virulenzfaktors, NGFG_01605, und Wirtsfaktoren (FLCN) in der Infektion von Gonokokken. NGFG_01605 wurde über Screening einer Transposonsammlung identifiziert und ist eine vermeintliche U32 Protease. Im Gegensatz zu anderen Proteinen dieser Familie, wird diese Protease nicht sekretiert und hat keine *ex vivo* Proteaseaktivität. Der Knockout von NGFG_01605 vermindert die Überlebensrate von Gonokokken in Epithelzellen. 3D-Modelle basierend auf T84-Zellen wurden für die Analyse der bakteriellen Transmigration entwickelt. Der Knockout von NGFG_01605 hat keinen Einfluss auf die Transmigration.

Bei der Suche neuer Wirtsfaktoren, die für die Adhärenz und/oder Internalisierung wichtig sind, wurde FLCN durch ein Screening einer shRNA Sammlung entdeckt. Wir konnten zeigen, dass dieser Faktor zwar nicht für die Adhärenz oder Invasion von *N. gonorrhoeae*, aber für das Überleben der Bakterien in der Wirtszelle essenziell ist. Da der programmierte Zelltod ein typischer Abwehrmechanismus gegen intrazelluläre Bakterien ist, haben wir Apoptose und Autophagie weiter untersucht und konnten zeigen, dass FLCN zwar keinen Effekt auf Apoptose hat, aber Autophagie inhibiert. Außerdem konnten wir zeigen, dass FLCN die Expression von E-cadherin inhibiert. Auch der Knockdown von E-cadherin verringerte Autophagie und erhöhte das Überleben von *N. gonorrhoeae*. Im Gebärmutterhals sind sowohl polarisierte als auch

nicht-polarisierte Zellen präsent. E-cadherin hat zudem unterschiedliche Einflüsse auf diese unterschiedlichen Zellen. Aus diesem Grund haben wir ein 3D-Modell entwickelt, um die Funktionen von FLCN besser zu verstehen. Wir entdeckten, dass FLCN zwar auch im 3D Modell wichtig für das Überleben ist, aber nicht durch Inhibition von Autophagie. Außerdem inhibiert FLCN die Expression und Verteilung von E-cadherin in 3D-Modellen. Da *N. gonorrhoeae* die Epithelzellbarierre durch sowohl Zell-Zell-Kontakte als auch transzelluläre Migration überwinden kann, untersuchten wir daraufhin die Rollen von FLCN und E-cadherin in der transzellulären Migration. Diese wird durch FLCN verspätet und durch Knockdown von E-cadherin erhöht.

Zusammengefasst, haben wir die Rolle von NGFG_01605 und den Zusammenhang von FLCN und E-cadherin während der Infektion von *N. gonorrhoeae* untersucht. Unser Fokus war hierbei das intrazelluläre Überleben sowie zelluläre Transmigration. Diese Arbeit ist die Erste, die FLCN und humanpathogenspezifische Infektion miteinander in Verbindung bringt.

1. Introduction

1.1 *Neisseria gonorrhoeae*

1.1.1 The genus of *Neisseria*

1.1.1.1 Taxonomy of *Neisseria*

Members of the genus *Neisseria* are Gram-negative β-proteobacteria, commonly found as commensals on animal and human mucosal surfaces. *Neisseria* spp are facultatively intracellular and are capable of living and reproducing either inside or outside cells**.** Conventional *Neisseria* phenotypic taxonomy only reliably identifies three species, *N. meningitidis*, *N. gonorrhoeae*, and *N. lactamica.* Therefore, the application of phylogenetic analyses of nucleotide sequence data to clarify species is necessary (Diallo *et al*., 2019). Analysis with single loci, such as 16S rRNA genes, poorly differentiated *Neisseria* species, due to distortions resulting from low resolution and horizontal gene transfer (HGT) (Maiden *et al.*, 1998). Phylogenies based on multi-locus sequence analysis (MLSA), such as the seven loci used in Multi Locus Sequence Typing (MLST)(Maiden *et al.*, 1998), the 53 ribosomal genes of ribosomal MLST (rMLST)(Jolley *et al.*, 2012), and the 246 loci of the *Neisseria* genus core genome MLST (cgMLST)(Bennett *et al.*, 2012), have significantly improved *Neisseria* species classification. Currently, there are 11 species in the *Neisseria* genus, of which two are pathogens. These are *N. gonorrhoeae* and *N. meningitidis.*

1.1.1.2 Genotype and Phenotype of *Neisseria*

Neisseria typically contains a 2.2 Mbp circular chromosome. Both *N. meningitidis* and *N. gonorrhoeae* are polyploid, containing two to five genome equivalents per growing gonococcal cell, with an estimated two chromosomal copies per gonococcal cell unit (Tobiason and Seifert, 2006). However, these organisms are still genetically haploid and cannot carry two different alleles in the same genomic locus (Tobiason and Seifert, 2010). Besides, the *Neisseria* contains a repertoire of genetic elements that enable increased genomic plasticity. The pathogenic *Neisseria* has conserved genetic systems that contribute to host colonization and survival, such as deoxyribonucleic acid (DNA) transformation by the highly repeated element DNA uptake sequences (DUS) and variation of displayed antigens (Rotman and Seifert, 2014). The morphology

varies among the different *Neisseria* species. *N. weaveri* and *N. bacilliformis* are rod-shaped; *N. animaloris* and *N. zoodegmatis* are coccobacilli; *N. canis*, *N. mucosa*, *N. subflava* and *N. cinerea* are diplococci, similar to *N. gonorrhoeae* (Liu *et al*., 2015).

1.1.1.3 Pathogenesis of *Neisseria*

N. gonorrhoeae and *N. meningitidis* are exclusively human pathogens. *N. gonorrhoeae* causes gonorrhea and *N. meningitidis* causes bacterial meningitis and septicemia. The others are commensal, localized at human nasal and oropharyngeal or residing at wide ranges of host and body sites (Liu *et al*., 2015). Also free-living *Neisseria* were found in the environment e.g. *N. sicca* (Liu *et al.*, 2015), *N. mucosa* (Sakai *et al.*, 1996). However, *N. mucosa* (Tronel *et al.*, 2001) and *N. oralis* (Tronel *et al.*, 2015) have the potential to cause disease. Many of the virulence traits of the pathogenic *Neisseria* are also present in the commensal species, such as iron scavenging and immunoreactive surface proteins (Marri *et al*., 2010, Saunders *et al*., 2006), presumably because they are essential for colonization, growth, and survival of the organisms within the human host. Interestingly, some known virulence factors are not absolutely required for virulence. For example, although the capsule is considered a major virulence factor of meningococci, the unencapsulated *N. meningitidis* strain α14 can still cause invasive disease (Schork *et al*., 2012). The determination of which genes (or combinations of genes) are responsible for virulence is an active field of investigation.

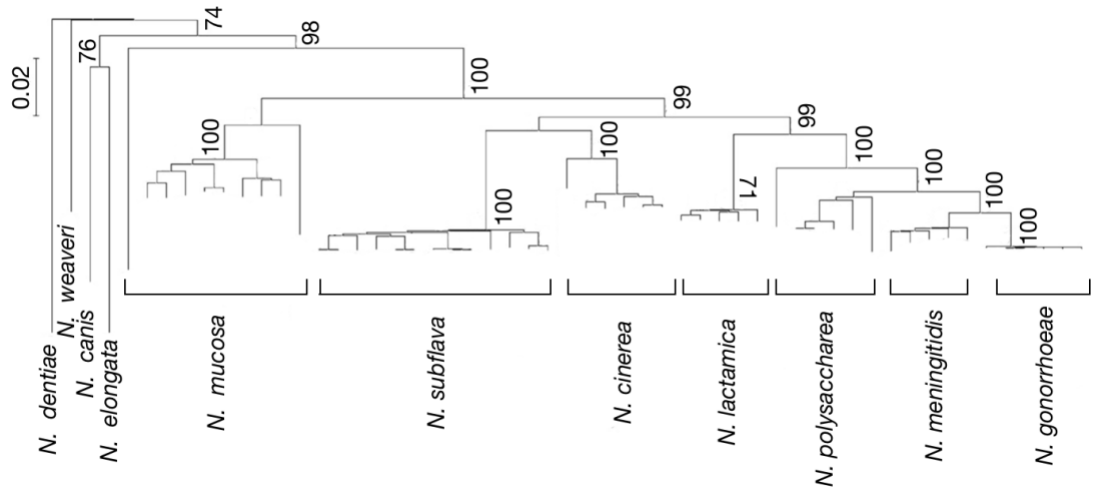

Figure 1: Taxonomy of *Neisseria*
Evolutionary relationships among *Neisseria* based on concatenated sequences from 246 genes, adapted from Bennett *et al* (2012). The evolutionary history was inferred using

the neighbor joining method. The percentages of replicate trees in which the associated taxa clustered together in the bootstrap test (500 replicates) are shown next to the branches. There are 11 species in *Neisseria*.

1.1.2 *Neisseria gonorrhoeae*

1.1.2.1 A brief history of *N. gonorrhoeae*

N. gonorrhoeae was first discovered 1878 by Albert Neisser and named after him. Albert Neisser isolated and visualized gonorrhoeae strains in samples from 35 men and women with the classic symptoms of genitourinary infection with gonorrhea (Hill *et al.*, 2016). Leistikow and Loeffler were able to grow *N. gonorrhoeae in vitro* in 1882 (Quillin and Seifert, 2018). In the next year, Max Bockhart proved that it is the cause of disease gonorrhea by inoculating the penis of a healthy man with the bacteria (Shah, 2016). Most media designed for the growth of *N. gonorrhoeae* have extremely complex compositions. Until 1977, a complete medium for the growth of *N. gonorrhoeae* was developed, using the same basic ingredients contained in commercial media but with fewer supplements (Jones and Talley, 1977).

1.1.2.2 Physiology of *N. gonorrhoeae*

The *Neisseria* species are exquisitely adapted to live within their respective tissue niches. This has affected their biochemical capacity, for example a restricted number of carbon sources in the tissue environment. One biochemical feature that distinguishes between different species of *Neisseria* is the ability to produce a starch-like polysaccharide in the presence of sucrose. In this way, polysaccharide-positive species, such as *N. polysaccharea*, can be differentiated from polysaccharide-negative species, such as *N. gonorrhoeae*. In addition, *N. gonorrhoeae* is positive for oxidase, catalase, superoxol and hydroxyproly-laminopeptidase activity and produces acid from the oxidative metabolism of glucose (McSheffrey *et al.,* 2015).

1.1.2.3 Genotype and phenotype of *N. gonorrhoeae*

The *N. gonorrhoeae* genome contains repeat elements and insertion sequences that contribute to genomic rearrangements and differences between species. There are approximately 2,000 10-mer DUSs found in chromosomes, contributing to approximately one every kilobase of DNA. The DUSs mediate species-specific DNA transformation (Marri *et al.*, 2010). Duplicated repeat

sequence 3 (dRS3) is the second most abundant repeat, appearing 200 times in *N. gonorrhoeae* (Marri *et al.*, 2010). dRS3 acts as a site for phage integration (Kawai *et al*., 2005). Additionally, phase variation, or the random switching between the ON and OFF state of genes, occurs by slipped-strand synthesis at polynucleotide tracts and short tandem repeats. More than 100 genes are phase regulated and many virulence factors are phase variable. The three major surface antigens, lipopolysaccharide (LOS), pilus and opacity-associated proteins (Opa), can undergo antigenic variation through a multigene phase variation process (Rotman and Seifert, 2014).
The overall shape of *N. gonorrhoeae* is spherical pairs together with adjacent sides flattened morphology. Four morphologically distinct clonal types were observed in *N. gonorrhoeae* cultures. Type 1 is small in size, dark gold, with an entire edge. Type 2 is similar to type 1 except for a crenated edge. Type 3 is bigger in size and light brown. Type 4 is bigger in size and colorless. Type1 colonies are pili positive**,** while the type4 colonies are pili negative (Jones and Talley, 1977). Of note, type 1 morphology was mostly found in the primary clinical isolates. Around 10% of the clinical isolates are of type 2 and type 3 morphology. After several generations of clinical isolates in culture, they present another phenotype, type 4.

1.1.2.4 Life cycle of *N. gonorrhoeae*

A combination of *in vitro* cell culture, human tissue culture and chimpanzee studies provides insight into how *N. gonorrhoeae* infects mucosal tissues. The bacteria adhere to the mucosal surface first and are then engulfed into a membrane-enclosed phagosome to translocate across the epithelial barrier and be released into the subepithelial space. Afterwards, *N. gonorrhoeae* has to survive within the tissue by acquiring essential nutrients from the host and evading the innate and adaptive immune responses (McSheffrey *et al*., 2015). In rare cases, gonococcus can enter the bloodstream and cause disseminated gonococcal infection (McCormack *et al.*, 1977).

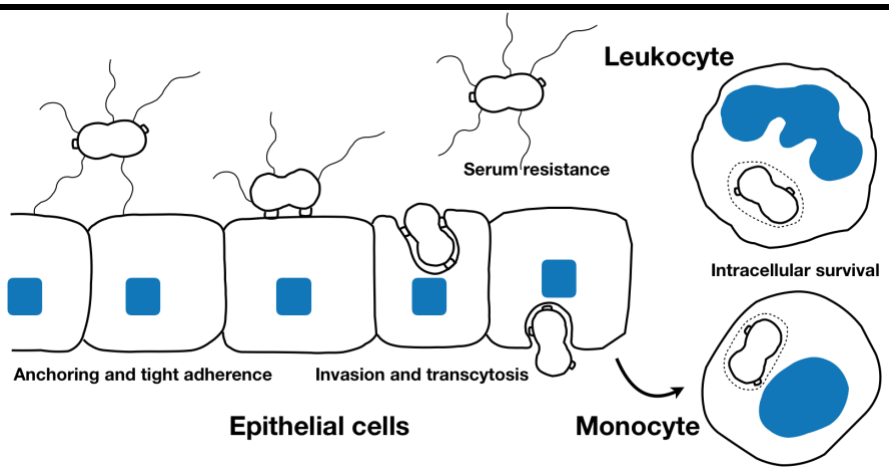

Figure 2: Life cycle of *N. gonorrhoeae*
Pili is a prerequisite for the *Neisseria* attachment to the epithelial cell surface. The surface-attached bacteria penetrate the epithelial cells while contained in a vacuole and may transcytose towards sub-epithelial tissues. The pathogenic *Neisseria* strongly interact with phagocytic cells, such as neutrophils and macrophages, which seem to provide them with an intracellular habitat. Adapted from reference Meyer (1977).

1.1.2.5 Pathogenesis of *N. gonorrhoeae*

Gonorrhea is the second most reported sexually transmitted disease (STD) in the world. An estimated 78 million cases of gonorrhea occur globally each year (Newman *et al*., 2015). The main means of gonorrhea transmission are sexual transmission through vaginal, anal, oral sex and perinatal transmission. *N. gonorrhoeae* infects lower genital tract and cervix in women, anterior urethra in men, mucosal surface of pharynx and rectum. The symptoms after infection vary from man to woman. The symptoms of men could be developed within one day to one year post infection, including pain or burning with urination, discharge from the penis, or testicular pain. Around 20% of the infected men could be without symptom (Harrison *et al*., 1979). Infection symptoms of women comprise burning with urination, vaginal discharge, vaginal bleeding between periods, or pelvic pain. Untreated pelvic inflammatory disease could result in infertility. 50% of the infected women are asymptomatic (McCormack *et al.*, 1977). The reason for asymptomatic infection is unknown. The asymptomatic carriers of *N. gonorrhoeae* are reservoirs of its transmission in the population. Rarely, *N. gonorrhoeae* disseminates to bloodstream leading to septic arthritis and skin lesions (Li and Hatcher, 2020). Because of the serious social and medicolegal consequences of misdiagnosing gonorrhea or misidentifying strains of *N. gonorrhoeae*, the Centers for Disease Control and Prevention (CDC) has recommended criteria for reporting diagnoses of gonorrhea, including suggestive diagnosis, presumptive diagnosis and definitive diagnosis (Miller, 2006).

1.1.2.6 Challenges and current progress of new therapeutic strategies

The emergence of multidrug-resistant isolates of *N*. *gonorrhoeae* drives the need for the urgent development of safe and effective vaccines and novel therapies. Antibodies provide a safe and effective means to target bacteria selectively for complement-mediated killing and/or elimination through opsonophagocytosis. Even though the phase variation of *N. gonorrhoeae* antigens, the lack of knowledge of the immune response it induced, and the absence of robust animal models mimic disease progression, progress have been made in the antibody-mediated therapy development. *N. meningitidis* serogroup B vaccine MeNZB, which is the outer membrane vesicle (OMV) of serogroup B, has been found to work against gonococcal infection (Edwards *et al*. 2018), but with the low efficiency. What is more exciting is that monoclonal antibody (mAb) 2C7, which recognizes a LOS epitope expressed by >95% of clinical isolates, drives the activity of complement to kill the bacteria (Gulati *et al*., 2019). Some commensals of the same genus work against *Neisseria* pathogens e.g. *N. lactamica* protects host against *N. meningitidis* infection (Evans *et al*., 2011) by natural immunity (Gold *et al*., 1978). They represent therefore potential new candidates for vaccine development (Gorringe *et al*., 2009; Vaughan *et al*., 2006). A better understanding of the host-pathogen interactions and an optimized *ex vivo* infection model will facilitate the development of new therapies.

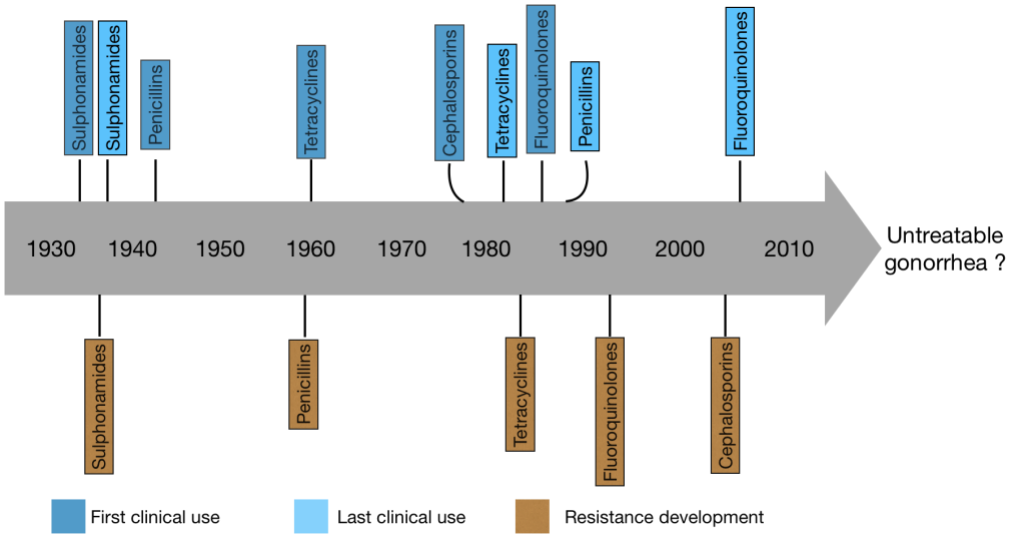

Figure 3: *N. gonorrhoeae* antibiotic resistance development
Since the first treatment of *N. gonorrhoeae* with antibiotics in the 1930s, *N. gonorrhoeae* have acquired genetic resistance determinants that prevent killing by all major classes of antibiotics that are used as first line treatment. As shown here, each new class of antibiotics that served as first line treatment for *N. gonorrhoeae* have been stopped as

all strains gained resistance. Recently, resistance was observed for the last available first line treatment for *N. gonorrhoeae* infection, the cephalosporins. The ability of *N. gonorrhoeae* to evolve resistance makes it a superbug and if new therapies are not developed soon, we may face an era of untreatable gonorrhea. Adapted from Quillin and Seifert (2018).

1.2 *N. gonorrhoeae* and host cell interactions

1.2.1 The adherence and invasion of *N. gonorrhoeae* into epithelial cells

Epithelial cells are the first responders and orchestrators of the early innate immune response during mucosal infection (Quayle, 2002). The epithelium maintains its selective barrier function through the formation of complex protein-protein networks that mechanically link adjacent cells and seal the intercellular space. The gonococci have evolved sophisticated and redundant mechanisms to adhere and invade into epithelial cells. The initial step in gonococcal infection is tethering of the bacterium to the apical side of the host epithelium. The attached gonococci induce focal polymerization of actin rearrangement (Giardina *et al*., 1998) and are then internalized by an actin- and clathrin-dependent process (Harvey *et al*., 1997). The internalized gonococci typically remain surrounded by a membrane-bound vacuole akin to a phagosome (Harvey *et al*., 1997). In rare cases, free *N. gonorrhoeae* was found in the cytoplasm in urethral epithelial cells (Apicella *et al*., 1996). Bacteria-containing vacuoles undergo a maturation process whereby they acquire bactericidal properties that effectively kill pathogens (Vieira *et al*., 2002). There are a batch of bacterial surface ligands and their respective cell receptors involved in the adherence and invasion process.

1.2.1.1 Type IV pili and their potential receptors CD46, CR3

Type IV pili are long, exquisitely thin and dynamic appendage on the bacterial surface. It is rapidly polymerizing and depolymerizing from a pool of pilin subunits. The extension, binding and retraction of type IV pili performs a diverse array of functions, including twitching motility, DNA uptake and microcolony formation (Craig *et al*., 2019). *N. gonorrhoeae* has one expression locus of pili and many promoterless partial-coding silent copies (pilS), which are reservoirs for pilin variation (Rotman *et al.*, 2016). The phase variation is dependent on recA-mediated homologous recombination (Stohl and Seifert, 2001). The initial attachment to the epithelial cells is mediated by pili and the host receptors CR3 (a CD11b/CD18 integrin heterodimer) or CD46 (Membrane cofactor protein). Questions remain as to whether the interaction of pili with CD46 functions to

mediate adherence or rather a downstream intracellular signaling event (Edwards *et al*., 2002; Kallstrom *et al*., 2001). Whereas pili constitute adhesive structures leading to adherence, it induces an immediate recruitment of caveolin-1 (Cav1) in the host cell to the infection site, which subsequently prevents bacterial internalization by triggering cytoskeletal rearrangements via downstream phospho-tyrosine signaling (Boettcher *et al*., 2010). Therefore, the adhered gonococci have to switch off the pili to invade (Faulstich *et al*., 2013). The clonal morphology of piliated *N. gonorrhoeae* refers to type 1 and 2 clonal morphology.

1.2.1.2 Opa proteins and their receptors CEACAM and HSPG

After the efficient attachment to the human target cells, the Opa proteins mediate an intimate binding and furthermore trigger the efficient invasion of the gonococci into the epithelial cells. *N. gonorrhoeae* has 11 Opa proteins. Opa genes are constitutively transcribed, but Opa protein expression undergoes phase variation at the translational level due to the presence of the pentameric coding repeat (CR) sequence 5'-CTCTT-3'. Modulation of the number of repeats occurs by slipped-strand mispairing during DNA replication, resulting in regular frameshifting (Stern *et al.*, 1986).
Receptor tropism of Opa proteins can be broadly divided into two categories. A relatively small number of Opa variants (e.g. Opa50) bind to heparan sulfate proteoglycan (HSPGs) and extracellular matrix (ECM) proteins, such as vitronectin and fibronectin (Chen *et al*., 1995; van Putten and Paul, 1995; Virji *et al*., 1999). Opa-HSPG facilitates bacterial binding to epithelial and endothelial cells via HSPGs and the ECM proteins. Binding of gonococci to HSPG receptors activates the lipid-hydrolyzing enzymes phosphatidylcholine-specific phospholipase C (PC-PLC) and the acid sphingomyelinase (ASM), generating ceramide (Grassmé *et al*., 1997). Efficient bacterial entry requires the additional interaction with the serum-derived extracellular matrix proteins fibronectin and vitronectin (Dehio *et al*., 1998). Vitronectin mediates binding to integrins and activation of protein kinase C (Freissler *et al*., 2000). Most Opa variants (e.g. Opa57) bind to the carcinoembryonic antigen family (CEACAM) (Duensing and van Putten, 1997; Gómez-Duarte *et al*., 1997). Opa-CEACAM is responsible for bacterial adherence and entry into host cells and interactions with the immune system (Sadarangani *et al*., 2011).

1.2.1.3 Major outer membrane protein PorB and receptor SREC-I

After invasion and transmigration, *N. gonorrhoeae* reaches the bloodstream. The serum of human adults contains phosphate in the range of 0.84 to 1.45 mM, making it a low-phosphate environment (Kuhlewein et al., 2006). The major outer membrane porin (PorB) functions for invasion in the low phosphate conditions. The PorB is a β-barrel protein that can form hydrophilic pores for the transport of small nutrient molecules, anions and waste products through the outer membrane of bacteria (Massari *et al*., 2003). PorB is stably expressed and has no phase variation. *N. gonorrhoeae* strains contain a single *porB* gene in one of two allelic forms PorB$_{IA}$ and PorB$_{IB}$. Function and structure analysis of the protein PorB$_{IA}$ disclosed that the amino acid at the position 92 differs between the two serotypes A and B. The amino acid in the PorB$_{IA}$ expressing strains is conserved either as arginine or histidine (Arg92/His92) and PorB$_{IB}$ expressing strains have a serine (Ser92). Further experiments indicated an important role of PorB$_{IA}$ in disseminating gonococcal infections in the low phosphate conditions (Rechner *et al*., 2007; Zeth *et al*., 2013). Host glycoprotein Gp96 and scavenger receptor (SREC) interact with PorB$_{IA}$ of disseminating *N. gonorrhoeae* in the low phosphate epithelial invasion pathway (Rechner *et al*., 2007). Moreover, PorB$_{IA}$-expressing bacteria are is more resistant to killing by normal human serum than gonococci with the PorB$_{IB}$ (van Putten *et al*., 1998).

1.2.1.4 LOS and its receptor ASGP-R

Aside from those two protein adhesins of *N. gonorrhoeae*, the glycolipids LOS is important for adherence and invasion. LOS is the most abundant gonococcal outer membrane molecule and plays a key role in many facets of pathogenesis. It mimics host glycans to avoid host recognition and defense (Ram *et al*., 2018). Besides, the gonococci variably express some of the genes encoding the glycosyltransferases needed for LOS biosynthesis, and this results in rapid and reversible alterations in the oligosaccharide structure. Its variable expression facilitates bacteria to escape host defense (Danaher *et al.*, 1995). LOS binds to asialoglycoprotein receptors (ASGP-R) for intimate attachment to the host cell and initiates invasion (Harvey *et al*., 2008).

1.2.2 The epithelial cell responses upon gonococcal infection

Programmed cell death is known to defend against bacterial infection by epithelial cells. Of note, epithelial cells shape the tissue immune microenvironment by producing cytokines and chemokines (Fichorova *et al*., 2001), releasing cellular factors such as damage-associated molecular patterns

(DAMPs) (Murakami *et al*., 2014) that can further activate immune cells and via production of antimicrobial peptides that control infecting microorganisms (Bals, 2000).

1.2.2.1 Autophagy

Autophagy is an intracellular degradation system that delivers cytoplasmic constituents to the lysosome and consists of several sequential steps—sequestration, transport to lysosomes, degradation, and utilization of degradation products (Mizushima, 2007). During autophagosome formation process, a cytosolic form of microtubule-associated protein 1A/1B-light chain 3 (LC3-I) is conjugated to phosphatidylethanolamine to form LC3-phosphatidylethanolamine conjugate (LC3-II), which is recruited to autophagosomal membranes. Autophagosomes fuse with lysosomes to form autolysosomes, and intra-autophagosomal components, including LC3-II in autolysosomal lumen are degraded by lysosomal hydrolases. Hence, lysosomal turnover of the autophagosomal marker LC3-II reflects autophagic activity, and detecting LC3 by immunoblotting or immunofluorescence has become a reliable method for monitoring autophagy (Tanida *et al*., 2008).
Autophagy is actively involved in the clearance of pathogens. In *Salmonella typhimurium*, autophagy receptor nuclear dot protein 52 kDa (NDP52) binds both Galectin-8 and LC3-II, and targets *Salmonella*-containing vacuole (SCV) for autophagic degradation to kill the pathogen (Thurston *et al*., 2012; Thurston *et al*., 2009). The autophagy of Group A *Streptococcus* (GAS) and measles virus infected cells is initiated by cytoplasmic tail of CD46-cyt1 interacting with scaffold protein Golgi-associated PDZ and coiled-coil motif-containing (GOPC), recruiting the class III PI 3-kinase VPS34/Beclin-1 complex (Sakai *et al.*, 1996). The piliated *N. gonorrhoeae* infection recruits CD46-cyt1 to the site of infection via type IV pilus (Meiffren *et al*., 2010). Sequentially the infection stimulates matrix metalloproteinases to cleave the CD46-cyt1 ectodomain causing its N-terminal shedding, and the presenilin/γ-Secretase complex to cleave its transmembrane domain causing its C-terminal release to cytosol (Weyand *et al.*, 2010). The GOPC is recruited to CD46-cyt1 to initiate autophagy and kill the early invaders (Kim *et al*., 2019). Consequently, the induction of autophagy during intracellular infection can lead to the capture, breakdown and eventual killing of intracellular pathogens, thereby aiding in their detection by the host cell and subsequent activation of the immune response.
However, some pathogens rely on induction of host autophagy to survive within host cells. In most cases, these bacteria actively induce autophagy but, at the

same time, block autophagosome maturation and fusion with the lysosome (Escoll *et al.,* 2016). An example is *Anaplasma phagocytophilum* that uses a secreted effector to promote autophagosome nucleation and stimulates its own growth by using the nutrients contained in the autophagosomes (Niu *et al.,* 2012). Thus pathogen-autophagy interplay is a complex relationship.

1.2.2.2 Apoptosis

The apoptosis pathway is evolutionarily conserved across metazoans. Apoptotic cell death culminates in the activation of cysteine–aspartic proteases (caspases), which degrade cellular components to prepare dying cells for clearance by phagocytes with minimal stress to surrounding cells and tissues (Los *et al*., 1995). Apoptosis is an active process and includes two distinct pathways: the intrinsic pathway (mitochondria mediated) and the extrinsic pathway (death receptor-mediated) (Singh *et al*., 2019). Apoptosis is able to eliminate pathogens at the early stage of infection without emitting alarm signals. For example, the obligate intracellular bacteria have to inhibit apoptosis to secure an intracellular niche for replication, otherwise they will die from apoptosis (Häcker *et al*., 2018). On the other side, apoptosis could also benefit pathogens. Increased apoptosis may assist the dissemination of intracellular pathogens or induce immunosuppression. Studies showed that infection of human intestinal epithelial cells with *Salmonella typhimurium* induced caspase-3–dependent and –independent cell death (Schauser *et al.* 2005). The role of apoptosis in *N. gonorrhoeae* infection is cell-type, strain phenotype and infection condition dependent. The study of Kepp et al. (2009) showed that Bim and Bmf synergize to induce intrinsic apoptosis upon PorB$_{IA}$ *N. gonorrhoeae* infection. However, Howie *et al* (2005) showed that type IV pilus retraction increases the ability of the cell to withstand apoptotic signals triggered by infection, therefore no apoptosis was observed upon infection. Thus pathogen-apoptosis interplay is a complex relationship as well.

1.2.2.3 Necrosis

Necrosis is characterized by membrane rupture, nuclear swelling, and the release of cellular content and is accompanied by caspase-independent inflammation. Necrosis is triggered by reactive oxygen species (ROS) production or danger signals, such as lysosomal destabilization, calpain release, and depletion of adenosine triphosphate (ATP), that are induced upon bacterial infection or physical damage (Ashida *et al*., 2011). Receptor-interacting protein 3

(RIP3) is a key mediator of programmed necrosis induced through death receptors or toll-like receptors (TLRs). During necrosis induction, RIP3 interacts with RIP1 to form a pro-necrotic complex, which is stabilized by phosphorylation of their serine/threonine kinase domains (Vandenabeele *et al*., 2010). Gonococcal infection induces production of the cellular inhibitor of apoptosis-2 (cIAP2) in human cervical epithelial cells. The intracellular cIAP2 protects the infected cells against an inflammatory, necrosis-like cell death during *N. gonorrhoeae* stimulation (Nudel *et al.*, 2015). Therefore, necrosis is an important mechanism to protect cells from bacterial infection.

1.2.2.4 Pyroptosis

Pyroptosis is coordinated by inflammasome-mediated caspase-1 or caspase-4 activation and accompanied by membrane rupture, DNA fragmentation, and the release of pro-inflammatory cytokines, including IL-1β and IL-18. *N gonorrhoeae* stimulation of monocyte-derived macrophages (MDMs) resulted in caspase 1 and 4–dependent cell deaths, indicative of canonical and noncanonical pyroptosis, respectively. The inflammatory pyroptosis is partly due to LOS (Ritter and Genco, 2018). Therefore, pyroptosis is also an important mechanism to protect cells from bacterial infection.

1.2.3 Humoral responses upon gonococcal infection

Most intracellular pathogens spread by moving from cell to cell through the extracellular fluids. The extracellular spaces are protected by the humoral immune response, in which antibodies produced by B cells and complement proteins cause the destruction of extracellular microorganisms and prevent the spread of intracellular infections (Janeway *et al*., 2001). *N. gonorrhoeae* is well-known for its extraordinary capacity to vary its surface antigen composition, both between strains and within the same strain over time. The ability of these variations in structure leads to heterogeneity in antigenic epitopes. In general, the local and systemic immune responses to gonococci are extremely modest, with a slight increase of serum immunoglobulin G (IgG) and IgA (Hedges *et al*., 1999). In addition, reinfection fails to induce a secondary antibody response (Song *et al*., 2008). Interestingly, almost all *N. gonorrhoeae* strains examined by Gulati and colleagues maintain expression of the LOS structure recognized by monoclonal antibody 2C7, despite these variations in LOS structure (Gulati *et al*., 1996). Aside from inhibiting strong antibody production, gonococci have developed two general mechanisms to evade complement attack. Firstly, they

bind to and inactivate complement cascade components and prevent membrane attack complex formation. *N. gonorrhoeae* recruits factor I to cleave the LOS-bound C3b to iC3b, which is the inactive form (Edwards and Apicella, 2002; Quillin and Seifert, 2018). Secondly, they shield themselves from complement by binding to complement regulators. *N. gonorrhoeae* binds to factor H in the cervix epithelium and to c4b-binding protein (C4BP) in the serum (Ram *et al.*, 1998). Both factor H and C4BP provide defense against direct complement-mediated killing. Thus *N. gonorrhoeae* is capable of evading the humoral response.

1.2.4 Cell-mediated immune response upon gonococcal infection

1.2.4.1 Professional phagocyte activation

N. gonorrhoeae infection triggers a potent, local inflammatory response by phagocytes, including neutrophils, dendritic cells (DCs) and macrophages. Neutrophils kill *N. gonorrhoeae* by production of reactive oxygen species and release of degrading enzymes, antimicrobial peptides and phagocytosis. Neutrophil-gonococci interaction is driven by Opa binding to CEACAM3, which ultimately promotes the efficient uptake of bound bacteria by an actin microfilament-dependent process (Sadarangani *et al.*, 2011). However, some gonococci survive and replicate within neutrophils, possibly by expressing virulence factors that defend against neutrophils' oxidative and non-oxidative antimicrobial components (Johnson and Criss, 2011). *N. gonorrhoeae* developed strategies to evade DCs and macrophage killing, as well. Gonococcal infection promotes secretion of DCs inhibitory factors such as IL-10 (Zhu *et al*., 2012), and suppresses DCs maturation (Yu *et al*., 2013). In macrophages, *N. gonorrhoeae* activates the cyclic-GMP-AMP synthase (cGAS) to produce IFN-β, which is detrimental to the host cells (Andrade *et al*., 2016). Therefore, *N. gonorrhoeae* evolved strategies to defend against phagocytes attack.

1.2.4.2 Lymphocyte activation

Lymphocytes are responsible for the specificity of adaptive immune responses, including T lymphocytes and B lymphocytes. *N. gonorrhoeae* infection activates different subtypes of T lymphocytes including activating T helper cells 1(Th1) to produce IFNγ, activating Th2 to produce IL-4, activating Th17 to produce IL-17 and activating regulatory T cells (Tregs) to produce IL10 (Kraus *et al*., 1970; Wyle *et al.*, 1977). However, gonococcal Opa proteins were able to suppress the activation and proliferation of $CD4_+$ T lymphocytes via binding to CEACAM1

(Boulton and Gray-Owen, 2002). Repeated infections among gonorrhoea patients are very common, and the ability of gonococci to inhibit the immune response may be in part due to the suppression of B lymphocytes (Hedges *et al*., 1999). The interaction of *N. gonorrhoeae* and CEACAM1 on human peripheral B lymphocytes also resulted in induction of cell death (Pantelic *et al.*, 2005). Gonococcal developed strategies to evade adaptive immune systems as well.

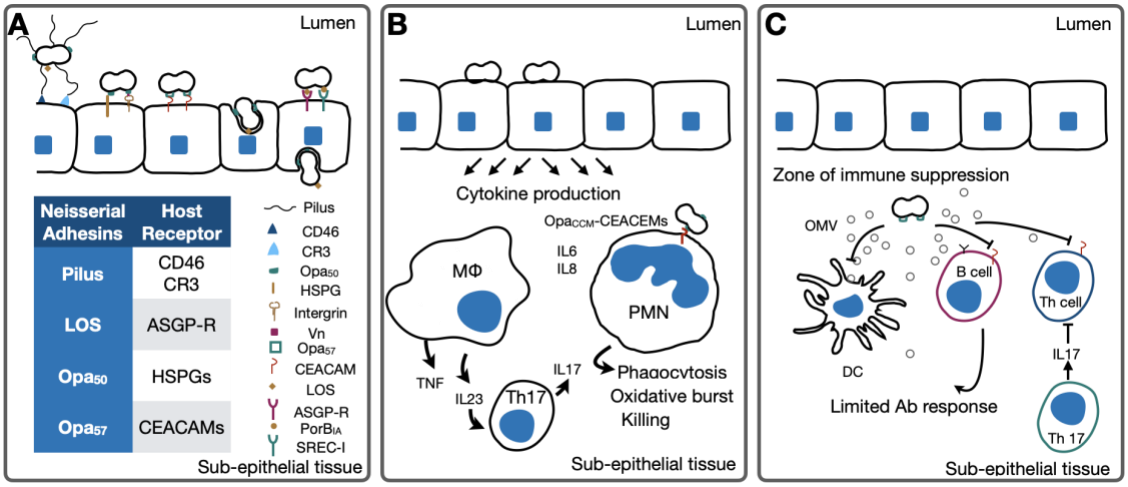

Figure 4: *N. gonorrhoeae* and host interactions
(a) adherence and invasion into the epithelial cells. The initial step in gonococcal infection is gathering of the bacterium to the host mucosal epithelium via the pilus, which attaches to the host receptors CD46 and/or CR3. Retraction of the pilus brings the bacteria into close contact with the host cells. Intimate attachment is mediated by Opa PorB$_{IA}$ and LOS. Intimate attachment triggers transcytosis of the bacterium through the epithelial cell and its exit into the subepithelial space. (b) Host cells are capable of detecting and killing gonococci. Epithelial cells recognize the gonococcus via the Toll-like receptors and can kill the bacteria via secretion of the antimicrobial peptide. The immune response is perpetuated by cytokines and chemokines released by the infected epithelial cells and macrophages. In particular, macrophages secrete IL-17 which drives a Th17 response to gonococcal infection. In response to host chemokines, neutrophils are recruited to the tissue. These cells engulf and kill the bacteria. (c) *N. gonorrhoeae* are able to evade and suppress the host immune response. The gonococcus releases outer-membrane vesicles (OMVs) upon infection. These OMVs contain Opa or PorB proteins that can bind to the surface of immune cells. For example, Opa binding to CEACAM1 inhibits the function of dendritic cells, B cells and Th cells. Furthermore, the gonococcal induced Th17 response suppresses the adaptive T cell response. Adapted from McSheffrey *et al.* (2015).

1.2.5 Tn5 transposon library screening identified NGFG_01605 as a new pathogenic factor

Even though the adhesin proteins of *N. gonorrhoeae* have been intensively studied to elucidate the initiation of infection, the virulence factors that contribute to their adaptation in the host cell have not been fully understood yet. In our group, a Tn5 transposon library has been constructed to screen for those potential virulence factors (Xian et al., 2014). Tn5 transposon is a composite transposon which contains three antibiotic resistance genes, *kan* (kanamycin), *ble* (bleomycin) and *str* (streptomycin), bracketed by two IS50 elements, ISSOL and IS50R. Both IS50 elements are delineated by 19-bp sequences, the inside end (IE) and the outside end (OE) (Fisette *et al*., 2003). Gonococcal genomic DNA was mutagenized in vitro by Tn5 transposon containing a kanamycin resistance marker. The gonococcal mutant library was used to infect human conjuctiva Chang cell line. The genomic DNAs of the mutant library (input library), the total cell-associated gonococci (output library 1) and the surviving gonococci (output library 2) were sequenced and compared. As a result, NGFG_01605 was identified as one of the potential candidates essential for infection. NGFG_01605 is a putative protease or U32 family peptidase, characterized by the consensus sequence E-x-F-x(2)-G-[SA]-[LIVM]-C-x(4)-G-x-C-x-[LIVM]-S containing two active site cysteine residues. Most of these proteases are virulence factors of human-pathogenic bacteria. Protease PrtC from *Porphyromonas gingivalis* ATCC 53977 was the first reported and is also the most studied U32 protease (Kato *et al*., 1992).

1.2.6 Folliculin (FLCN) was identified as a potential host factor for gonococcal infection

Parallel to the screen for the novel virulence factor, a short hairpin RNA (shRNA) screening assay to search for new host factors involved in the gonococcal pathogenesis was performed in our group as well. shRNA is an artificial RNA molecule with a tight hairpin turn that can be used to silence target gene expression via RNA interference (RNAi). shRNA library of HeLa cells was constructed by Winkler (2015). Briefly, the pGIPZ vectors, which coded for 10,000 different shRNAs, together with psPAX and pMD2.G plasmids were transfected to 293T cells to produce lentivirus. Virus was used to transduce HeLa2000 cells, which were then selected in puromycin-containing medium to produce the knockdown cell library. Fluorescencently labeled *N. gonorrhoeae* N2013 (pili$_{+}$, Opa$_{+}$, PorB$_{IA}$) were used for the screen. FACS analysis was used to distinguish the highly infected and uninfected populations. The genomic DNA isolated from different cell populations were sent for sequencing to compare the frequency of shRNA insertions. As a result, FLCN was identified as one of the candidates that could play a role in gonococcal infection.

FLCN is a 64 kDa protein, localized in the cytosol and the nucleus. FLCN mutation is related to the disease Birt-Hogg-Dubé syndrome (BHD). BHD patient develop often fibrofolliculomas, lung cysts, spontaneous pneumothorax, and have an increased risk for kidney tumors.
FLCN has an N-terminal Longin domain and a C-terminal DENN (Pacitto *et al*., 2015) and has been connected to multiple cellular processes including mammalian target of rapamycin (mTOR) signaling, transforming growth factor β (TGF-β) and AMP-activated kinase (AMPK) signaling, autophagy and the formation of lysosomes. However, the functions of FLCN in regulating those pathways are cell type- and microenvironment-dependent. FLCN regulates mTOR in a cell type-dependent manner. FLCN-deficient mouse kidneys displayed elevated levels of phospho-mTOR and phosphorylated ribosomal protein S6 (phospho-S6), demonstrating activation of mTOR pathway (Baba *et al*., 2008; Chen *et al*., 2008). However, another study revealed that endogenous FLCN localizes to the lysosomal surface to activate mTOR1 in response to amino acid starvation in human embryonic kidney (HEK)-293T cells (Tsun *et al*., 2013). FLCN has been demonstrated to be essential for TGF-β signaling (Hong *et al*., 2010b). This finding has been expanded upon by experiments which show that FLCN also regulates apoptosis through TGF-β (Cash *et al.*, 2011). Additionally, FLCN has been demonstrated as a negative regulator of AMPK. Loss of FLCN results in constitutive activation of AMPK, which induces autophagy (Possik *et al*., 2014). Moreover, knockdown of FLCN in HK2 cells resulted in the accumulation of the autophagic marker sequestosome 1 (SQSTM1/p62), which signals impaired autophagy, and was reversed by FLCN re-expression (Dunlop *et al.,* 2014). Except for AMPK, transcription elongation factor B (TEFB) and transcription enhancer factor 3 (TEF3) are well characterized as master regulators of the autophagy-lysosome pathway in response to starvation (Jeong *et al.*, 2018). FLCN inactivation was correlated with an increase in TFE3 activation (Hong *et al.*, 2010a).
It is intriguing that all these pathways are also connected to cell polarization and integrity. Cell polarity is triggered by cell-cell adhesion via junction proteins, e.g. E-cadherin and Zonula occludens-1 (ZO-1). E-cadherin is a single-pass type I transmembrane glycoprotein of 120 kDa that consists of five extracellular cadherin (EC) repeats with binding sites for Ca^{2+} (Ogou *et al*., 1983). These homophilic E-cadherin dimerize in cis at the cell's surface and the homodimer can then interact in trans with an adjacent E-cadherin homodimer on a neighboring epithelial cell to form adherens junctions (Shapiro *et al*., 1995). E-cadherin interacts with p120-ctn and β-catenin by its intracytoplasmic tail (Devaux *et al*., 2019). P0071, one of the interacting proteins of FLCN is a

homolog of P120-ctn (Hatzfeld *et al*., 2014). FLCN has been demonstrated to affect E-cadherin polarization in a cell-type dependent manner (Medvetz *et al.*, 2012; Goncharova *et al*., 2014). Moreover, FLCN was shown to function in endocytic trafficking (Nookala *et al*., 2012). Rab7A was identified as a FLCN interacting protein, as well. Their interactions regulate the endosomal recycling and lysosomal degradation of epidermal growth factor receptor (EGFR) (Laviolette *et al*., 2017). FLCN is critical for cilia formation, a cell structure of the endometrium, fallopian tubes and cervix cells (Lenz and Dillard, 2018). Recent study shows that FLCN regulates epithelial cell size in response to fluid flow via autophagy (Zemirli *et al*., 2019).
FLCN has multiple functions in regulating cell growth, survival and morphology pathways, which are critical in *N. gonorrhoeae* infection as well. It is of high interest to relate FLCN and human obligate pathogen infection, which has not previously been reported.

1.3 Three-dimensional microenvironment

The traditional flat two-dimensional (2D) monolayers composed of a single cell type have provided critical insight into understanding host-pathogen interactions and infectious disease mechanisms. But such models lack many essential features present in the native host microenvironment that are known to regulate infection, including three-dimensional (3D) architecture, multicellular complexity, gas exchange and nutrient gradients, and physiologically relevant biomechanical forces (Barrila *et al*., 2018).

1.3.1 The cervix microenvironment

N. gonorrhoeae infects humans exclusively and initiates infection in the female reproductive tract at the cervix. The mucosal surface of the human cervix varies significantly and is generally divided into three regions: the ectocervix, consisting of multilayered, non-polarized, stratified, squamous epithelial cells; the endocervix, containing a single-layer of polarized, columnar cells; and the transforming zone, where epithelial cells progressively change from stratified squamous to columnar cells (Hafes *et al*., 1982). Those epithelial cells play a crucial role in the initiation, maintenance, and regulation of innate and adaptive response in collaboration with immune cells. These include mounting physical (intercellular junctions, mucus) and immune barriers (pathogen-recognition receptor-mediated pathways), which collectively and ultimately lead to specific chemokine or cytokine release. The cytokines subsequently recruit subsets of

immune cells tailored to a particular immune context and response, such as DCs and lymphocytes. The human cervical tissue explant has been established for gonococcal infection. They showed that *N. gonorrhoeae* preferentially colonizes the ectocervix by activating integrin-β1, which inhibits epithelial shedding. *Neisseria gonorrhoeae* selectively penetrates into the squamocolumnar junction (TZ) and endocervical epithelia by inducing β-catenin phosphorylation, which leads to E-cadherin junction disassembly (Yu *et al*., 2019).

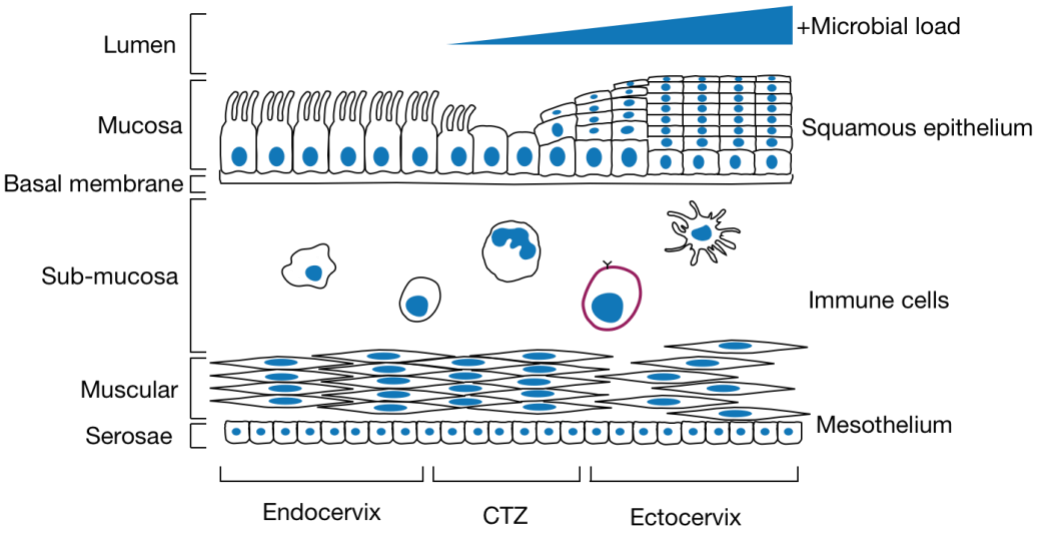

Figure 5: The cervix microenvironment
Microscopic illustration of the cervix. The cervix is divided into the three main compartments, namely, the microbe-laden ectocervix and “sterile” endocervix, which are bordered by the cervical transformation zone and their associated immune cells. The endocervix has ciliated epithelial cells and the ectocervix has ciliated epithelial cells and squamous stratified epithelial cells. Adapted from de Tomasi *et al* (2019).

1.3.2 The advantage of *ex vivo* models to study the host-pathogen interactions

Traditionally, the interaction was studied via a single pathogen and a single host cell type grown as a flat monolayer. It enabled important and fundamental understanding of the mechanisms, but it was difficult to relate the *ex vivo* and *in vivo* responses. Therefore, it is important to consider the context in which the investigations are performed. Reconstructing the host microenvironment is the key to study host-pathogen interactions. There are many unique features of the *in vivo* microenvironment, such as multicellular complexity, microbiota, oxygen tension and biomechanical forces, which affect the host-pathogen interaction.

The cellular factors, like polarized epithelial cells, act as a barrier against infection. The tissue residing microbiota, which reciprocally interacts with the host, contributes to tissue function. In addition, the biochemical cues, like mucin and ECM, and biophysical forces, like fluid shear and pressure, affect infection as well. Hydrodynamic calculations suggest that fluid shear forces on the exposed epithelial brush border microvilli are 200 times greater than those between microvilli (Guo *et al*., 2000). However, no single *ex vivo* models fulfill this requirement. It is important to choose the right models depending on the scientific questions to be answered.

1.3.3 *Ex vivo* models to study gonococcal infection

Several cell culture systems exist for the development and application of 3-D models of human tissues for infectious disease research, including the rotating wall vessel (RWV) bioreactor, the ECM-embedded/organoid models and organ-on-a-chip models (Barrila *et al*., 2018).

(i) The RWV bioreactor

The rotating wall vessel is an optimized form of suspension culture that facilitates formation of self-organizing 3-D tissue-like aggregates by allowing cells the spatial freedom to colocalize and self-assemble based on natural affinities within a low-fluid-shear environment (Barrila *et al*., 2018). The HEC-1A cell line was used to develop the RWV gonococcal infection model. As shown in the study, the model recapitulates several functional/structural characteristics of the cervix, including cell differentiation, the presence of junctional complexes/desmosomes and microvilli, and the production of membrane-associated mucins and TLRs (Łaniewski *et al*., 2017). Meanwhile there are some limitations to this technology. It is difficult to recapture the full extent of 3-D architecture, multicellular complexity and physical forces of the in vivo tissue. Furthermore, it is not suitable to study the bacterial transmigration.

(ii) ECM-embedded/organoid models

Organoid is a piece of organ-like tissue. Traditionally, it refers to embedding or culture of the cell lines, stem cells, primary cells or tissue explants on top of ECM scaffolds to allow cells to self-assemble into 3-D structures. Recently, the concept shifted to the 3-D models derived from stem cells, progenitor cells, or primary explants (Fatehullah *et al*., 2016). There are different ways to study the bacterial infection using these models such as addition of pathogen directly to the media, microinjection into the lumen, shearing of models into fragments followed by pathogen addition and complete disruption of 3-D models into flat monolayers followed by pathogen addition (Barrila *et al*., 2018). Limitations were found in

those models as well. Heterogeneity in viability, size and shape of organoids were normal within a culture and across different samples. Extracellular matrix for embedding the cells has batch to batch variation, which affects the cell growth and differentiation. What's more, the growth factors exhibit batch to batch variation as well.

(iii) Organ-on-a-chip models

The chips for organs are designed with micrometer-sized fluidic channels separated by thin, flexible and porous membranes that allow development of different tissues in adjacent chambers and keep their ability to interact (Bhatia *et al*., 2014). A variety of platforms have been developed using everything from cell lines to primary cells. Such models can be used toc study the host-bacteria interaction in a high throughput fashion. However, limited cell types have been added to the ECM to mimic the cell complexity of the *in vivo* tissue. Therefore, each of the *ex vivo* 3D models have their advantages and disadvantages, so it is important to choose the right model depending on the scientific questions to be answered.

1.4 Aim of the study

N. gonorrhoeae is human obligate pathogen. Gonococci has multiple and phase-varied surface structures, which enable them to evade host attack. The bacterial and cellular factors involved in establishing adherence and invasion have been well characterized. However, the molecular bases for survival and transmigration to deeper tissue are less understood. Previous work in our group identified a novel bacterial and a novel host factor involved in the gonococcal infection process. The aim of this work was to determine their functions respectively in the gonococcal pathogenesis. Both molecular and biochemical methods were employed to determine which infection steps are regulated by those factors in the first place. We further explored their effects on the programmed cell death upon infection, since programmed cell death is the common mechanism manipulated by pathogens to favour their host adaptation. Moreover, their cellular localisation and interacting proteins were studied as well to better understand their function. Both non-polarised and polarised cell are present in the native tissue, where *N. gonorrhoeae* infects *in vivo*. Therefore, one of the aims of this work was to establish relevant 3D infection models and use them to better understand the roles these proteins play in the polarised cells, especially in terms of bacterial survival and transmigration. The goal of this study was therefore to better understand the gonococci and host interactions from both the pathogen and host side and to relate the 2D and 3D models.

2. Results

2.1 NGFG_01605 is essential for gonococcal survival in epithelial cells

2.1.1 NGFG_01605 is a cytosolic protein

NGFG_01605 is annotated as a putative U32 protease with a hitherto unknown catalytic type and PrtC of *P. gingivalis* is its homologous protein (Figure 6A). It is highly conserved in *Neisseria*, with only 5 aa difference between *N. gonorrhoeae* and its homolog in *N. meningitidis* (Figure 6B). NGFG_01605 was first identified as a potential *N. gonorrhoeae* virulence factor in disseminated gonococcal infection (Xian, 2014). NGFG_01605 knockout has been confirmed to decrease gonococcal survival, but no complementation is made to prove it.

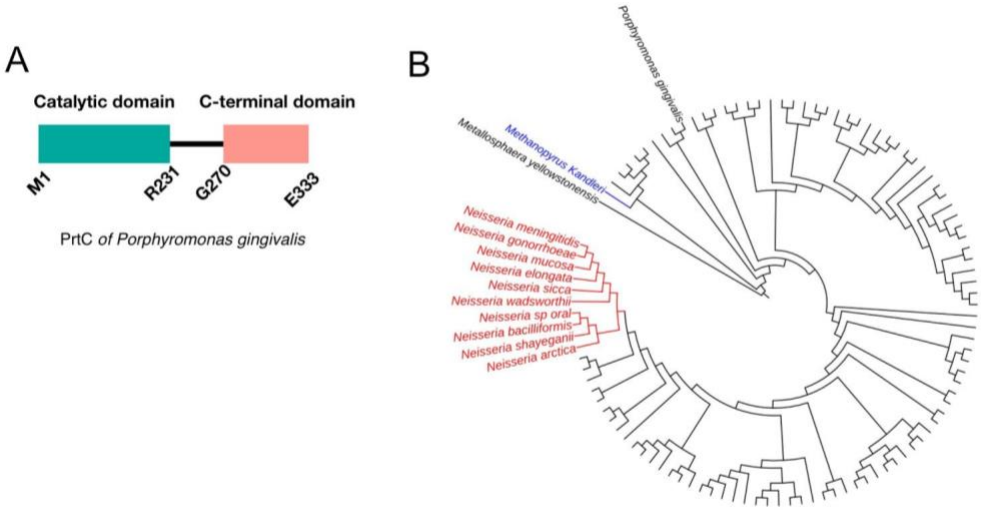

Figure 6: NGFG_01605 is predicted to be a protease
(A) The conserved domains of PrtC of *P. gingivalis*, which is a homologous protein of NGFG_01605. (B) The phylogenetic tree of the homologous proteins of NGFG_01605.

2.1.2 Recombinant NGFG_01605 purification

NGFG_01605 is 579 amino acids in length with a mass of 50 kDa. The coding DNA sequence of NGFG_01605 was cloned into the vector pET28b at BamHI and HindIII restriction sites, which fused an N-terminal His-tag to the protein. The vector was transformed in *E. coli* soluBL21 (Xian, 2014). The *E. coli* soluBL21 culture was induced by 0.25 mM IPTG and was incubated at 25 °C and 200 rpm for 4 h. The bacterial pellet was collected for NGFG_01605 purification by Ni-NTA resin in native condition as described in 4.2.7. SDS–PAGE analysis of a

representative protein purification using Ni-NTA show equal volumes of the cell lysate, the flow-through, and the eluate from the column. The eluate was further purified by anion exchange column (HiTrap Q) and gel filtration (Figure 7). The fractions of NGFG_01605 from gel filtration were collected and concentrated for *ex vivo* assay.

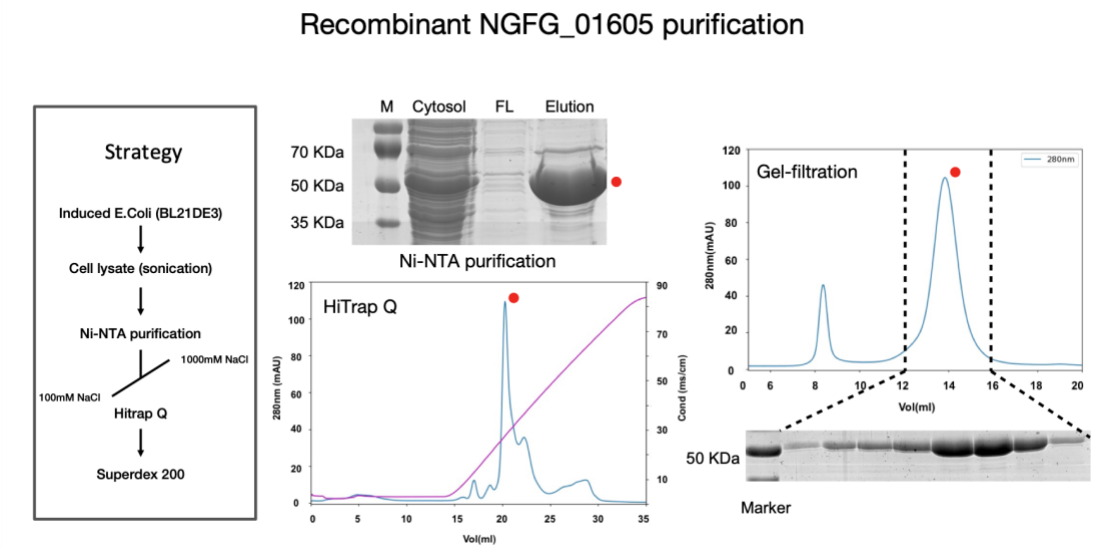

Figure7 Recombinant NGFG_01605 purification
The left panel shows the strategy to purify the recombinant NGFG-01605 from *E. coli* (soluBL21). The middle panel shows the Ni-NTA purification and HiTrap Q for further purification. The right panel shows the gel-filtration for the final purification and collection. The SDS-PAGE shows that the collected fractions were the same size as NGFG_01605.

No signal peptide has been predicted for NGFG_01605 secretion. As shown in the Figure 8D, it is localized in the cytosol, membrane, but not found in the supernatant. PrtC degraded soluble and reconstituted fibrillar type I collagen, heat-denatured type I collagen, and azocoll. The activity of PrtC was enhanced by Ca^{2+}. In other collagenase families, e.g. M9 family, Zn^{2+} is the cofactor. However, the substrate specificity of other U32 proteases has not been characterized in detail (Zhang *et al*., 2015). Azocasein is a nonspecific protease substrate. Hydrolysis of the casein releases the azo dye into the media where it is detected by absorbance at 440 nm. In this study, azocasein assay was employed to determine the protease activity of NGFG_01605. The proteolytic cleavage of azocasein was tested by either purified NGFG_01605 or in combination with a cofactor. As shown in the Figure 8 A-C, NGFG_01605 displayed no protease activity compared with the positive control trypsin.

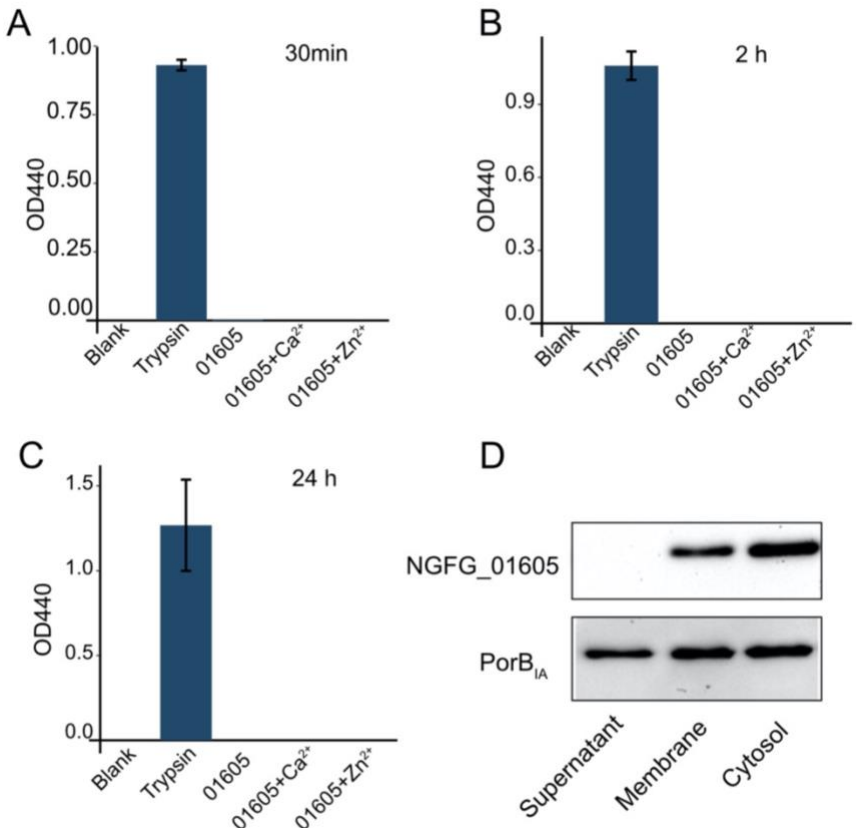

Figure 8: NGFG_01605 is not secreted and has no protease activity *ex vivo*
The purified recombinant NGFG_01605 with or without cofactor was incubated with azocasein for different periods of time. Trypsin was used as a positive control. OD_{440} was measured as shown from A to C (three biological replicates, mean ± s.d). (D) The supernatant proteins of N2009 liquid culture were precipitated by acetone, while the bacterial membrane and cytosol proteins were isolated by centrifugation at 100,000 rpm for 2 h. Samples were analyzed by SDS-PAGE and Western blot with the anti-NGFG_01605 antibody.

2.1.3 Exploring NGFG_01605 interacting proteins by co-immunoprecipitation

Aside from protein structure, the interacting partner proteins could provide insights into the molecular bases of its function as well. Therefore, the interacting proteins of NGFG_01605 were analyzed by co-immunoprecipitation of the native His-tag NGFG_01065 incubated with N2009 lysate. As shown in Figure 9, different incubation methods were employed including incubation of his-NGFG_01605 with gonococcal lysate first then incubation with Ni-NTA beads, and incubation of his-NGFG_01605 with Ni-NTA beads first and then with gonococcal lysate. However, no interaction partners have been found by this method.

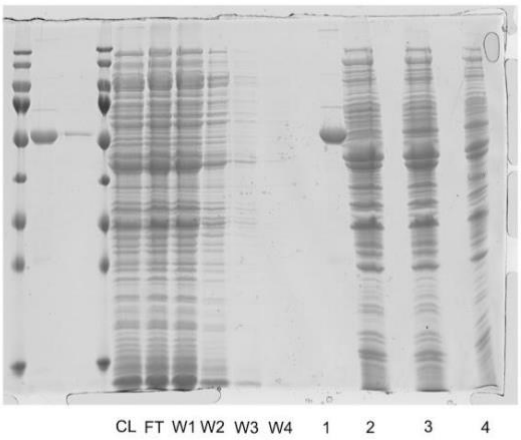

Figure 9: Immunoprecipitation of His-NGFG_01605 in the presence of *N. gonorrhoeae* lysate
Failure of establishment of co-Immunoprecipitation of His-NGFG_01605 as observed by silver stained SDS-PAGE. The very left of the gel is the marker, purified recombinant NGFG_01605 and elute of Ni-NTA beads after incubation. The rest of the gel shows the pull-down process. CL, cytosol; FL, flowthrough; W1 to W4, wash 1 to 4; 1; purified recombinant NGFG_01605; 2 to 4 represent different incubation combinations, 2 represents Ni-NTA beads incubated with gonococcal lysate, 3 represents gonococcal lysate incubated first with recombinant His-NGFG_01605 then with Ni-NTA beads, 4 represents Ni-NTA beads incubated with recombinant His-NGFG_01605 first then with gonococcal lysate.

The interaction proteins of NGFG_01605 were then analyzed by co-immunoprecipitation of FLAG-tagged NGFG_01065 expressed in the N2009. The anti-FLAG M2 affinity gel was used to pull down FLAG-tagged NGFG_01605 and its interacting proteins. As shown in Figure 10, no interaction partners had been pulled down compared to negative control N2009. This result was further confirmed by anti-FLAG (Figure 11B) and anti-NGFG_01605 (Figure 11C) immunoblots.

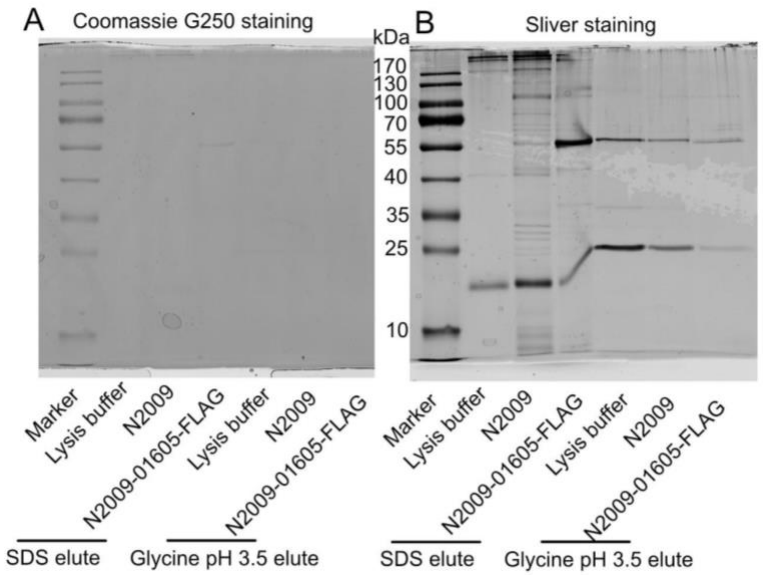

Figure 10: Co-Immunoprecipitation of NGFG_01605 with Flag tag
Co-Immunoprecipitation of NGFG_01605 Flag tag was analyzed by both coomassie stained and silver stained SDS-PAGE.

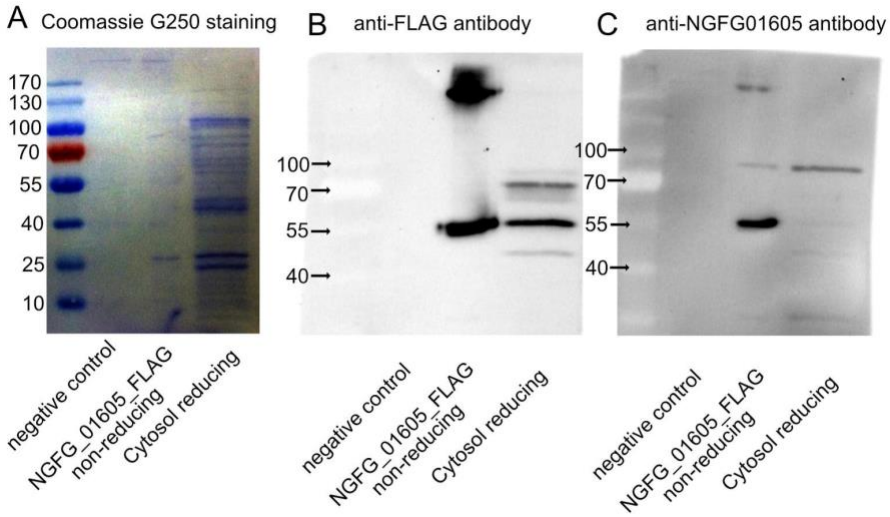

Figure 11: Co-Immunoprecipitation of FLAG-tagged NGFG_01605
Co-Immunoprecipitation of NGFG_01605 Flag-tag was observed by coomassie staining (A) and immunoblotting with anti-FLAG antibody (B) and anti-NGFG-01605 antibody.

2.1.4 NGFG_01605 is essential for gonococcal survival

To better understand the role of NGFG_01605, complementation strains of NGFG_01605 in N2009 were constructed to see whether it could restore gonococcal survival efficiency. The complementary strains were made by introducing PLAS:pilE_NGFG01605 plasmid with spectinomycin selection

marker. The successful complemented strains were sequenced by the primers PLAS-fseI-for and PLAS-pacI-Rev. Furthermore, the immunoblots showed a successful complementation (Figure 12A). N2009 is the wild type, N00125 and N00126 are the NGFG_01605 knockout strains, N00127 and N00128 are complementary strains. The growth curve was compared among NGFG_01605 wild type, knockout and complemented strains of N2009. All of the strains, except the complemented strain N00128, have similar growth rates as shown in the Figure 12B.

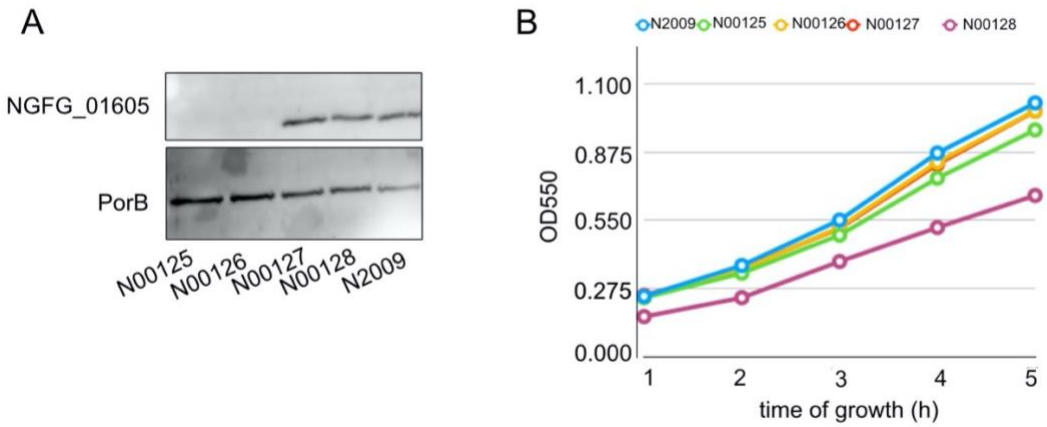

Figure 12 Complementation of knockout strains with NGFG_01605 in N2009
The NGFG_01605 knockout strains were complemented with the PLAS:NGFG01605 plasmid. N2009 is the wild type strain, N00125 and N00126 are the NGFG_01605 knockout strains, N00127 and N00128 are the complemented strains. The complementation was confirmed by Western blot as shown in (A). (B) The growth curves of the NGFG_01605 wild type, knockout and complementation strains of N2009.

Gentamicin protection assay and differential staining were combined to define the adherence, invasion and survival of *N. gonorrhoeae*. The difference of NGFG_01605 wild type, knockout and complemented strains of N2009 in adherence, invasion and survival in Chang cells were compared. As shown in the Figure 13A, NGFG_01605 did not affect adherence (left panel). NGFG_01605 knockout N00125 showed a higher invasion while the knockout N00126 did not, therefore, the role of NGFG_01605 in invasion has to be further clarified (Figure 13A middle panel). NGFG_01605 is essential for gonococcal survival as shown in the Figure 13A (right panel) since the knockout strains had significantly less survival compared with the wild type strains, and the complementation strains increased survival. The Figure 13B illustrates the differential staining method, the intracellular gonococci in red and extracellular ones in yellow.

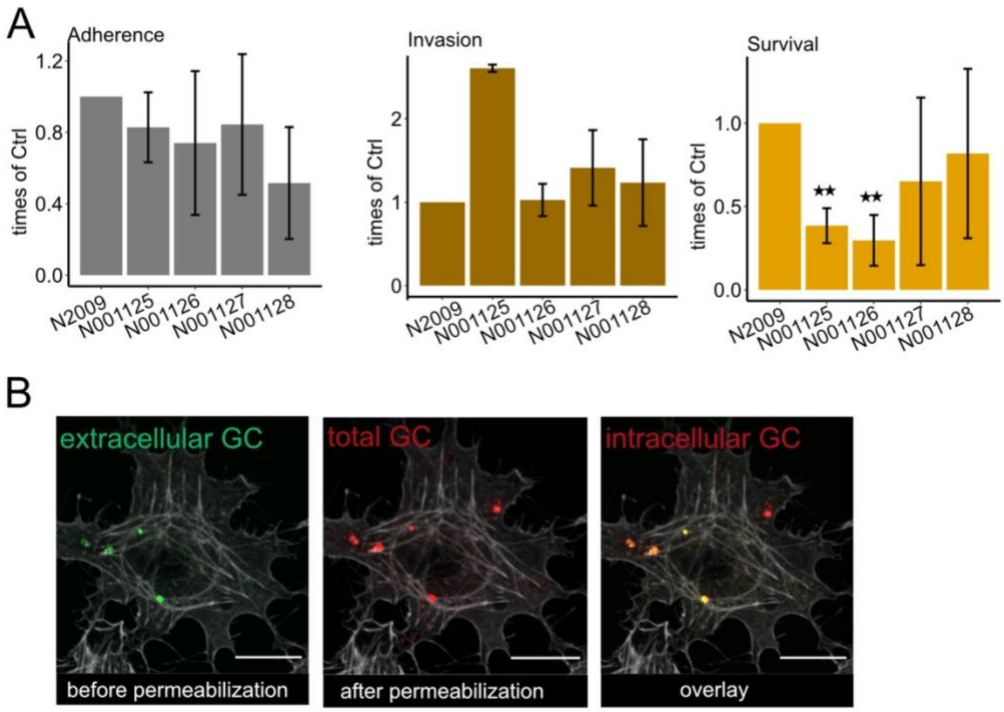

Figure 13 NGFG_01605 might be critical for *N. gonorrhoeae* survival in Chang cells

Gentamicin protection assay was used to quantify adhered and survival GC. Immunofluorescence staining was used to determine invaded GC. The extracellular GC (green) were, after decoration with the primary anti-GC antibody, stained with two secondary antibodies coupled to different fluorophores (before and after cell membrane permeabilization). The intracellular GC (red) were stained only once with the anti-GC antibody and one secondary antibody (after cell membrane permeabilization). (A) shows the adherence, invasion and survival of the NGFG_01605 wild type (N2009), knockout (N00125 and N00126) and complementation (N00127 and N00128) strains. The adherence and survival GC were determined by gentamicin assay and the invasion GC by differential staining and confocal microscopy quantification. Three biological replicates, mean ± s.d, *P<0.05, student's t-test. (B) Illustration of employing immunofluorescence staining to determine invaded GC. The extracellular bacteria with double staining are depicted in yellow and the intracellular bacteria stained once are depicted in red. Scale bars represent 20 μm.

2.1.5 Knockout NGFG_01605 does not affect gonococcal transmigration

After revealing that NGFG_01605 is critical for *N. gonorrhoeae* survival in 2D cell culture, we were interested in investigating its role in transmigration. T84, the colon epithelial cells, were used to develop the infection models on transwell for 10 days. FITC-dextran assay was performed to make sure the bacterial integrity was about 96%. Mature models were kept in antibiotic-free medium 24 h before

infection. NGFG_01605 wild type, knockout and complemented strains of N2009 were used to infect the models with the MOI of 50. The transmigrated *N. gonorrhoeae* were collected and plated for counting at 6 h and 24 h post infection. No *N. gonorrhoeae* was collected at the 6 h post infection. *N. gonorrhoeae* transmigrated and reached the bottom of the transwell at 24 h post infection. The knockout N00125 had a significantly less transmigration compared with wild type N2009. However, the NGFG_01605 knockout N00126 had a similar transmigration efficiency compared with wild type. In addition, the complementation strains (N00127 and N00128) had similar transmigration rates compared with the knockout strains (Figure 14). Therefore, knockout of NGFG_01605 does not affect gonococcal transmigration.

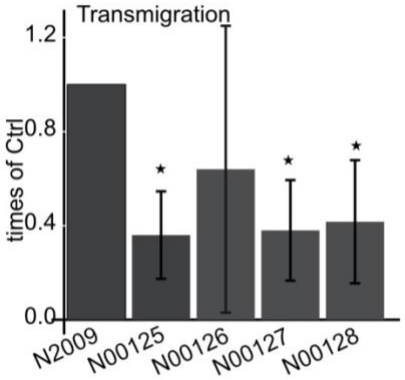

Figure 14: NGFG_01605 knockout does not affect N2009 transmigration
The T84 models grown on transwell for 10 days were infected with NGFG_01605 wild type (N2009), knockout (N00125 and N00126) and complementation (N00127 and N00128) strains in N2009 background with MOI 50. The number of transmigrated bacteria of the wild type was set to 100%. Colony forming units (CFU) are plotted in times of control (three biological replicates, mean ± s.d, *P<0.05, student's t-test).

2.2 FLCN is essential for gonococcal survival

2.2.1 FLCN is essential for gonococcal survival in 2D cell culture

2.2.1.1 FLCN is essential for gonococcal survival in HeLa2000 in the presence of FBS

A combined approach of shRNA library screening, flow cytometry, and next-generation sequencing was used to identify novel host factors involved in *N. gonorrhoeae* infection. FLCN was determined as one of the candidates important for the attachment and/or invasion of gonococci (unpublished data). To

investigate the function of FLCN more precisely, we generated a stable shRNA expressing HeLa2000 cell line for the suppression of FLCN expression. Before the single knockdown clone isolation by FACS, we used the FLCN knockdown pool for gentamicin protection assay. The FLCN knockdown pools were infected with N2013 (pili$_{+}$, PorB$_{IA}$, Opa$_{+}$), E1recA (pili$_{+}$, PorB$_{IB}$, Opa$_{+}$), and N927(pili$_{-}$, PorB$_{IA}$, Opa$_{-}$). N2013 was the strain used for the screening assay. It is pili positive and expresses the PorB$_{IA}$, which mediates the invasion in the low phosphate condition (HEPES). E1recA is constitutively pili positive and unable to switch off pilus expression due to the absence of recA, but with the PorB$_{IB}$ gene. N927 is pili negative and with the PorB$_{IA}$ gene. The infection was carried out in HEPES medium, which means both the PorB$_{IA}$ and Opa proteins, if present, can mediate the invasion. As shown in Figure 15, the effect of FLCN on gonococcal adherence was strain dependent, however, it is important for gonococcal survival since less N927 survived in the FLCN knockdown pools.

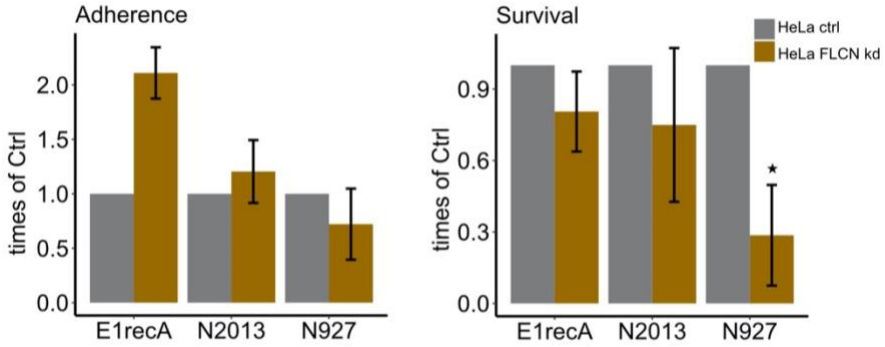

Figure 15: *N. gonorrhoeae* tends to survive worse in FLCN knockdown pools of HeLa2000

HeLa2000 with empty pLVTHM (ctrl) and FLCN shRNA knockdown pools were infected with N2013 (pili$_{+}$, PorB$_{IA}$, Opa$_{+}$), E1recA (Pili$_{+}$, PorB$_{IB}$, Opa$_{-}$), and N927(pili$_{-}$, PorB$_{IB}$, Opa$_{-}$) for 1 h at the MOI of 50. The infection medium is HEPES. Gentamicin protection assay was performed. (A) 1% saponin was used to permeabilize the infected cell and to release the intracellular GC, total GC were quantified by dilution plating. Shown are adherent GC, which were calculated by total GC minus surviving GC. (B) 50 μM gentamicin was added to the infected cells for further 2 h to kill the extracellular GC. Saponin treatment was performed afterwards to quantify the survival GC. Three biological replicates were performed.

To further study the role of FLCN in gonococcal infection, single knockdown clones were selected by FACS and confirmed by immunoblot (Figure 16A). The knockdown efficiency is about 50%. *N. gonorrhoeae* has two main invasin proteins, PorB$_{IA}$ and Opa. In the first set of experiments, gonococci N2013 and

N927, which contain PorB$_{IA}$, were selected for the gentamicin assay in the HEPES medium. As shown in Figure 16B and 16C, FLCN did not significantly affect the PorB$_{IA}$-mediated adherence and survival. In the second set of experiments, gonococci N931 (pili^{-}, PorB$_{IB}$, Opa$_{50}$) and N924 (pili^{-}, PorB$_{IB}$ Opa^{-}) were used for infection. Opa-mediated gonococcal invasion is usually performed in high phosphate conditions, such as RPMI and DMEM medium, to exclude the effect of PorB$_{IA}$-mediated invasion, which is phosphate dependent. The vitronectin and fibronectin in the FBS function as co-ligands for Opa-mediated invasion and improve the invasion efficiency. As shown in Figure 17A, FBS increases the N931 adherence and survival in HeLa2000. FLCN did not affect the adherence in both infection conditions. FLCN was essential for gonococcal survival in the infection condition with FBS. As shown in Figure 17B, FBS increases the N924 adherence and survival in HeLa2000 as well. N924 has a higher adherence efficiency (about 60 GC/cell) to HeLa2000 compared to that of N931 (about 15 GC/cell) with FBS in infection medium. However, the survival rate of N924 in HeLa2000 (around 0.0008 GC/cell) is significantly lower than that of the N931 (about 0.0023 GC/cell), pointing to a lower internalization of these bacteria. FLCN did not affect N924 adherence and survival. In conclusion, FLCN had no effect on gonococcal adherence but was essential for N931 survival.

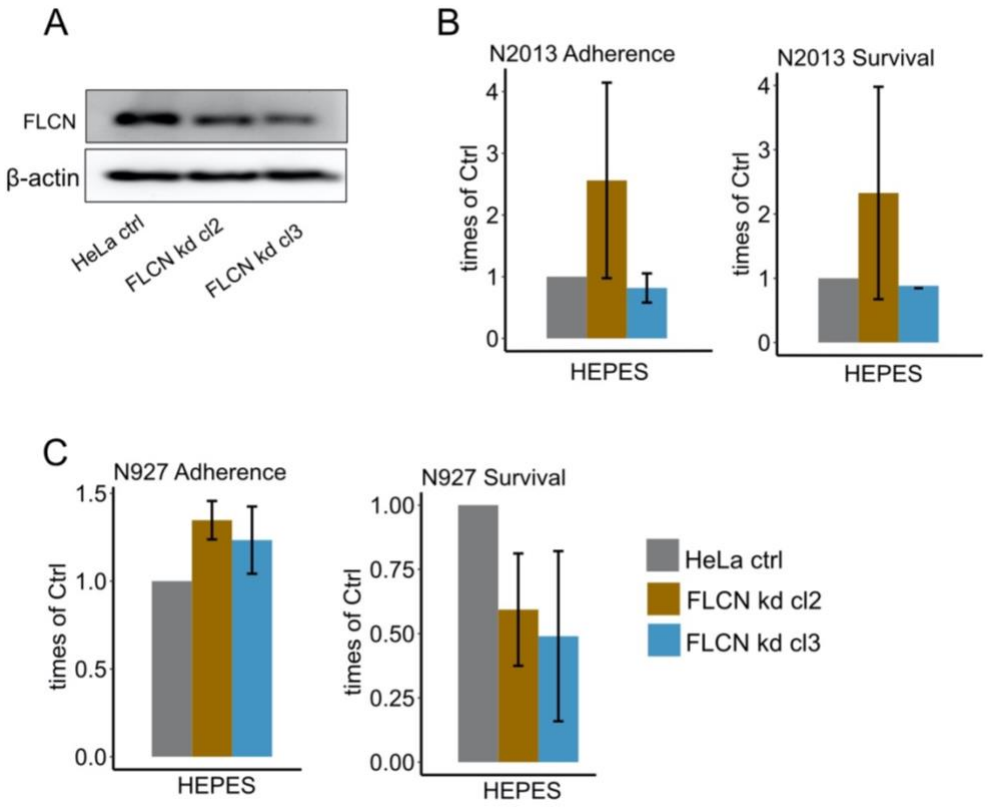

Figure 16: FLCN does not affect PorB$_{IA}$-mediated survival in HeLa2000
HeLa2000 with empty pLVTHM (ctrl) and the FLCN shRNA knockdown single cell clones were infected with N2013 (pili^{+}, PorB$_{IA}$, Opa^{+}) and N927(pili^{-}, PorB$_{IA}$, Opa^{-}) respectively for 1 h with the MOI of 50 in the HEPES medium. (A) FLCN protein was detected by Western blotting of HeLa2000 and its FLCN knockdown clones. The knockdown efficiency is about 50%. (B)1% saponin was used to permeabilize the N2013 infected cell to count the total cell-associated bacteria. 50 μM gentamicin treatment and followed 1% saponin permeabilization were used for assessing the survived bacteria. Adhered bacteria = total cell-associated bacteria – survival bacteria. three biological replicates, mean ± s.d. (C) The adherence and survival of N927 in the infected cells as described in (B).

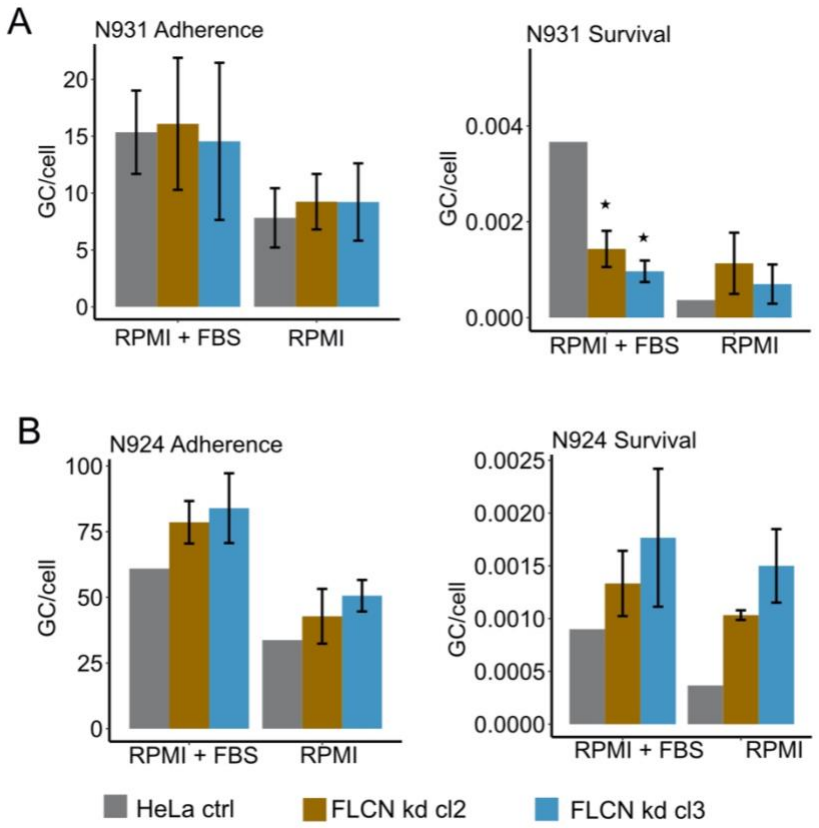

Figure 17: FLCN is important for *N. gonorrhoeae* survival in HeLa2000
HeLa2000 with empty pLVTHM (ctrl) and the FLCN shRNA knockdown single clones were infected with N931 (pili^{-}, PorB$_{IB}$, Opa$_{50}$) and N924 (pili^{-}, PorB$_{IB}$, Opa^{-}) for 2 h at the MOI of 50. The infection media were RPMI and RPMI plus FBS. (A) 1% saponin was used to permeabilize the N931 infected cell to count the total cell associated bacteria. 50 μM gentamicin treatment followed by 1% saponin permeabilization was applied to assess the surviving bacteria. Adhered bacteria = total cell-associated bacteria – survival bacteria. three biological replicates, mean ± s.d. (C) the adherence and survival of N924 in the infected cells as described in (B).

In addition to knockdown of FLCN in HeLa2000, overexpression of FLCN by transfecting the pCDNA3-FLCN-Flag expression plasmid into HeLa2000 was carried out to see the effects on gonococcal survival. The FLCN was highly expressed in the HeLa2000 cell transfected with the pCDNA3-FLCN-Flag plasmid as shown in Figure 18A. The HeLa2000 transfected with control empty vector and HeLa2000 overexpressing FLCN were infected with N931 in both RPMI and RPMI with FBS conditions. As shown in Figure 18B, FLCN overexpression did not affect the gonococcal adherence in both infection conditions, but significantly increased the N931 survival when FBS was present in the infection medium. Taken together, these results indicate that FLCN is essential for gonococcal survival in HeLa2000 when FBS is present in the infection medium. Whether this role of FLCN is Opa-mediated invasion pathway specific has to be further studied.

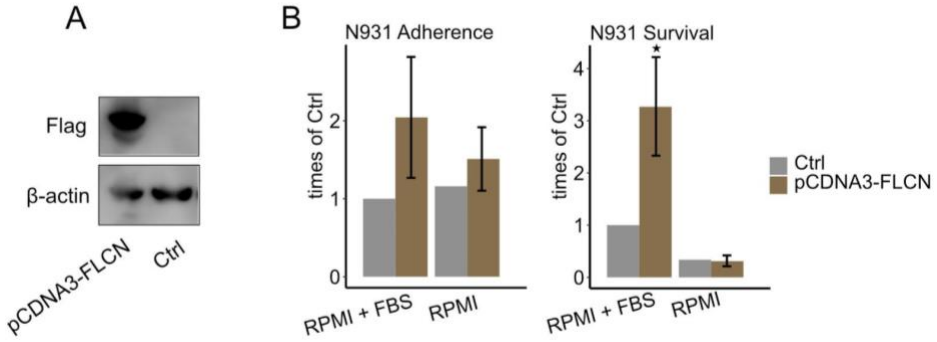

Figure 18: FLCN overexpression increased *N. gonorrhoeae* intracellular survival
HeLa2000 with empty pCDNA3 (ctrl) and the FLCN overexpression cell lines were infected with N931 (pili-, PorB$_{IB}$, Opa$_{50}$) for 2 h in RPMI plus FBS. (A) FLCN protein was detected by Western blot of HeLa2000 and FLCN overexpression cells. (B) 1% saponin was used to permeabilize the N931 infected cell to count the total cell-associated bacteria. 50 μM gentamicin treatment followed by 1% saponin permeabilization was applied to count the survival bacteria. The adhered bacteria were defined as total cell-associated bacteria minus survival bacteria (three biological replicates, mean ± s.d, *P<0.05, student's t-test).

2.2.1.2 FLCN is essential for gonococcal survival in UOK cells in the presence of FBS

The FLCN knockdown efficiency by shRNA in HeLa2000 is about 50%. The knockdown efficiency is relatively low. Therefore, UOK257 and UOK-FLCN were introduced for further studies. UOK257 is a kidney epithelial cell line derived from Birt-Hogg-Dubé syndrome (BHD) patients. It contains an insertion of a C at nucleotide 1733 of FLCN, resulting in a frameshift mutation that is assumed to

destroy the function of FLCN. FLCN was reintroduced by the plasmid pUbC-FLCN-SMAR in UOK-FLCN (Wong and Harbottle, 2013). The western blot (Figure 19) confirmed that there was no functional FLCN expression in UOK257. The ability of *N. gonorrhoeae* to adhere and survive in UOK-FLCN was compared to that in HeLa2000. As it can be seen in the Figure 19, the ability of gonococci to adhere to cells depends on the derivative used. N924 bound to UOK-FLCN better than to HeLa2000, while the N931 behaved in an opposite way. As to the survival, both N924 and N931 had significantly higher survival rates in the UOK-FLCN than in the HeLa2000. In this way, UOK cells were a better system to study the role of FLCN in gonococcal survival.

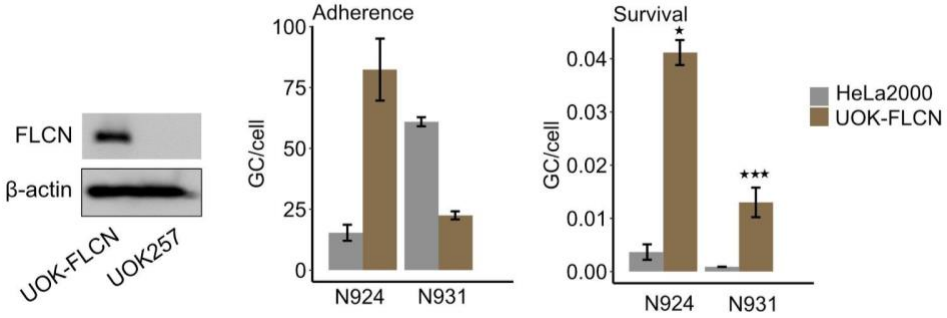

Figure 19: *N. gonorrhoeae* better survives in UOK-FLCN than in HeLa2000
HeLa2000 and UOK-FLCN were infected with N931 (pili-, $PorB_{IB}$, Opa_{50}) and N924 (pili-, $PorB_{IB}$, Opa-) respectively for 2 h at the MOI of 50. The infection medium is RPMI plus FBS. The left panel shows the western blot detecting FLCN protein in UOK cells. The middle panel shows the adhering bacteria of both N924 and N931 infected HeLa2000 and UOK-FLCN. The right panel shows the surviving bacteria after gentamicin treatment of both N924 and N931 infected HeLa2000 and UOK-FLCN (three biological replicates, mean ± s.d, *P<0.05, student's t-test).

To investigate whether the increased survival of gonococci in the presence of FLCN was a consequence of better invasion or impaired intracellular killing, we investigated adherence, invasion and survival by differential immunofluorescence staining and gentamicin protection assay in parallel (Rechner *et al.*, 2007). One set of the infected samples was treated with 1% saponin to quantify the total cell-associated bacteria. The second set was incubated with gentamicin for another 2 h to kill the extracellular bacteria and intracellular survival of bacteria was determined in CFU assays. Adherence was calculated as the total number of bacteria minus the number of intracellular survivors. The third set of samples was fixed with 4% PFA and stained twice with anti-gonococcal antibodies. The first staining was done before permeabilizing the host cell membrane, followed by the staining with secondary antibody coupled to a certain fluorophore. The second staining was carried out after the permeabilization of the membrane and was

followed by the staining with the secondary antibody coupled to a different fluorophore than the one used in the first staining. Hence, invaded bacteria were only labelled with one fluorophore, whereas extracellular bacteria were double labelled (Figure 21). Confocal images were taken, and invasion was quantified by FIJI analysis. These assays were performed with UOK cells. As shown in Figure 20, FLCN did not affect adherence nor invasion, but was critical for the survival of N931. In order to find out whether this effect depends on surface adhesin proteins or not, we used the N924 (Opa-, PorB$_{IB}$, pili-) as a negative control. FLCN did not affect adherence nor invasion, but was critical for the survival of N924, although the survival efficiency was clearly reduced compared to the bacteria expressing Opa-adhesins. Taken together with the data of N931 and N924, we assumed that FLCN played a role in gonococcal survival in UOK cells independently of their surface adhesins.

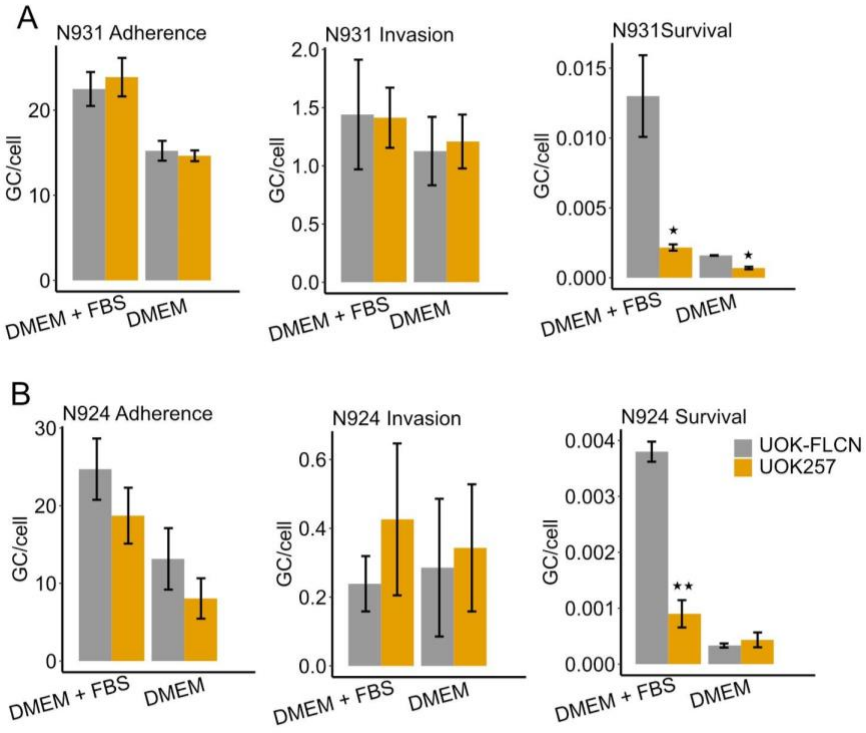

Figure 20: FLCN is essential for *N. gonorrhoeae* survival in UOK257 cells independently of Opa in the presence of FBS

Gentamicin protection assay was used to quantify adhered and surviving GC. Immunofluorescence staining was used to determine invading GC. The extracellular GC was stained twice with the same anti-GC primary antibody and then stained with secondary antibodies coupled to different fluorophores, the intracellular GC was stained only once with the anti-GC antibody and subsequent secondary antibody. At least 70 cells were quantified per sample. N931 (pili-, PorB$_{IB}$, Opa$_{50}$) and N924 (pili-, PorB$_{IB}$, Opa-)

were used for infection (three biological replicates, mean ± s.d, *P<0.05, **P<0.01, Student's t-test). (A) shows the adhered, invaded and surviving N931 in UOK-FLCN and UOK257 cells. (B) shows the adhered, invaded and surviving N924 in UOK-FLCN and UOK257 cells

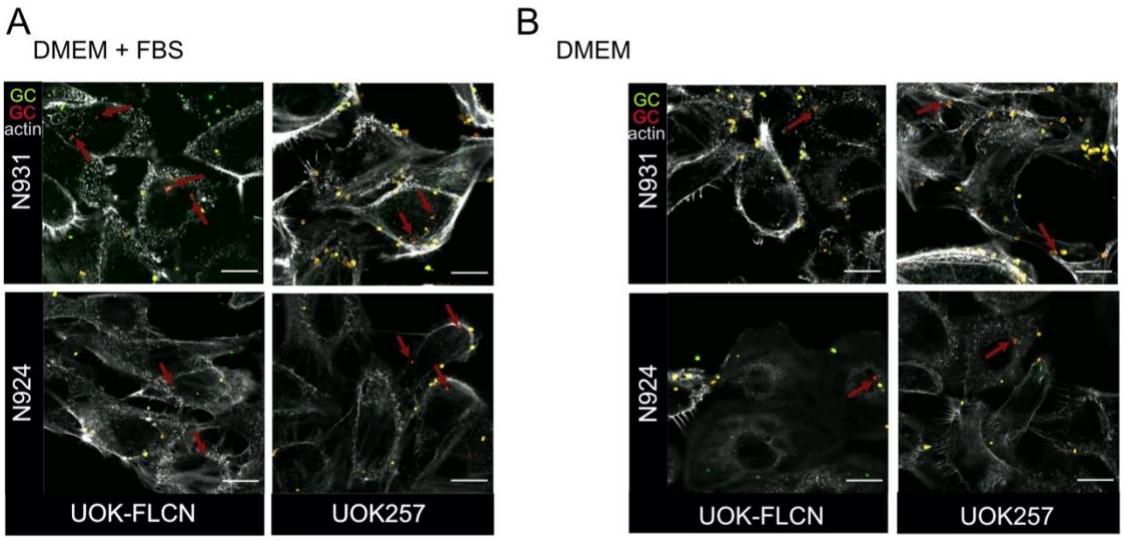

Figure 21 Illustration of employing immunofluorescence staining to determine invading gonococci

The extracellular GC was stained twice with the anti-GC antibody and secondary antibodies coupled to different fluorophores before and after the permeabilization of the cell by 0.1% triton, while the intracellular GC was labelled with only one fluorophore by antibody staining after the permeabilization. The extracellular GC shown here are yellow and intracellular ones are red. F-actin was shown in gray. (A) UOK-FLCN and UOK cells were infected with N931 and N924 respectively in DMEM plus FBS medium. (B) UOK-FLCN and UOK cells were infected with N931 and N924 respectively in the DMEM condition. Scale bars represent 20 μm.

To further test this assumption, UOK-FLCN and UOK257 cells were used to infect with N313 (pili-, $PorB_{IB,}$ Opa_{57}) and N927 (pili-, $PorB_{IA}$, Opa-) in the DMEM and HEPES medium respectively. As shown in Figure 22, FLCN was not essential for either $PorB_{IA}$ or Opa_{57} mediated adherence and survival. Additionally, we revealed that the efficiencies by which cells could kill gonococci were significantly lower in UOK-FLCN than in UOK257 with FBS in the infection medium whereas the killing efficiency was similar in UOK-FLCN and UOK257 in DMEM medium without FBS (Figure 23). hiFBS is prepared by heating to 56 °C for 30 minutes to inactivate complement, a group of proteins present in serum that are part of the immune response. The hiFBS was added to DMEM and gentamicin assay was performed. Different from the result obtained using non-inactivated FBS, FLCN had no effects

on the adherence and survival of N931 (Figure 24) in the presence of hiFBS. Therefore, FLCN favors *N. gonorrhoeae* survival in a FBS dependent fashion, and heat-sensitive factors play a role in this process.

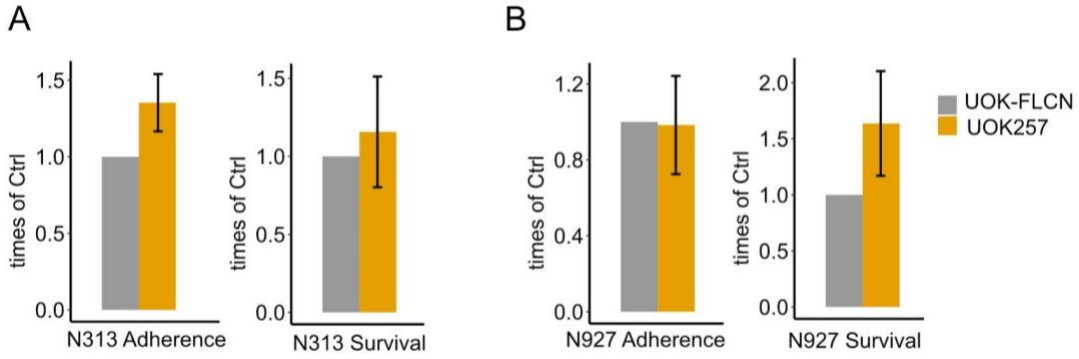

Figure 22: FLCN does not affect Opa_{57} and $PorB_{IA}$ mediated intracellular survival
UOK-FLCN and UOK257 were infected with Opa_{57} N313 in DMEM and $PorB_{IA}$ N927 in HEPES (three biological replicates, mean ± s.d). (A) 1% saponin was used to permeabilize the N313 infected cell to count the total bacteria. 50 μM gentamicin treatment followed by the 1% saponin permeabilization was applied to count the surviving bacteria. Adherence bacteria was determined by total bacteria minus survival bacteria (B) The adherence and survival of N927 in the infected cells as described in (A).

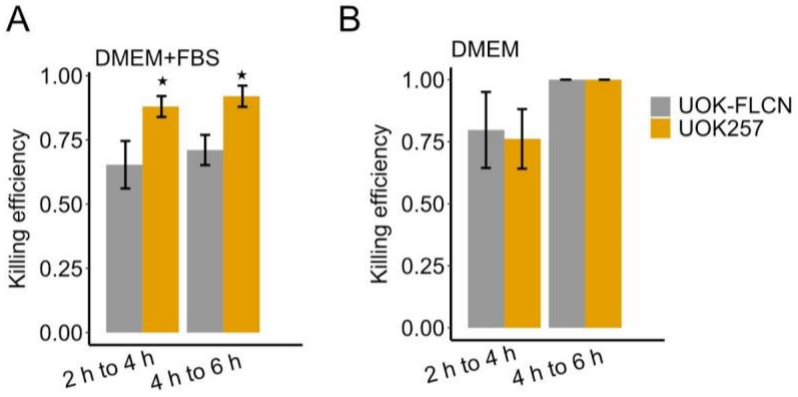

Figure 23: FLCN decreases the bacterial killing efficiency of the cells in the presence of FBS
The UOK257 cells were infected with *N. gonorrhoeae* N931 for 2 h. The total cell-associated bacteria were counted by saponin treatment and dilution plating. Meanwhile 50 μM gentamicin treatment for 2 h, 4 h and 6 h were followed respectively to count the surviving bacteria at each time point post infection. The killing efficiency was defined by (total GC-surviving GC)/total GC (three biological replicates, mean ± s.d, *P<0.05, Student's t-test). (A) the killing efficiency of *N. gonorrhoeae* by UOK cell in DMEM plus FBS condition. (B) the killing efficiency of *N. gonorrhoeae* by UOK cell in DMEM condition.

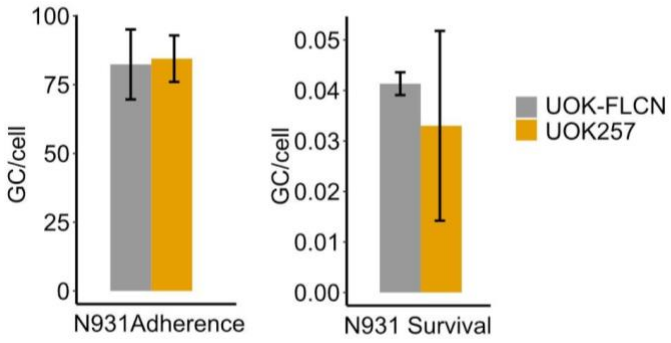

Figure 24: FLCN does not affect *N. gonorrhoeae* survival in the presence of hiFBS
UOK-FLCN and UOK257 were infected with N931 in DMEM with hiFBS for 2 h. 1% saponin was used to permeabilize the N931 infected cell to count the total cell-associated bacteria. 50 μM gentamicin treatment and following 1% saponin permeabilization were applied to count the surviving bacteria (three biological replicates, mean ± s.d). adhered bacteria = total cell-associated bacteria – survival bacteria.

To assess if the cell type played a crucial role for the observed effect, FLCN knockdown cell lines were made in the Hec-1-B, the endometrial adenocarcinoma cell line, as well. Single knockdown clones were isolated by FACS and the knockdown efficiency was tested by western blot shown in Figure 25A. The results of the gentamicin protection assay of Hec-1-B pLVTHM empty vector (control) and FLCN shRNA knockdown cells infected N931 showed that FLCN was essential for gonococcal survival in Hec-1-B cells, which was consistent with the results for HeLa2000 and UOK cells. Therefore, FLCN is essential for *N. gonorrhoeae* survival when FBS is present in the infection medium.

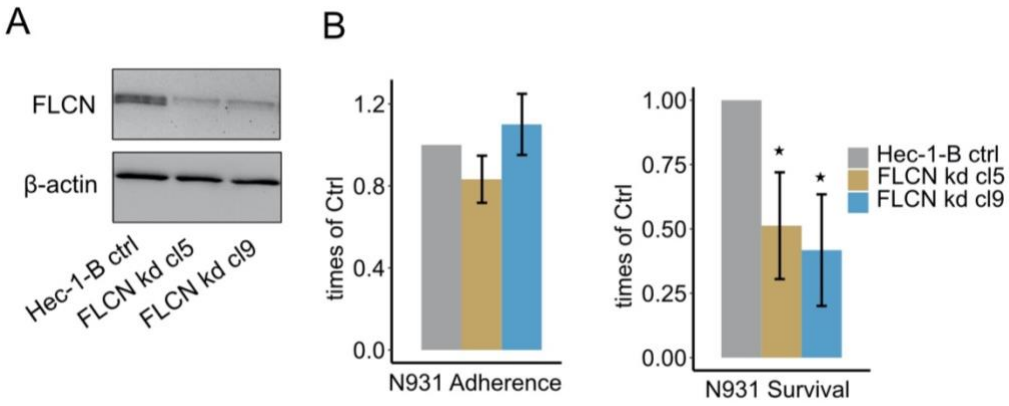

Figure 25: FLCN is essential for *N. gonorrhoeae* survival in Hec-1-B cells
Hec-1-B pLVTHM empty vector (control) and its FLCN shRNA knockdown single clones were infected with N931 for 2 h at the MOI of 50 in DMEM plus FBS medium. (A) FLCN,

of Hec-1-B and its knockdown clones, was detected by Western blotting (B) 1% saponin was used to permeabilize the N931 infected cell to count the total cell-associated bacteria. 50 μM gentamicin treatment and following 1% saponin permeabilization were used to assess the surviving bacteria (three biological replicates, mean ± s.d, *P<0.05, student's t-test). Adhered bacteria = total cell associated bacteria – survival bacteria.

2.2.2 *N. gonorrhoeae* infection does not affect FLCN expression

FLCN is essential for *N. gonorrhoeae* survival in different epithelial cell lines as displayed above. We were curious about whether the infection will affect the expression of FLCN. To this purpose, we infected two cell lines, including Hec-1-B (cell line derived from cervix) and End1 (endocervix cells) for different periods of time. UOK-FLCN is not included since its FLCN expression is under the control of a promoter in the plasmid and this artificial promotor might not be influenced by infection as opposed to the endogenous promotor. Three independent experiments were carried out. From the representative immunoblots, we could see that the protein levels of FLCN did not change during at least 4 h post infection (Figure 26).

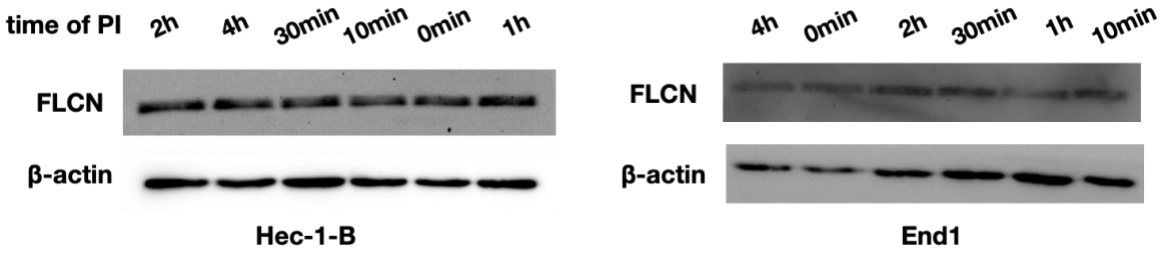

Figure 26: The amount of FLCN does not change upon *N. gonorrhoeae* infection
Cells were infected with N931 at MOI 50 in the DMEM plus FBS condition. Infected cells were harvested at different time points after infection and analyzed by SDS-PAGE and Western blot. (A) Representative Western blot shown changes of FLCN in Hec-1-B upon N931 infection (B) Representative Western blot shown changes of FLCN in End1 upon N931 infection.

2.2.3 FLCN does not affect apoptosis

Infection with various pathogens results in the inhibition or activation of apoptotic cell death. Many bacteria kill immune or epithelial cells by apoptosis allowing them to subvert immune reactions or to invade tissues. Gonococcal infection induces apoptosis in the epithelial cells by activating caspase 3 (Kepp *et al*., 2009). We were interested whether FLCN influences apoptosis upon infection or

not. Here, PARP-1 the substrate of cleaved caspase 3 was used as the indicator of apoptosis. Caspase 3 cleaves PARP-1 into 89 kDa and 24 kDa fragments. Non-infected and infected UOK cells were maintained in three different conditions, which were DMEM, DMEM plus hiFBS and DMEM plus FBS. Two gonococcal strains N931 and N924 were tested. Staurosporine (STS) treated and no infection cells were the positive control and negative control respectively. As shown in the immunoblot (Figure 27), STS induced apoptosis of both UOK-FLCN and UOK257 cells indicated by the 89 kDa PARP-1 fragment. N931 and N924 induced apoptosis in the DMEM infection condition without significant difference between the FLCN positive and negative cells. In the conditions where hiFBS and FBS were present, gonococcal infection barely promotes apoptosis. Hence, the role of FLCN supporting bacterial survival we observed is independent of the regulation of apoptosis.

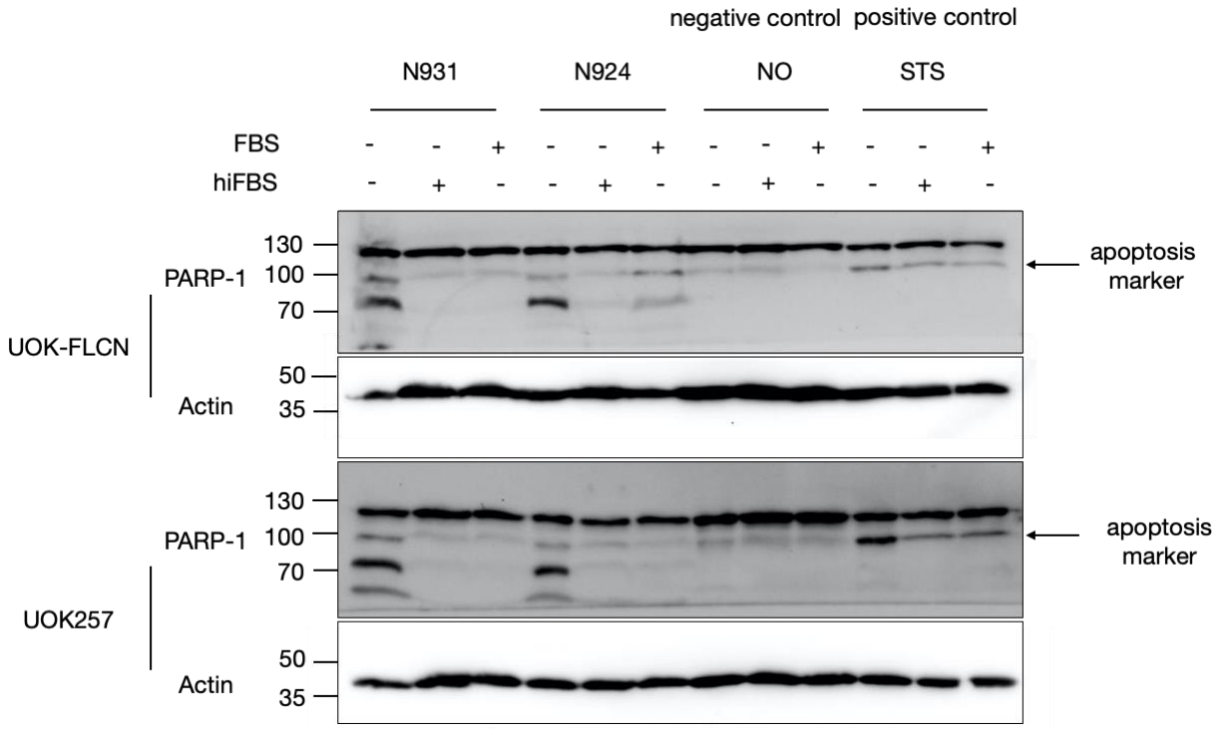

Figure 27: FLCN does not affect apoptosis of UOK cells upon *N. gonorrhoeae* infection

UOK cells were non-treated, STS treated for 24 h, N931 infected for 24 h and N924 infected for 24 h respectively. Meanwhile, those samples were divided into three groups by the infection medium: DMEM, DMEM with hiFBS and DMEM with FBS. Infected cells were collected for Western blot. The upper lane shows the cleavage of PARP-1 of UOK-FLCN cells with different treatments. The lower lane shows the cleavage of PARP-1 of UOK257 cells with different treatments.

2.2.4 FLCN favors gonococcal survival by inhibiting autophagy

2.2.4.1 FLCN inhibits autophagy upon gonococcal infection

As reported previously (Kim *et al*., 2019), *N. gonorrhoeae* modulates the autophagy flux to evade intracellular killing. We therefore wanted to determine whether gonococcal infection induces autophagy in UOK cells or not, using immunoblotting to monitor the level of the autophagosome marker LC3B II. During autophagy the cytosolic LC3B I conjugate to phosphatidylethanolamine to form LC3B II, which is recruited to autophagosomal membranes. LC3B II is degraded by lysosomal enzymes upon fusion of the lysosome with the autophagosome (Yoshii and Mizushima, 2017). Blocking of LC3B II degradation by Bafilomycin A1 (BafA1) gives information about the total amount of LC3B-II. As shown in the Figure 28A, B, FLCN does not affect autophagy of UOK cells. However, FLCN inhibits autophagy upon gonococcal infection. The total amount of LC3B II has increased significantly in the FLCN negative cells (UOK257) upon infection, while that in the FLCN positive cells (UOK-FLCN) did not change. Therefore, we assumed that FLCN inhibits the autophagic flux to support the survival of intracellular gonococci.

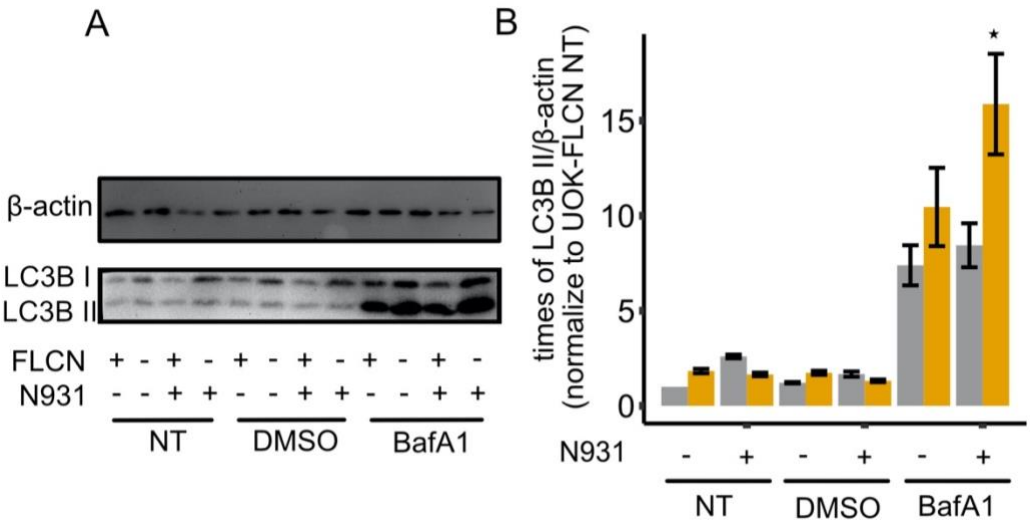

Figure 28: *N. gonorrhoeae* infection induces autophagy and FLCN inhibits the autophagy
(A)Representative immunoblot displaying LC3B I, LC3B II, and β-actin of UOK-FLCN and UOK257 cells. The cells were non-treated, DMSO-treated and 5 nM BafA1-treated for 16 h in the absence or presence of GC N931 infection. (B) Densitometry quantification of LC3 II levels in three independent immunoblots (described in A). Data

represent the mean ± s.d with three independent repeats; significance was determined using student t-test, *P<0.05.

2.2.4.2 BafA1 blockage of autophagy reverses the effects of FLCN in favoring gonococcal survival

In order to test our hypothesis, we carried out gentamicin protection assay using non-treated (NT) cells, solvent DMSO-treated cells, and 5 nM BafA1-treated cells (16 h). The cells were infected with N931 for 2 h in DMEM plus FBS. The adherence and survival of *N. gonorrhoeae* were quantified. As shown in Figure 29, there was no difference between UOK-FLCN and UOK257 in the adherence of *N. gonorrhoeae* in all the three different cell treatments. However, the survival of *N. gonorrhoeae* was increased in the BafA1-treated cells and the FLCN-dependent survival benefit was counteracted (Figure 29). CD46 is crucial for activating autophagy upon gonococcal infection (Kim *et al*., 2019). CD46 has two isoforms for its C-terminal part, CD46-cyt1 and CD46-cyt2. CD46-cyt1 is essential for autophagy activation. We found that the FLCN positive cell (UOK-FLCN) has a lower ratio of CD46-cyt1/cyt2 compared with FLCN negative cell (UOK257). While higher expressions of CD46-cyt1 and CD46-cyt2 were determined in the FLCN positive cell (Figure 30).

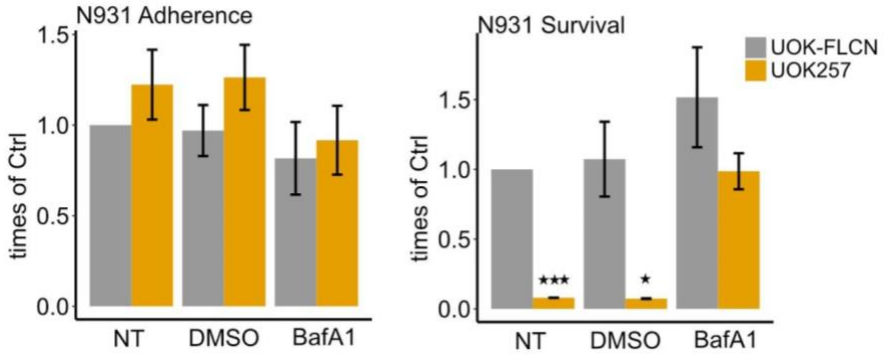

Figure 29: BafA1 treatment reversed the FLCN-favored intracellular *N. gonorrhoeae* survival
The UOK cells were non-treated, solvent DMSO treated or BafA1 treated for 16 h before N931(MOI 50) 2 h infection. 1% saponin was used to permeabilize the infected cell to count the total cell-associated bacteria and the adhered bacteria was determined by total cell-associated bacteria minus survival bacteria as shown in the left panel. 50 μM gentamicin treatment, followed by 1% saponin permeabilization was applied to count the surviving bacteria as shown in the right panel. Data represent the mean ± s.d with three independent repeats; significance was determined using student t-test, *P<0.05 **P<0.001.

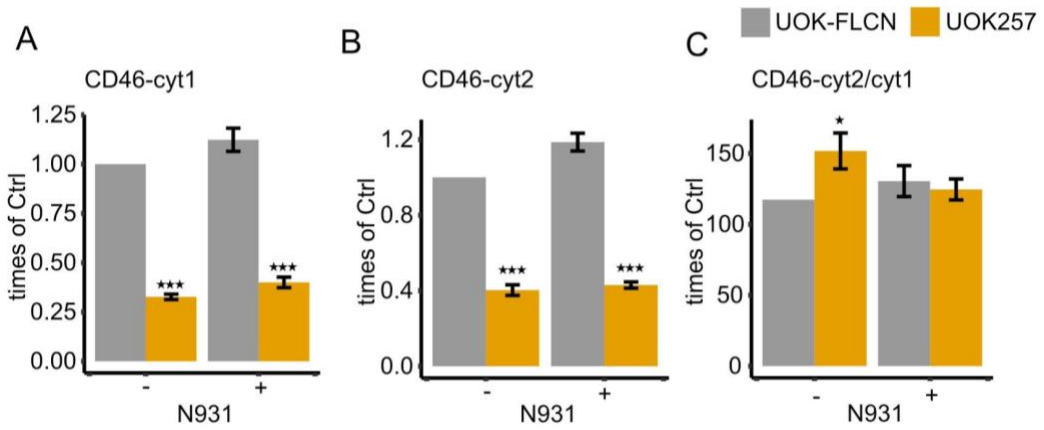

Figure 30: FLCN increases CD46-cyt1, CD46-cyt2 and the ratio of CD46-cyt2/cyt1
UOK-FLCN cells with or without gonococcal infection (MOI 50, 2 h) were harvested for mRNA isolation and qPCR quantification of CD46-cyt1, CD46-cyt2 and CD46-cyt2/CD46-cyt1. GAPDH was used as an internal control. Data represent the mean ± s.d with three independent repeats; significance was determined using student t-test, *P<0.05 **P<0.001.

2.2.4.3 Confocal microscopy shows that the intracellular gonococcal are killed in the lysosome

Autophagy delivers cytoplasmic material, organelles and intracellular pathogens to lysosomes for degradation. LAMP1 (lysosomal associated membrane protein 1) is routinely used as a lysosome marker and LAMP1-positive organelles are often referred to as lysosomal compartments (Cheng *et al*., 2018). To better visualize the intracellular autophagy killing process of *N. gonorrhoeae*, we constructed the LAMP1-YFP UOK257 cell lines and mCherry-*N. gonorrhoeae*. Both N931 and N924 are pili negative and difficult to transform. Hence, MS11 (a wild type stain) was selected for the experiment. As shown in Figure 31A, MS11 and its fluorescence derivative N00130 (MS11-mCherry) have the same Opa phenotype as N931. Furthermore, the gentamicin protection assay revealed that the MS11-mCherry had similar survival defects in the FLCN negative cell line UOK257 (Figure 31B). LMAP1-YFP UOK257 cells were infected with N00130 MOI 5 for 2 h. Fixation and DAPI staining for the nucleus were performed afterwards. We saw that *N. gonorrhoeae* (cyan) were surrounded by the LAMP-1 (magenta), which revealed the bacteria had been delivered to the lysosome (Figure 31C). The fluorescence signal strength of the bacteria inside of the lysosome was weaker than the one of the free bacteria, which indicated that bacteria were dying in the lysosome. *N. gonorrhoeae* developed strategies to

modify lysosome. LAMP-1 has been shown to be recruited to the infection site and cleaved by IgA of *N. gonorrhoeae* (Lin *et al*., 1997). Meanwhile, FLCN was

reported to regulate the peri-nuclear localization of LAMP1 upon serum and amino acid deprivation (Starling *et al*., 2016). We were interested in whether FLCN participated in regulating LAMP-1 distribution upon gonococcal infection or not. We saw FLCN change LAMP-1 distribution from cytosol to peri-nuclear zone upon infection (Figure 32). However, the differences between FLCN positive and negative cells in terms of LAMP-1 distribution have to be confirmed in the future.

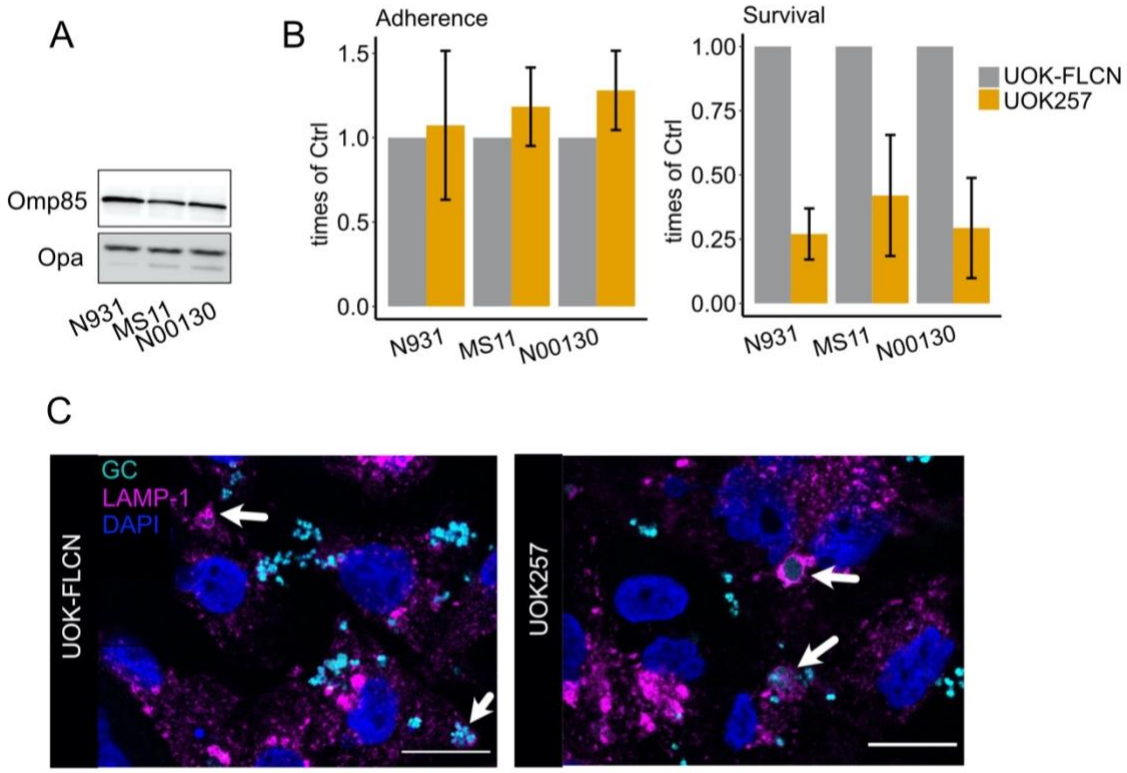

Figure 31: Intracellular *N. gonorrhoeae* was killed in the lysosome
N. gonorrhoeae MS11 was transformed with plasmid PLAS:pilEmCherry. The mCherry positive colonies were selected by Spectinomycin. The UOK cells were transduced with LAMP-1-YFP lentivirus to produce the constantly LAMP-YFP expressing cells. (A) Western blot detecting Omp85 and Opa of different *N. gonorrhoeae* derivatives, including positive control N931, wild type MS11 and the fluorescence derivative N00130 (MS11-mCherry). (B) Gentamicin protection assay of UOK cells infected with N931, MS11 and MS11-mCherry derivatives. Adherence and survival of *N. gonorrhoeae* were quantified. Data represent the mean ± s.d with three technical repeats (C) The confocal images of UOK-LAMP-YPF cells infected with MS11-mCherry gonococci.

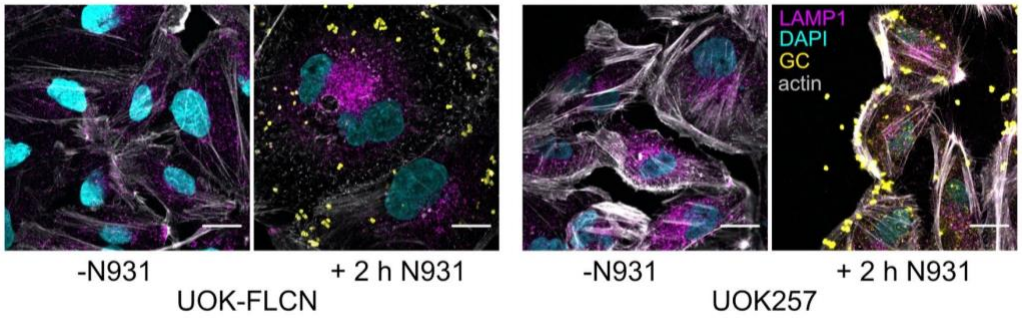

Figure 32: FLCN regulates peri-nucleus localization of LAMP-1 upon infection
The UOK cells were maintained in DMEM plus FBS condition. Cells were either not infected or infected with N931 gonococci for 2 h. Subsequently, immunofluorescence staining was performed. LAMP-1 is shown in magenta, *N. gonorrhoeae* in yellow, nucleus in cyan and F-actin in gray. Scale bars represent 20 µm.

2.2.5 FLCN interferes with E-cadherin

2.2.5.1 FLCN interferes with E-cadherin both at transcriptional and translational levels

Autophagy influences cell polarization probably by the control of cell junction protein expression (Nighot and Ma, 2016). In this study, we found that FLCN inhibited both the transcription and translation of E-cadherin in UOK cells (Figure 33A, B). To rule out the possibility that this was a cell-type specific phenomenon, we tested single clones of Hec-1-B FLCN knockdown cells (Figure 25A) for E-cadherin expression. E-cadherin expression was hardly detectable in control knockdown cells but detectable in Hec-1-B FLCN knockdown cells (Figure 33C), supporting a role of FLCN in suppressing E-cadherin expression. Different from the adherence junction protein E-cadherin, the tight junction protein ZO-1 was not influenced by the presence or absence of FLCN in UOK cells (Figure 33D, 35), indicating that FLCN influenced selectively adherence junctions.

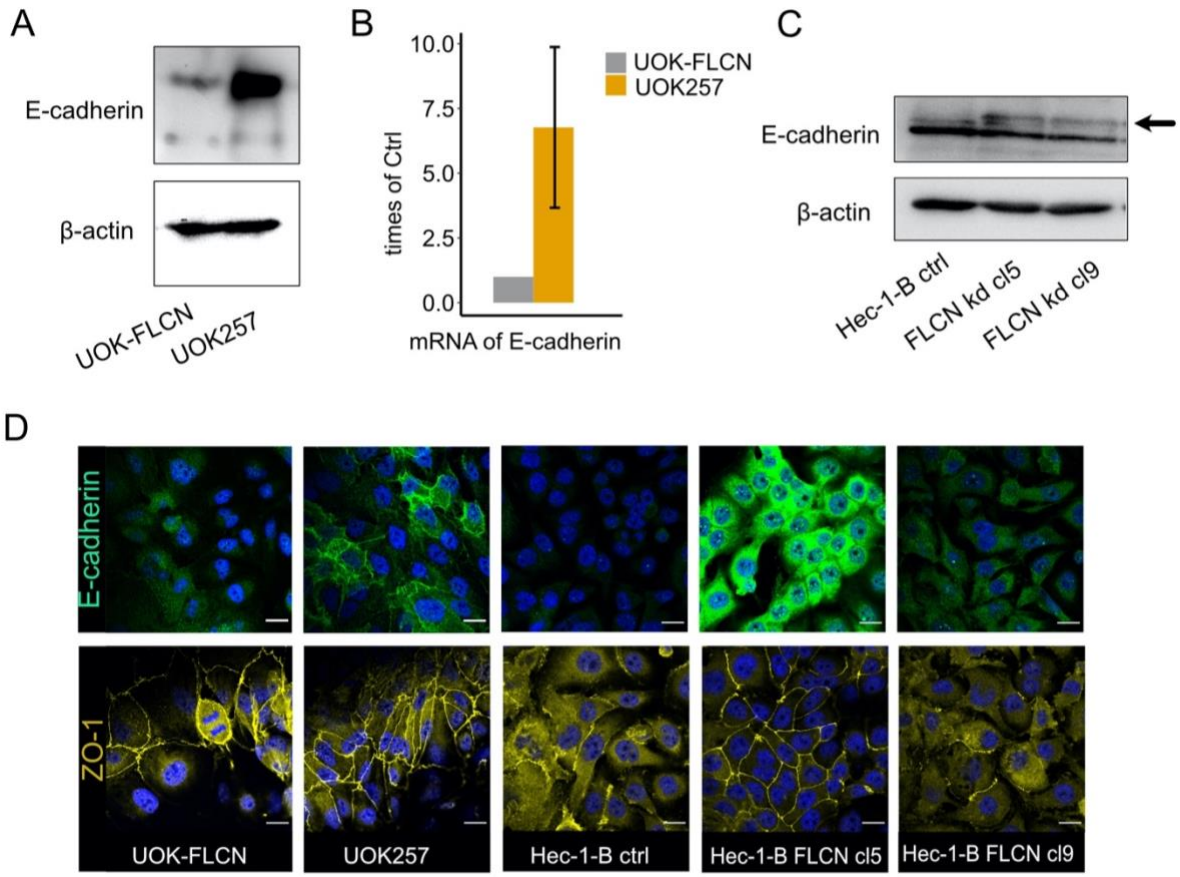

Figure 33: FLCN negatively regulates E-cadherin in 2D cell culture
(A) qPCR of E-cad in UOK-FLCN and UOK257 cells. GAPDH was used as an internal control. (B) Western blot detecting E-cadherin of UOK-FLCN and UOK257 cells. Data represent the mean ± s.d with three independent repeats. (C) Western blot detecting E-cadherin of the control and FLCN knockdown cells of Hec-1-B. (D) Immunofluorescence staining of E-cadherin in UOK-FLCN, UOK257 and the control and FLCN knockdown cells of Hec-1-B. E-cadherin shown in green, nucleus in blue, scale bars represent 20 µm.

2.2.5.2 E-cadherin shortly increases upon gonococcal infection

E-cadherin has been shown to be important for bacterial infection as cellular receptor for infection (Rubinstein et al., 2013; Ortega et al., 2017). We were interested to know whether the gonococcal infection will affect the E-cadherin. We infected the UOK257 cells, the E-cadherin positive cells, with N931 for 0 h, 0.2 h, 0.5 h, 2 h and 4 h. Samples were collected for mRNA isolation followed by qPCR analysis and immunoblot. As shown in Figure 34A and B, *N. gonorrhoeae* infection increases E-cadherin both at mRNA and protein levels at the early stage of infection (< 2 h). The level of E-cadherin decreases to more or less the level comparable to the non-infected samples at 4 h post infection.

Overexpression of FLCN in the UOK257 cell was carried out to further test the effect of FLCN on E-cadherin. However, there was no significant difference between the UOK257 empty vector cells and UOK257-FLCN-overexpression cells (Figure 34C).

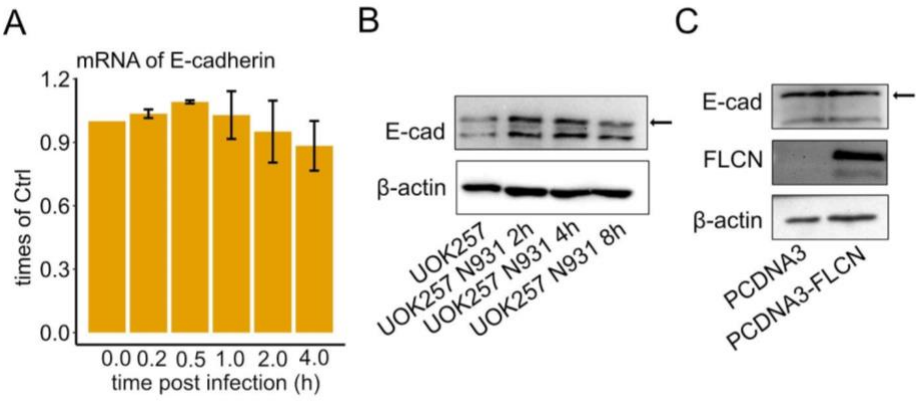

Figure 34: E-cadherin expression increased shortly upon *N. gonorrhoeae* infection
The UOK257 cells were infected with N931 for 10 min, 30 min, 1 h, 2 h and 4 h. Samples were collected for mRNA isolation to determine the E-cadherin transcription level by qPCR. Data represent the mean ± SEM with three technical repeats (A) and Western blot to detect the translation level of E-cadherin (B). UOK257 cells were transfected with empty vector pCDNA3 and FLCN overexpression vector pCDNA3-FLCN. Samples were collected to check the E-cadherin translational levels in different conditions by Western blot.

2.2.5.3 E-cadherin increases autophagy and inhibits gonococcal survival

To elucidate the role of E-cadherin in gonococcal infection, we constructed an E-cadherin knockdown cell line in UOK257. E-cadherin has a long half-life. The knockdown cells were kept in culture for 10 passages after FACS sorting. The successful knockdown was shown by both Western blot and immunofluorescence staining (Figure 35A, B). To check whether E-cadherin had a role in autophagy flux regulation, we determined the LC3-II levels in both non-treated and BafA1-treated cells. Three independent experiments revealed that autophagy was increased in the presence of E-cadherin (Figure 35C, D). In addition, gentamicin protection assay was used to determine the adherence and survival of gonococci in control and E-cadherin knockdown cells. E-cadherin did not affect the adherence but decreased the survival rate of gonococci (Figure 35E). To further investigate if the bacterial survival defect in E-cadherin positive cells was mediated by autophagy, we compared the survival of gonococci in mock-treated and BafA1-treated cells. The inhibition of autophagy counteracted

the survival defects in the E-cadherin control cell line (Figure 35E). Therefore, E-cadherin inhibits gonococcal survival by increasing autophagy.

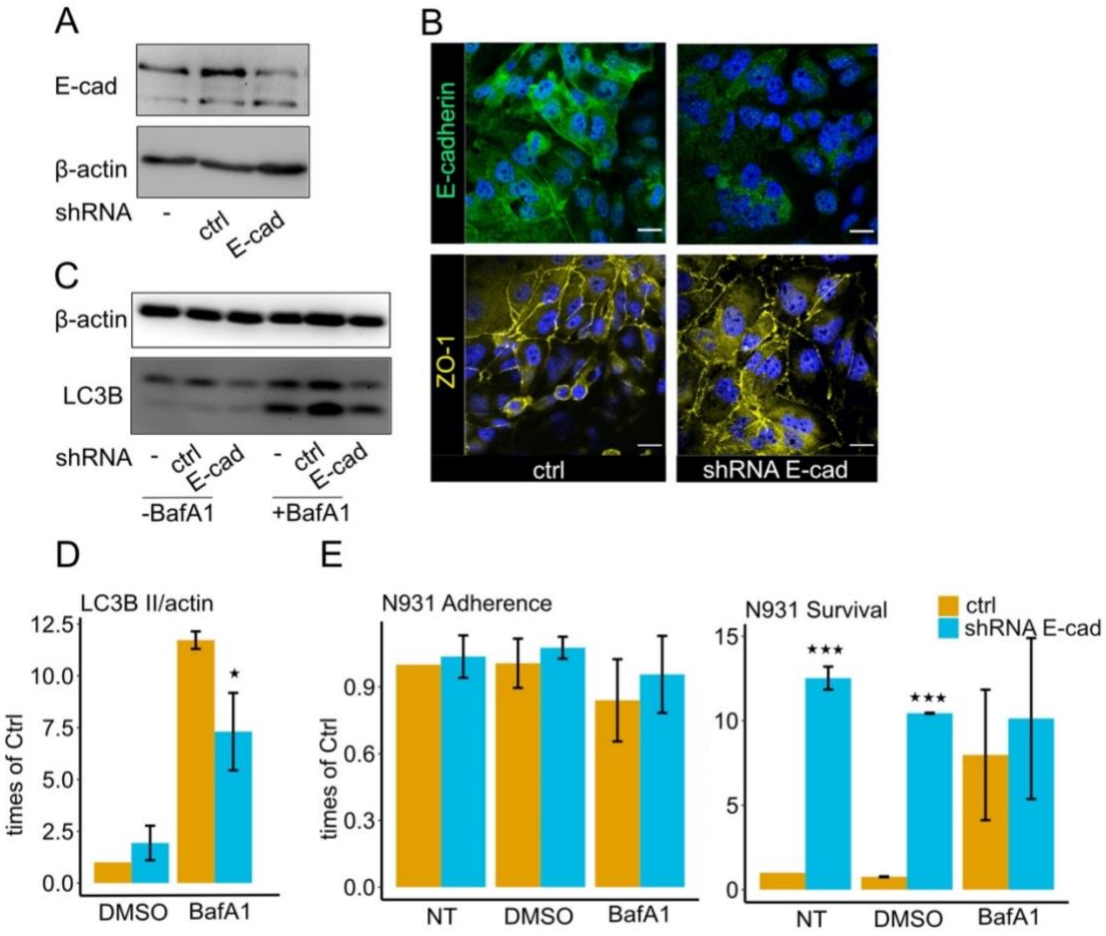

Figure 35: E-cadherin knockdown in UOK257 cell increases GC survival in 2D cell culture

(A) Western blot detecting E-cadherin in non-treated, control shRNA and E-cadherin shRNA-transfected UOK257 cells. (B) Immunofluorescence staining of E-cadherin and ZO-1 in the control and E-cadherin knockdown cells of UOK257. E-cadherin in green, ZO-1 in yellow and nucleus in blue, scale bars represent 20 μm. (C) Representative immunoblot displaying LC3B I, LC3B II, and β-actin in the control and E-cadherin knockdown of UOK257 cells. The cells were either treated with solvent DMSO or 5nM BafA1 for 16 h. (D) Densitometry quantification of LC3 II levels in three independent immunoblots (described in C). LC3B II in each lane were normalized to the β-actin. The normalized values were expressed to that of the non-treated UOK257 sample. Data represent the mean ± s.d with three independent repeats; significance was determined using student t-test, *P<0.05. (E) Adherent (left) and surviving (right) GC from samples of non-treated and 5 nM BafA1-treated cells for 16 h of UOK257-ctrl and UOK257-Ecad-shRNA. The cells were infected with N931 (MOI 50) for 2 h. Data represent the mean ±

s.d with three independent repeats; significance was determined using student t-test, **P<0.001.

2.2.6 FLCN delays *N. gonorrhoeae* transmigration in 3D

2.2.6.1 FLCN interferes with E-cadherin membrane association in 3D

To reach deeper tissues, gonococci have to overcome the epithelial barrier during infection, of which the cell-cell communication and cell polarization are critical markers (Wang *et al*., 2017, Heydarian *et al*., 2019). Therefore, we seeded the UOK cells on the transwell membrane to induce cell polarization. Similar to the results of 2D cell culture, the FLCN did not affect the ZO-1 polarization, but it decreased the amount of E-cadherin and no membrane association of E-cadherin was found in UOK-FLCN (Figure 36).

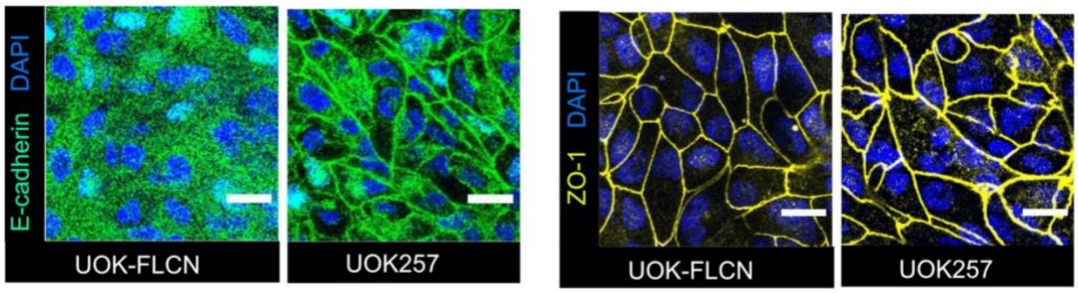

Figure 36: FLCN inhibits E-cadherin membrane association in the 3D cell culture Confocal microscopy of transwell models of UOK-FLCN and UOK257. The models were cultured for 10 days and then fixed and decorated with E-cadherin (green) or ZO-1 (yellow) antibodies and DAPI (blue). Z-stacks were made and reconstructed using FIJI. Shown are Z-projections (XY, 3 stacks). Scale bars represent 20 µm.

2.2.6.2 FLCN delays gonococcal transmigration

E-cadherin is critical for bacterial transmigration. To determine whether FLCN affects gonococcal transmigration, we infected the transwell samples with N931 from the apical side. Both colony collection from the bottom of the transwell and immunofluorescence staining were used to monitor the transmigration. As shown in Figure 37A, gonococcal infection did not affect the barrier integrity until 4 days post infection in the DMEM plus FBS medium by FITC assay. The delayed transmigration of N931 through UOK-FLCN was supported by the data from dilution plating of the bacteria collected from the bottom of the transwell, which showed a 7-fold higher transmigration in FLCN-negative cells at 48 h post infection (Figure 37B). In line with the colony plating assay, the confocal

microscopy showed a similar trend of transmigration. *N. gonorrhoeae* remained at the top of the cells 24 h after infection. Bacteria transmigrated to the basal side of the epithelial layer after 96 h of infection in the UOK257 but not in the UOK-FLCN as seen by orthogonal and Z-projections of the Z-stacks of images (Figure 37C).

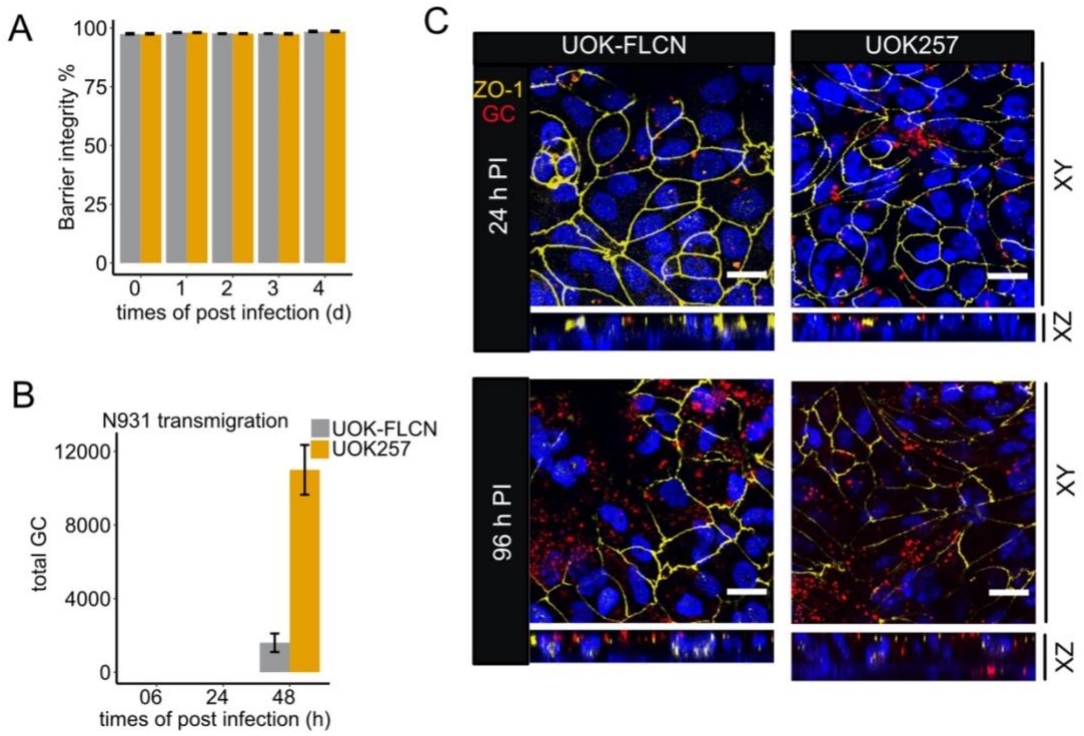

Figure 37: FLCN delays *N. gonorrhoeae* transmigration in the 3D cell culture
The transwell 3D cell culture was infected with N931 (MOI 50) in the DMEM plus FBS condition. (A) Barrier integrity of N931-infected UOK-FLCN and UOK257 models was measured by 4 kDa FITC-dextran assay. Shown are mean ± s.d from three biological replicates. (B)Transmigration of N931 in the UOK-FLCN and UOK257 transwell models. Shown are the colonies collected from the bottom of the transwells. Three biological replicates were performed. (C) Confocal microscopy of N931-infected transwell models at different time points. Shown are Z-projections (XY) and orthogonal view (XZ). Scale bars represent 20 µm.

2.2.6.3 E-cadherin decreases gonococcal transmigration

We next tested if the delayed transmigration in the UOK-FLCN cell was due to the defect in E-cadherin membrane polarization. We therefore seeded control and E-cadherin UOK knockdown cells on transwell membranes (Figure 38A). The transwell samples were infected with N931 at MOI 50 for 96 h. As shown in

Figure 38B, the majority of the gonococci were on the apical side of the cells 24 h pi and more of them transmigrated with the progression of time until 96 h pi. Infection did not affect the barrier integrity (Figure 38C). However, transmigration was strongly increased upon E-cadherin knockdown in the absence of FLCN expression (Figure 38D). Therefore, FLCN delays the gonococcal transmigration independently of E-cadherin. Except E-cadherin, EGFR is essential for *N. gonorrhoeae* transmigration (Edwards *et al.*, 2013). We showed that EGFR was polarized at the basolateral side of the cells and partially translocated to the apical side upon infection (Figure 39). It will be interesting to quantify the difference in terms of EGFR localization between FLCN positive and negative cells in the future.

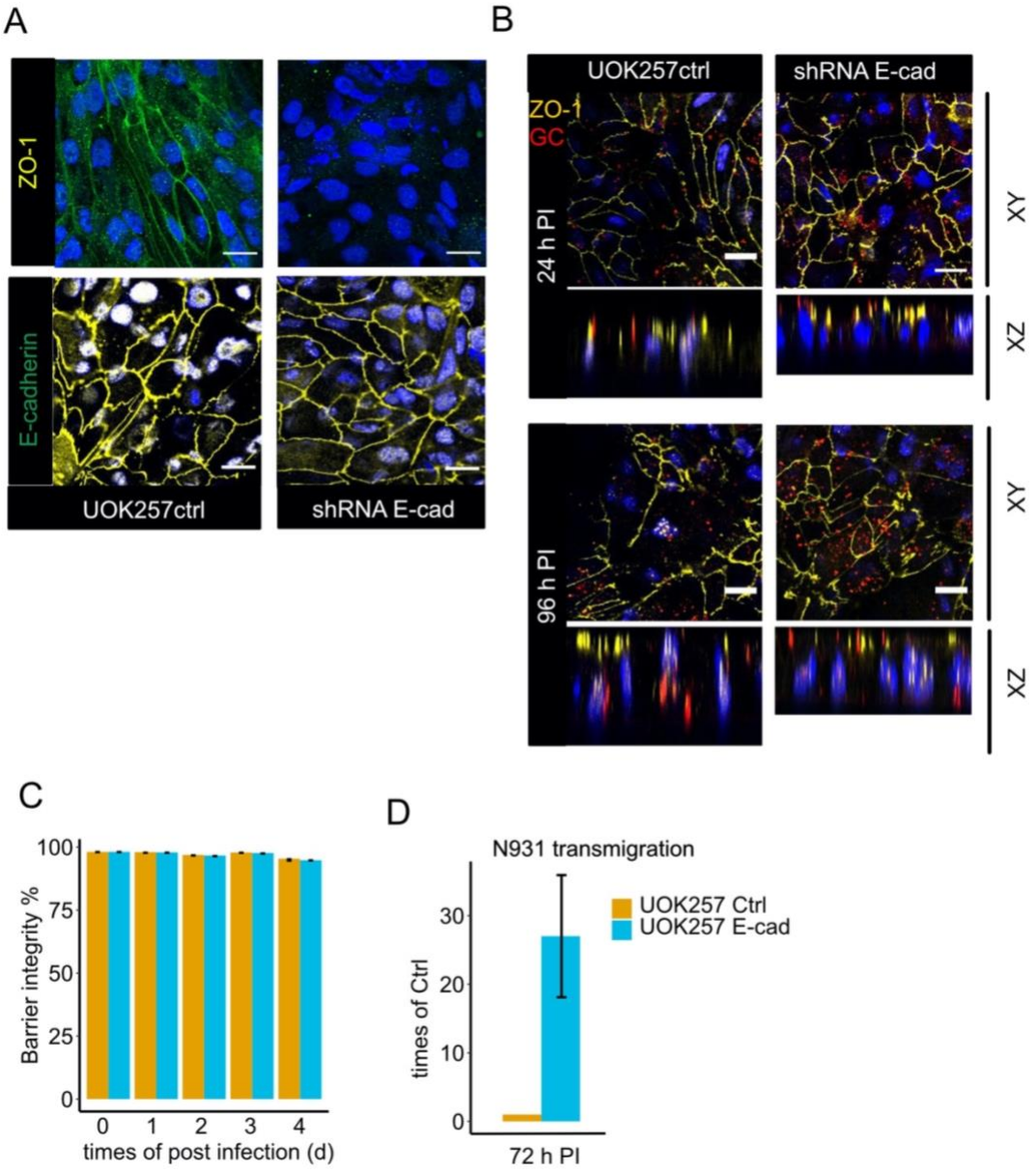

Figure 38: E-cadherin interferes with *N. gonorrhoeae* transmigration
UOK257 shRNA Ctrl and UOK257 E-cadherin knockdown cells were infected with N931 (MOI 50) in the DMEM plus FBS condition. (A) Confocal microscopy of the transwell models of the control and E-cadherin knockdown UOK257. The samples were stained with ZO-1 (yellow) or E-cadherin (green) and DAPI (blue). Z-stack was made and reconstructed with FIJI. Shown were XY projections. Scale bars represent 20 µm. (B) Confocal microscopy of N931-infected transwell models at different time points. Shown are Z-projections (XY) and orthogonal view (XZ). Scale bars represent 20 µm. (C) Barrier integrity of N931-infected UOK257 shRNA Ctrl and UOK257 E-cadherin knockdown models was measured by 4 kDa FITC-dextran assay. Shown are mean ± s.d from three biological replicates. (D) Transmigration of N931 in the UOK257 shRNA Ctrl and UOK257 E-cadherin knockdown models after 3 d infection. Shown are mean ± s.d from three biological replicates.

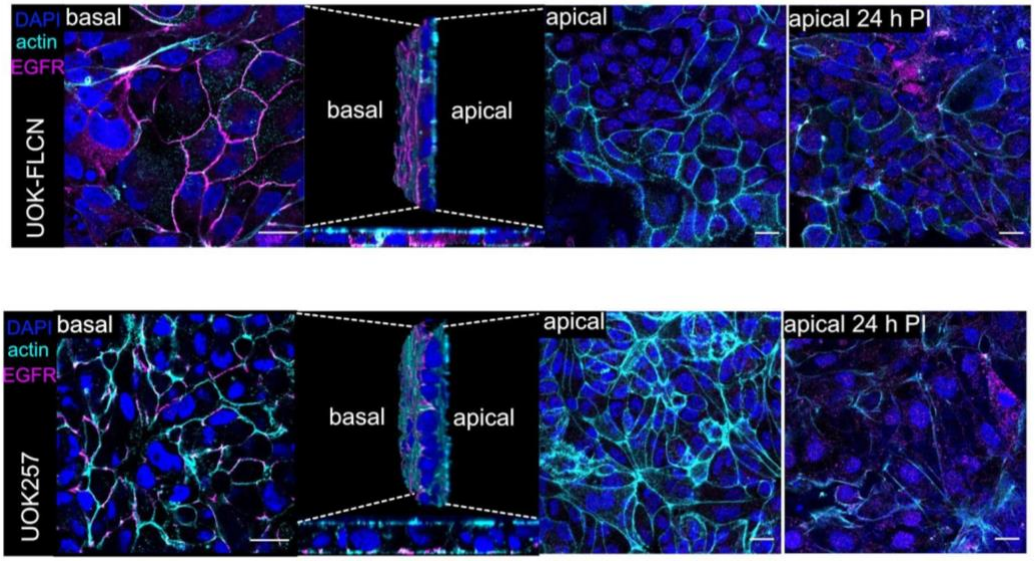

Figure 39: EGFR localizes at the basolateral side of the polarized cells and partially translocates to the apical side upon infection.
The mature UOK-FLCN and UOK257 3D models were wither not infected or N931-infected for 24 h. The samples were fixed and decorated with anti-EGFR antibodies (magenta), phalloidin (F-actin, cyan) and DAPI (blue). Z-stack was made and reconstructed with FIJI. Shown are Z-projections and orthogonal views. Scale bars represent 20 µm.

2.2.6.4 *N. gonorrhoeae* maintains the Opa phenotype during transmigration

N. gonorrhoeae constantly change their surface structures via phase and antigenic variation during the pathogenesis process. It has been reported that expression of Opa proteins interferes with the transmigration of *N. gonorrhoeae* across polarized epithelial cells (Stein *et al*., 2015). *N. gonorrhoeae* might switch off the Opa expression upon infection to accelerate the transmigration (Heydarian *et al*., 2019). Therefore, we collected the adhered, surviving and transmigrated *N. gonorrhoeae* N931 to check their Opa expression by Western blot. As shown in Figure 40, N931 kept its Opa expression upon infection of the UOK-FLCN, UOK257, UOK257 pLVTHM (control), and UOK257 E-cadherin knockdown models. The improved transmigration either by loss of FLCN or by loss of E-cadherin is not related to the Opa expression.

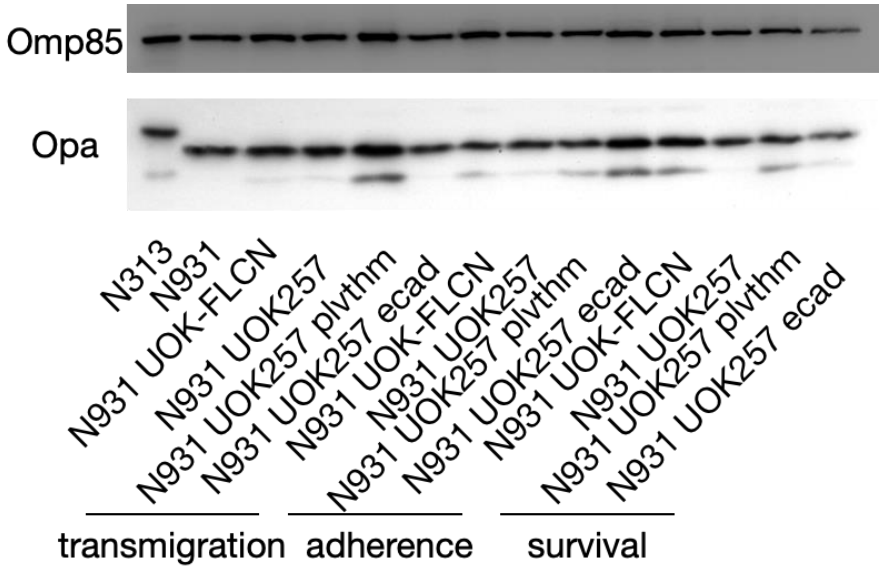

Figure 40: Opa genotype did not change before and after the transmigration
The UOK-FLCN and UOK257 models were infected with N931 in the DMEM plus FBS conditions. The adhering, surviving and transmigrated *N. gonorrhoeae* were collected and plated on GC agar plates. The colonies were lysed and analyzed by SDS-PAGE and Western blot using anti-Opa and anti-Omp85 antibodies.

2.2.6.5 Gonococcal infection does not decrease barrier integrity in the presence of FBS

It is interesting to observe the phenomenon that *N. gonorrhoeae* infection did not break the barrier integrity even 4 d post infection. This is different the previous studies based on other types of epithelial cells (Heydarian et al. 2019). Therefore, we tested the role of FBS in maintaining the barrier function upon bacterial infection. The mature models of UOK257 shRNA control and UOK257 E-cadherin knockdown were kept in the DMEM, DMEM plus hiFBS and DMEM plus FBS 24 h before infection. The models were infected with N931 at MOI 50. FITC dextran assays were performed to check the barrier integrity at 6 h, 1 d, 2 d, 3 d and 4 d post infection. Medium was changed at those time points to remove the non-attached bacteria and to provide cells with enough nutrients. As shown in Figure 41, the barrier integrity of infected models in the DMEM started dropping at day 1 post infection and reached around 50% integrity at day 2 and day 3 post infection. However, the models maintained in both DMEM plus hiFBS and DMEM plus FBS conditions showed that barrier integrity barely changed upon infection by day 4 post infection. Those data indicate that both FBS and

hiFBS play an important role in maintaining the UOK cell barrier integrity upon bacterial infection.

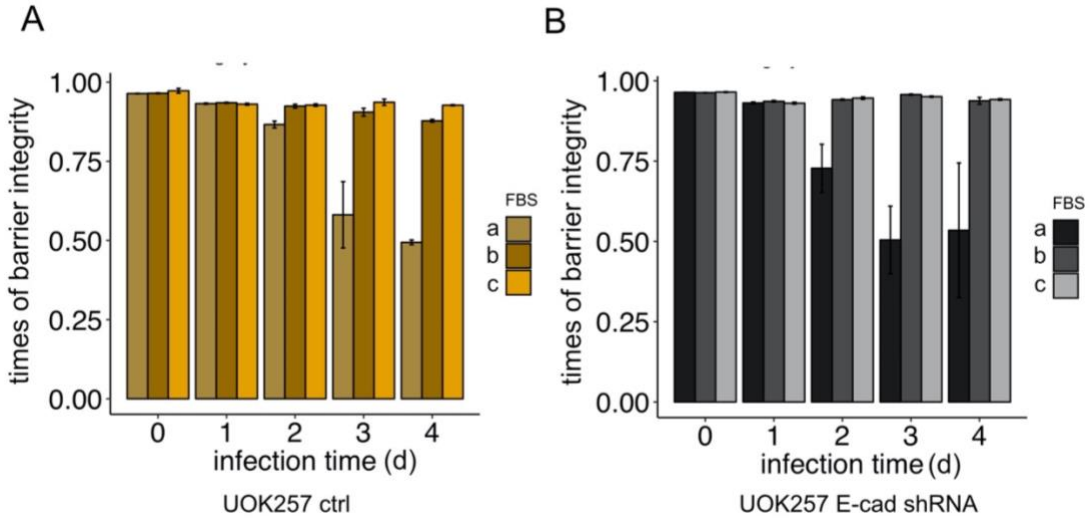

Figure 41: FBS maintains the UOK cell barrier integrity upon *N. gonorrhoeae* infection

UOK257 Ctrl models were kept in the medium of DMEM (a), DMEM plus hiFBS(b) and DMEM plus FBS (c) respectively before infection with N931 of MOI50. (A) Barrier integrity was measured by 4 kDa FITC-dextran assay at different time points after infection. Shown are mean ± s.d from three biological replicates. (B) The barrier integrity of UOK257 E-cadherin knockdown models upon *N. gonorrhoeae* infection. Shown are mean ± s.d from three biological replicates.

2.2.7 FLCN is essential for gonococcal survival in 3D

2.2.7.1 Optimization of gentamicin treatment for survival assay

N. gonorrhoeae reaches the deeper tissue either by paracellular transmigration or by transcellular transcytosis. Therefore, it is critical to check the function of FLCN in gonococcal survival in the 3D models. The infection was performed from the apical side of the cells. As shown above, the bacterial infection did not break the barrier function in the presence of FBS. Therefore, we want to test how fast gentamicin could difuse from the basal compartment of transwell across the transwell membrane to kill the extracellular bacteria associated with the basal part of the cells. Four groups of treatment were designed to estimate the time (Figure 42A). The first group was of 500 µl *N. gonorrhoeae* suspension (10_6 GC) (a), the second group was of *N. gonorrhoeae* suspension with 50 µM gentamicin (b), the third group was of 500 µl *N. gonorrhoeae* suspension loaded from the apical side of the transwell membrane and 1000 µl medium at the bottom (c1 and

c2), the fourth group was the same as group 3 except with a 50 μM gentamicin in the medium at the bottom (d1 and d2). The amounts of bacteria from each group and both from the apical and basal side of the membrane were quantified by serial dilution plating and colony counting. As shown in Figure 42B, gonococci reached a balanced distribution between the upper and bottom parts of the membrane after 2 h incubation displayed by c1 and c2. Meanwhile, gentamicin diffused from d2 into d1 as the survival bacteria of d2 was significantly lower than of c2 after 2 h incubation. The less concentrated gentamicin took 4 h to kill the bacteria as shown by d1 and d2 of 4 h. Thus, the 4 h gentamicin incubation was sufficient to kill the extracellular bacteria and this time was used for determining the number of the intracellular surviving bacteria in the infection models.

2.2.7.2 FLCN is essential for gonococcal survival in 3D

To check whether the FLCN was critical for gonococcal survival, we infected the transwell samples with N931 at MOI 50 for 48 h. The culture medium was changed at 6 h and 24 h post infection to remove the unattached bacteria and replace the used medium. After infection, one set of the samples was intensively washed with the infection medium and 1% saponin was added to break the cell membrane. Dilution plating was done to count the total cell-associated bacteria. The other set of cell samples were further treated with 50 μM gentamicin at both apical and basal sides for 4 h to kill the extracellular bacteria. Dilution plating was performed afterward to count the survivors. These experiments demonstrated that FLCN increases gonococcal survival in this 3D culture (Figure 42C). In addition, a gentamicin protection assay was performed to check the role of E-cadherin on adherence and survival *N. gonorrhoeae*. As shown in Figure 42D, the E-cadherin was critical for *N. gonorrhoeae* adherence (left) but was not important for survival (right).

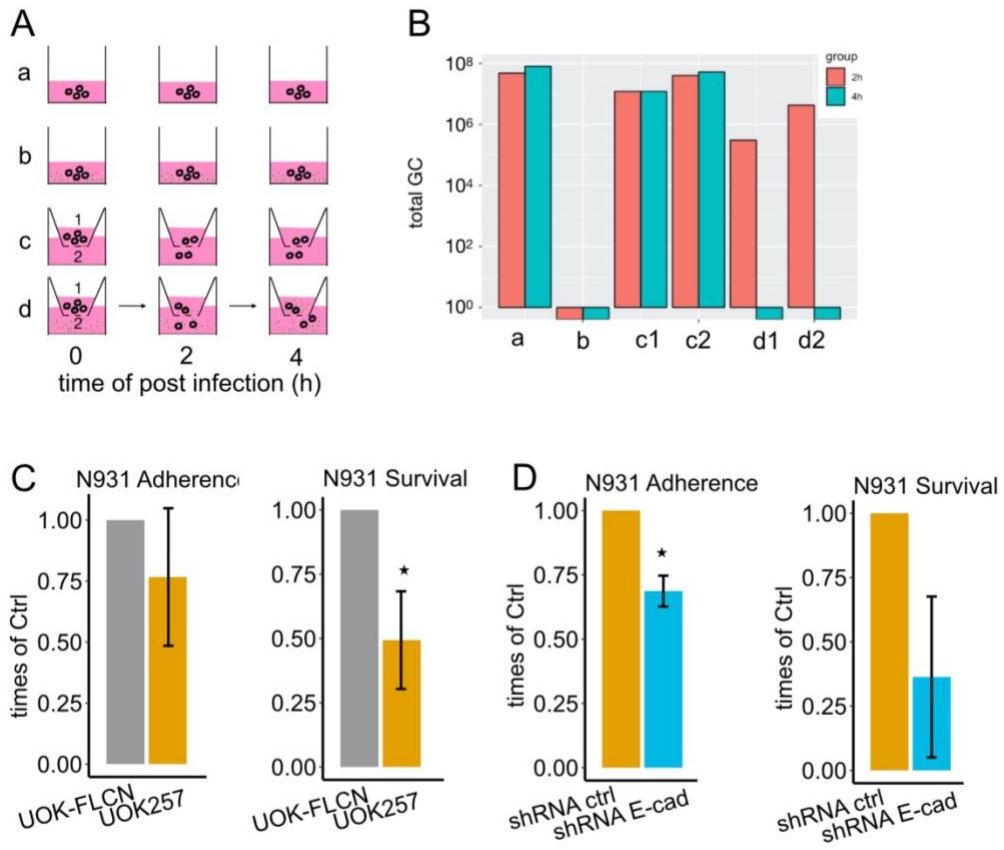

Figure 42: FLCN is essential for *N. gonorrhoeae* survival in the 3D models
Gentamicin protection assay was used to define the adherence and survival gonococci of the 3D models. The gentamicin treatment time was optimized as shown by (A) the scheme of the experiment and survival of *N. gonorrhoeae* with different gentamicin incubation time. (C) The adherence and survival of *N. gonorrhoeae* of the UOK-FLCN and UOK257 models. Shown are mean ± s.d from three biological replicates. (D) The adherence and survival of *N. gonorrhoeae* in the UOK257 Ctrl shRNA and UOK257 E-cadherin knockdown models. Shown are mean ± s.d from three biological replicates.

2.2.7.3 FLCN does not affect autophagy in 3D

FLCN is critical for *N. gonorrhoeae* survival in the 2D cell culture by interfering with autophagy. We were interested in the molecular bases of how FLCN affects *N. gonorrhoeae* in the 3D models. Therefore, the mature models were treated with BafA1 for 16 h to block the degradation of LC3B II before harvesting for Western blot. As shown in Figure 43, there was no significant difference among FLCN positive and negative, E-cadherin positive and negative models.

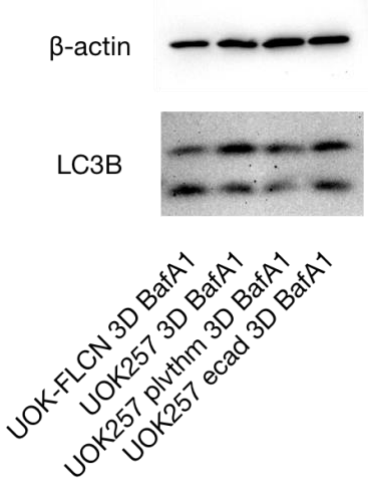

Figure 43: FLCN did not affect autophagy in the 3D models of polarized cells
The 3D models were incubated with BafA1 for 16 h before sample collection. The samples were analyzed by SDS-PAGE and Western blot to detect LC3B.

2.2.7.4 FLCN is polarize to the apical side and gonococcal infection increases FLCN

In addition, we checked the localization and expression of the FLCN in the 3D models. Considering the fact that UOK-FLCN is a FLCN complemented cell line, we used the FLCN wild type cell line Hec-1-B. The Hec-1-B cells were seeded together with supportive fibroblasts on the top of small intestinal submucosa (SIS) scaffold. The mature models were paraffin embedded and sectioned at the XZ direction. Immunofluorescence staining showed that FLCN accumulates at the apical side (Figure 44A). Furthermore, the whole non-infected and infected transwell models were fixed and stained with anti-FLCN and anti-*N. gonorrhoeae* antibodies. As shown in the Figure 44B, FLCN was more or less equally distributed in Hec-1-B without infection. FLCN tended to aggregate at the site of gonococci upon infection and its amount was increased as well.

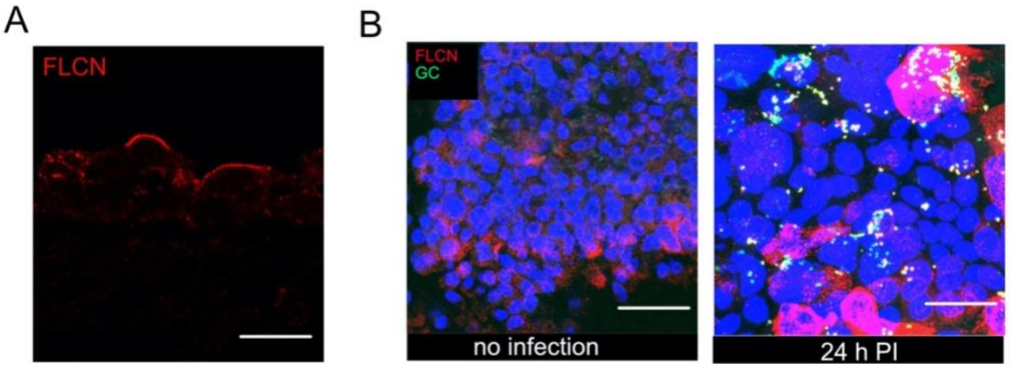

Figure 44: FLCN increased upon *N. gonorrhoeae* infection in the 3D models
The UOK-FLCN model was paraffin embedded and sectioned for immunofluorescence staining of FLCN (red) as shown by (A). The UOK-FLCN models were infected with N931 for 24 h and fixed and stained with anti-FLCN (magenta) and anti-gonococci antibodies (yellow) as shown by (B). Scale bars represent 20 μm.

3. Discussion

Neisseria gonorrhoeae, the host-adapted human pathogen, is the causative agent of gonorrhea. The continued worldwide incidence of gonorrheal infection, coupled with the rising resistance to multiple antibiotics, highlights the need to better understand the molecular basis of *N. gonorrhoeae* infection. *Neisseria gonorrhoeae* starts infection by colonizing the cell surface, followed by invasion of the host cell, intracellular persistence, transcytosis and exit into the subepithelial space. A large number of studies have well established the host-pathogen interactions in the initial adherence and invasion steps. However, the mechanisms of intracellular survival and traversal are poorly understood so far. Besides, most of the previous studies about *N. gonorrhoeae* were performed in the conventional semi-confluent culture of cells (2D cell culture). Although they have provided insights into host-pathogen interactions, many information about the native infection microenvironment, like cell polarization and barrier function, are still missing. In this study we explored the molecular bases of *N. gonorrhoeae* pathogenesis both from the aspects of a bacterial virulence factor and a host factor. Since the non-polarized and polarized cells are both present in the cervix, and additionally, junction proteins represent different properties on these different cells, we established 3-D models to further explore the function of those bacterial and host factors in pathogenesis.

The bacterial factor NGFG_01605 did not affect gonococcal adherence but was critical for its survival in epithelial cells in 2D cultures. However, its role on invasion has to be further clarified to avoid the clonal effects. The knockout of NGFG_01605 does not gonococcal transmigration in the 3D cultures. We did not resolve the molecular bases of NGFG_01605 in regulating bacterial infection, because we failed to find its interacting proteins.

The host factor FLCN did not affect *N. gonorrhoeae* adherence and invasion but was essential for bacterial survival in the host cells. FLCN increased *N. gonorrhoeae* survival independent of the bacterial surface molecules, which are critical for their adherence and invasion. Since programmed cell death (apoptosis and autophagy) are host defense mechanisms against intracellular pathogens, we further explored both mechanisms and determined that FLCN did not affect apoptosis but inhibited autophagy. Blocking autophagy by BafA1 also benefited *N. gonorrhoeae* survival. Furthermore, FLCN inhibited the expression of E-cadherin, and knocking down the E-cadherin decreased the autophagy flux which improved the *N. gonorrhoeae* survival. In summary, this work reveals a novel

facet of autophagy regulation by FLCN-E-cadherin axis upon infection in non-polarized cells.
Since the non-polarized and polarized cells are both present in the cervix, and additionally, E-cadherin represents different properties on these different cells, we established several 3-D models to better understand the function of FLCN in an emulated environment. We found that FLCN was critical for *N. gonorrhoeae* survival in the 3-D emulated environment as well, but not through inhibiting autophagy, like we observed in 2-D cell culture. Furthermore, FLCN does not only inhibit the E-cadherin expression but also disturbs its polarization in the 3-D models. Due to the distinct roles of E-cadherin in polarized cells, FLCN-E-cadherin axis may here have different function in *N. gonorrhoeae* survival and not by regulating autophagy. Since *N. gonorrhoeae* is able to cross the epithelial cell barriers through both cell-cell junctions and transcellular migration, we further explored the roles FLCN and E-cadherin play in transmigration. FLCN delayed *N. gonorrhoeae* transmigration, whereas only knocking down E-cadherin increased *N. gonorrhoeae* transmigration. This suggests FLCN but not E-cadherin may play a dominant role in transmigration. In summary these observations strongly indicate that the function of FLCN and E-cadherin possibly depends on the cell polarity and their local environment.

3.1 Bacterial virulence factor: NGFG_01605

NGFG_01605 has been confirmed in this study as a cytosolic protein without protease activities. It is critical for gonococcal survival in Chang cells (Figure 13). However, we could not determine in this study whether the increased survival is a result of better invasion as shown by its knockout N00125 or by better evasion of killing shown by its knockout N00126 (Figure 13). Therefore, more knockout clones need to be included in the study. Interestingly, we found that the NGFG_01605 knockout decreases the amount of adhesin protein Opa (data not shown), which is critical for gonococcal adherence and invasion. But whether the loss of Opa is resulted from NGFG_01605 knockout has to be further explored. In addition to epithelial cells, NGFG_01605 knockout did not affect gonococcal survival in neutrophils (data not shown). However, this is not a solid conclusion yet. We performed this experiment using the strains with the background of N2009. The type of Opa expressed by this strain is difficult to specify due to the phase variation. According to the previous studies neutrophils express CEACAM3 (Sadarangani *et al*., 2011), which binds to Opa$_{57}$. It is important to explore the role of NGFG_01605 in gonococcal survival in neutrophils by using the strains expressing Opa$_{57}$.

3.2 Host factor: FLCN

FLCN is a protein that in humans is associated with Birt-Hogg-Dubé syndrome, which acts as a tumor suppressor. FLCN has participated in many pathways like the AMPK and mTOR. Only few studies discussed the relationship between FLCN and pathogen infection in *Caenorhabditis elegans*, indicating that the loss of FLCN activates AMPK-dependent pro-inflammatory cytokine expression and phagocytosis in macrophages and confers pathogen resistance (El-Houjeiri *et al*., 2019). In our study, we explored the interactions between human obligate pathogen *N. gonorrhoeae* and epithelial cells from the aspect of adherence, invasion, survival and transmigration of gonococci.
N. gonorrhoeae has four types of surface structure that are essential for its adherence and invasion, namely $PorB_{IA}$, Opa, pili and LOS. $PorB_{IA}$ only functions in the low phosphate condition, e.g. HEPES. The other three surface structures work both at low phosphate condition and high phosphate condition e.g. DMEM and RPMI, but the efficiency varies. In addition to phosphate, FBS has been reported to affect adherence and invasion efficiency (Kuhlewein *et al.*, 2006). In our study, N2013 ($pili^{+}$, $PorB_{IA}$, Opa^{+}) was the strain used for shRNA screening, but it is a weaker invader due to the presence of pili, which blocks invasion (Faulstich *et al*., 2013). Hence the *Neisseria* strains expressing individual adhesin, including N931 (Opa_{50}), N927 ($PorB_{IA}$), N313 (Opa_{57}) and N924, were used to explore the role of FLCN on their infection. The $PorB_{IA}$-mediated adherence and survival of N927 in HEPES were not affected by FLCN. The Opa_{57}-mediated adherence and survival of N313 in DMEM were not affected by FLCN. The only difference we observed is the Opa_{50} mediated survival of N931 in DMEM. Except for Opa-HSPG interactions, vitronectin / fibronectin and integrin interactions facilitate the Opa_{50} positive *Neisseria* infection efficiency. Therefore, we added 10% FBS, which contains vitronectin/fibronectin, into DMEM for infection. FLCN is essential for the Opa-HSPG-vitronectin-integrin mediated pathway as well. Interestingly, FLCN favored N924 survival, which is Opa negative, in the DMEM plus FBS condition as well. This indicates that FLCN is essential for gonococcal survival independent of surface structures. In most of the later studies, if not specified, we have therefore used N931 and DMEM plus FBS for performing experiments.

3.2.1 Adherence

3.2.1.1 FLCN did not affect adherence

The primary event establishing infection is bacterial adherence to the mucosa epithelium, which is mediated through distinct bacterial surface structures including Type IV pili, Opa, LOS, and PorB$_{IA}$ (Quillin and Seifert, 2018). In this research, we used *N. gonorrhoeae* with different surface structures, e.g pili (N2013), Opa (N931 and N313), and PorB$_{IA}$ (N927) as well as different epithelial cell line, HeLa2000, Hec-1-B and UOK257. Our results revealed that FLCN had no effects on gonococcal adherence independent of the bacterial surface structures and host cell lines. This data implies FLCN is not involved in regulating cellular receptors of the bacterial adhesins. Among those receptors, the pilus receptor is controversial.

Whereas both nonpiliated and under piliated variants frequently arise when *N. gonorrhoeae* are grown *in vitro*, all clinical isolates of *N. gonorrhoeae* are piliated (Swanson *et al*., 1987). CD46 has been reported as a pilus receptor, however, several studies argued a controversial role of CD46 as a pilus receptor. CD46 undergoes alternative splicing and is expressed in four major isoforms, BC1, BC2, C1, and C2. All four isoforms have either the cytosolic tail cyt1 or cyt2. Using Chinese hamster ovary (CHO) cells transfected with the four isoforms, Kallström and colleagues (Kallstrom *et al*., 2001) showed that piliated gonococci bind to BC1-expressing cells (Lee *et al*., 2002). However, Tobiason and Seifert found that the level of pilus-mediated gonococcal adherence does not correlate with the amount of surface-expressed CD46. Furthermore, Kirchner et al. (Kirchner *et al*., 2005) discovered that piliated gonococci bind to epithelial cells in a CD46-independent manner by using CHO and Madin-Darby canine kidney (MDCK) cell lines stably transfected with specific CD46 isoforms and RNA interference. In this study, we compared the CD46-cyt1(BC1 and C1) and CD46-cyt2 (BC2 and C2) expressions between FLCN positive and negative cells (Figure 30). CD46-cyt2 is the dominant isoform in the UOK cell, which is about 100 times higher than CD46-cyt2. Both expression of CD46-cyt1 and CD46-cyt2 was lower in UOK257 than in UOK-FLCN, whereas the ratio of C46-cyt2/cyt1 is significantly higher in the UOK257 than in the UOK-FLCN. Those two isoforms have distinct cellular functions. Activation of CD46-cyt1 leads to binding of the scaffold protein GOPC and promotes autophagy. CD46-cyt2 participates in the pathways regulating pathogen infection (Lee *et al*., 2002). Our data revealed that FLCN did not affect pilus mediated *N. gonorrhoeae* adherence. FLCN knockout decreases the expression of CD46. Therefore, our study implies that pilus receptors are redundant and CD46 is not the only one.

3.2.1.2 FLCN decreases E-cadherin expression and polarization

Discussion

The E-cadherin is known as the epithelial cadherin on the surface to form adherence junctions. In our study, we found that FLCN interferes with E-cadherin expression both in UOK cells and Hec-1-B cells (Figure 33A, B and C). Moreover, it interrupts E-cadherin polarization (Figure 36). Controversial regulation of E-cadherin by FLCN has been reported. FLCN deletion in primary alveolar epithelial cells (AECs) interferes with E-cadherin expression. TSC2-null kidney epithelial cells (FLCN negative) have decreased membrane localization of E-cadherin (Goncharova *et al*., 2014). However, Hatzfeld *et al* (2014) showed that the FLCN-p0071 protein complex is a negative regulator of cell-cell adhesion. p0071 is a member of the armadillo repeat-containing protein family, which includes p120-catenin (p0071's closest homolog) and β-catenin. Similar to this study, Medvetz *et al* (2012) reported that the loss of FLCN increased adherence junction in UOK cells. In addition, both p120-catenin and p0071 regulate RhoA activity and FLCN-deficient cells have low levels of RhoA (Medvetz *et al.*, 2012). The study of Noren *et al* (2001) showed that induction of cell-cell junctions inhibited RhoA, which indirectly supports that FLCN negatively regulates E-cadherin. Taken together with the results of previous studies and our study, it indicates that the role of FLCN on E-cadherin regulation is cell-type dependent. Additionally, E-cadherin plays an important role in bacterial adherence.

In our study, we discovered E-cadherin knockout did not affect gonococcal adherence in 2D cultures (Figure 35E), whereas it significantly decreased adhered bacteria in the 3D cultures (Figure 42D). Previous studies showed that E-cadherin was a receptor for some pathogens during infection. *Fusobacterium nucleatum*, a pathogen associated with oral plaque formation and colorectal cancers, binds E-cadherin through its FadA adhesin (Rubinstein *et al*., 2013). *Listeria monocytogenes,* the causative agent of severe food poisoning, internalizes when internalin A (InlA) and InlB bind to E-cadherin and the hepatocyte growth factor receptor on the basolateral surface of epithelial cells (Ortega *et al*., 2017). In this research, E-cadherin knockdown did not affect gonococcal adherence in 2D, which indicates that E-cadherin is not a receptor of bacterial adhesin in this context. While in the 3D culture the FLCN-mediated inhibition of E-cadherin had a tendency of increasing adherence, the shRNA-mediated knockdown of E-cadherin decreased adherence. This data implies that E-cadherin is a receptor for adherence and FLCN regulates other proteins which are critical for bacterial adherence in addition to E-cadherin in the 3D microenvironment. Taking those 2D and 3D adherence data together indicates that FLCN has a different regulation network in these two conditions. E-cadherin

has a different function for bacterial infection in a context dependent fashion as well.

3.2.2 FLCN does not affect gonococcal invasion

Subsequent to adherence, gonococci utilize Opa or PorB or LOS to intimately bind to and invade into host cells (Faulstich *et al*., 2013). In this study, we found that FLCN did not affect gonococcal invasion both in the absence or the presence of FBS. Representative stains N931Opa$_{50}$ (Figure 20A) and N924 (Figure 20B) were used. Opa-HSPG interactions are mediated through a pathway that begins with the highly localized recruitment of HSPG receptors, F-actin, and tyrosine phosphorylated proteins at the attachment sites. This process activates two lipid hydrolysis enzymes, the PC-PLC and an acidic sphingomyelinase (SMase). A second pathway of uptake through Opa$_{HSPG}$ occurs through bacterial binding to vitronectin / fibronectin, which interacts with $\alpha_V\beta_5$ or $\alpha_5\beta1$ integrin receptors on host cells. In our study we showed that N931 (Opa$_{50}$) had a higher efficiency of both adherence and invasion when FBS is present compared with that when FBS is absent (Figure 20A). It implies that both pathways work in the FBS condition. The Gal(b1-4)GlcNAc residues, found on particular gonococcal LOS moieties and common to most strains of gonococci, serve as a ligand for the human ASGP-R. N924, which expresses none of the invasive proteins, e.g PorB$_{IA}$ and Opa, might invade the cell through LOS-ASGP-R pathway. We revealed in this study that FLCN did not affect the invasion of N924. Interestingly, FBS increases N924 adherence but does not affect the invasion (Figure 20B). Previous studies reported that the biotin in FBS increases ASGP-R expression (Collins *et al*., 1988). Moreover, the gonococcal infection increases the expression of ASGP-R (Porat *et al*., 1995). This might explain the increased adherence of N924 in the presence of FBS. Furthermore, our data indicates that coreceptors are needed for the ASPG-R-mediated invasion process.

3.2.3 FLCN is essential for gonococcal survival

After *N. gonorrhoeae* invading cells, few viable intracellular bacteria were recovered, which led to the assumption that *N. gonorrhoeae* is a weak invader. In our study, we found that in the N931 (MOI 50) infected UOK-FLCN cells, there was about 1.5 GC/cell for invasion while only 0.013 GC/cell for survival after the 2 h infection (Figure 20). FLCN is critical for gonococcal survival as we saw 0.013 N931/cell and 0.004 N924/cell for survival in FLCN positive cell while only

0.002 N931/cell and 0.001 N924/cell for survival in FLCN negative cell (Figure 22). FLCN does not favor survival when hiFBS is present in the infection medium as well (Figure 24). As discovered above, we revealed that the better bacterial survival is not conveyed by increasing invasion, indicating that FLCN plays a role in regulating bacterial evasion from cellular killing.

3.2.3.1 FLCN does not affect apoptosis upon gonococcal infection

Apoptosis plays a critical role in the elimination of infected cells. It is activated through either the intrinsic (mitochondrial mediated, e.g. the STS induced) or extrinsic (death receptor mediated, e.g. TNF-α induced) apoptotic pathways. PARP is a 116-kDa nuclear protein that mediates DNA repair in response to cell stress and is required to maintain cell viability. During programmed cell death, the protein is cleaved by caspase 3 or caspase 7, a terminal step in the caspase cascade. These suicidal caspases cleave PARP-1 into 89 kDa and 24 kDa apoptotic fragments (Chaitanya *et al*., 2010). In our study, apoptosis was barely detected upon gonococcal infection in the presence of FBS (Figure 27). What is interesting here is that FLCN might play a role in inhibiting apoptosis. There was less 89 kDa-PARP1 in the non-treated and STS-treated UOK-FLCN than in the UOK257 cells (Figure 27). Previous study showed that the role of apoptosis in *N. gonorrhoeae* survival is cell-type, strain phenotype and infection condition dependent. PorB$_{IA}$ - expressing *N. gonorrhoeae* infection induces intrinsic apoptosis (Kepp *et al*., 2009) while type IV pilus positive gonococcal infection triggers no apoptosis (Howie *et al.*, 2005). What is in common is that the gonococcal infection protects cells from induced apoptosis, e.g. STS or TNF-α induced, independent of the surface structure (Binnicker *et al.*, 2003; Howie *et al*., 2005; Morales *et al*., 2006). FLCN inhibits induced apoptosis. Gonococcal infection inhibits induced apoptosis as well. Therefore, it will be interesting to check the survival of the gonococci in the UOK-FLCN and UOK257 cells, which were treated by apoptosis inducers in the future.
Moreover, the infected cells without FBS protection displayed a different cleavage pattern of PARP-1, including two more fragments with the size close to 70 kDa and 55 kDa (Figure 27). In addition to being the substrate of caspases, PARP-1 could also be cleaved by other cell death related proteases, e.g. cleavage into 40 and 70 kDa fragments by calpain-1, cleavage into 55 kDa fragments by Granzyme-A (Chaitanya *et al*., 2010). Since calpain-1 and Granzyme-A promote necrosis as well, our data indicated that the gonococcal infected cells in the absence of FBS might undergo other types of programmed cell death. Therefore, it is important to explore further the cleavage fragments of

PARP-1 of the cells maintained with or without FBS. We could gain a bigger picture on how FLCN affects the gonococcal survival by understanding whether FBS deprivation of cells had effects on cell death or not.

3.2.3.2 FLCN is essential for gonococcal survival by decreasing autophagy

Except apoptosis, autophagy kills most of the early invaders of *N. gonorrhoeae*. Autophagy is a well-established host defense mechanism against intracellular pathogens. In our study, we found that Opa$_{50}$ gonococcal infection barely induced autophagy in FLCN positive cells while significantly increased autophagy in FLCN negative cells. The autophagy in FLCN positive cells, with and without infection, was lower than in the FLCN negative cell. The blockage of the autophagy by BafA1 counteracted the survival advantages conveyed by FLCN (Figure 28, 29). Recently, two studies have reported that autophagy mediated the killing of the intracellular *N. gonorrhoeae* (Kim *et al*., 2019; Lu *et al*., 2018). Particularly, the piliated *N. gonorrhoeae* with its Opas phase switched off, induces autophagy by the CD46-cyt1/GOPC pathway (Kim *et al*., 2019) while in the study of Lu *et al.* (2018), the phenotype of used gonococci was not specified. Therefore, our study for the first time, showed that the intracellular Opa$_{50}$ phenotype was killed by autophagy and FLCN played a role in regulating the process. We also showed in this study that gonococci were killed in the LAMP1 positive vacuoles (Figure 31C). Additionally, we observed a potential phenotype that FLCN regulates the distribution of LAMP-1 upon infection. LAMP1 of the infected UOK-FLCN cell localized at the peri-nuclear space while that of the UOK257 cells distributed everywhere in the cell (Figure 32). FLCN has been reported to promote the peri-nuclear clustering of lysosomes following serum and amino acid withdrawal (Starling *et al*., 2016). Apart from the distribution of LAMP-1 being important for its function, LAMP-1 is reported to be cleaved by IgA of *N. gonorrhoeae* in the early stage of infection (less than 4 h). This ultimately remodels lysosomes and blocks lysosome/autophagosome fusion and/or prevents degradation of autophagolysosomal contents (Lin *et al*., 1997). Therefore, it will be interesting to check the levels and localization of LAMP-1 in a quantitative way to further explore the role of FLCN in gonococcal mechanism of autophagy evasion.

FLCN was essential for gonococcal survival in 3D culture (Figure 42C) but it had no effect on autophagy (Figure 43). No significant changes of FLCN expression were found before and after infection in 2D (Figure 26). While in the 3D cultures, FLCN polarizes at the apical side of the cells. The gonococcal infection increases

FLCN (Figure 44). Therefore, our study indicates that the role of FLCN on gonococcal survival is context and environment dependent.

3.2.3.3 E-cadherin blocks gonococcal survival by increasing autophagy

FLCN interferes with E-cadherin. As we discussed above, E-cadherin did not affect *N. gonorrhoeae* adherence. However, we found E-cadherin was essential for gonococcal survival in 2D cell culture (Figure 35E). E-cadherin is a positive regulator of autophagy in this context (Figure 35C and D). Evidence from previous study demonstrates that E-cadherin regulates membrane localization of LKB1, which is critical for AMPK activation (Sebbagh *et al.*, 2009). AMPK activation plays a positive role in regulating autophagy. Hence, further study on the activation of AMPK in E-cadherin wild type and knockdown cells might provide better evidence for its role in autophagy regulation. Similar to the results of adherence in 3D cultures, FLCN-mediated inhibition of E-cadherin increases survival while the shRNA-mediated knockdown of E-cadherin has a tendency of decreasing survival. Meanwhile, E-cadherin did not affect autophagy in the 3D cultures. This data indicates that FLCN regulates other factors in the 3D to play a role in survival and the role of E-cadherin on bacterial survival is context dependent.
Moreover, we found that *N. gonorrhoeae* infection in 2D shortly increases the E-cadherin at protein level followed by a decrease (Figure 35B). It has been reported that bacterial infection affects the expression of E-cadherin. *CDH1* is the gene coding for E-cadherin. *Chlamydia trachomatis* infection causes a DNA methylation of the *CDH1* promoter and downregulation of E-cadherin expression (Rajić *et al*., 2017). Therefore, it would be interesting to investigate the methylation of *CDH1* promoter upon gonococcal infection in the E-cadherin wild type and knockdown cells to better understand the role of E-cadherin in gonococcal infection.

3.2.4 FLCN delays gonococcal transmigration

3.2.4.1 FBS maintains the barrier integrity and delays gonococcal transmigration

In this study we found that FBS maintains the UOK cells barrier integrity of infected models at least 4 d post infection by the FITC dextran assay. The transmigrated gonococcal could be collected at bottom as early as 24 h post infection in DMEM condition, whereas the transmigrated gonococcal were

collected at 48 h to 72 h post infection in DMEM plus FBS condition. The less collected bacteria could be from the result of two possibilities, which are less transmigration and less release from the cells to medium. The FBS concentration influences barrier integrity according to previous studies. Derk *et al.* (2015) showed that high serum concentrations (15%) altered monolayer integrity, as indicated by low TEER measurements when compared with TEER values for lower serum concentrations (2%). While Hennig *et al*. (1992) reported that porcine endothelial cells maintained in low serum (1%) medium have a lower barrier function than that maintained in high serum (5%) medium due to Zinc deficiency. Therefore, those studies indicated that FBS has a role in regulating the barrier function in a concentration dependent manner. It is important to compare the barrier integrity of UOK cells maintained in medium with or without FBS. What more, as we discussed before the vitronectin and fibronectin facilitate Opa_{50} mediated invasion by integrins $\alpha_V\beta_5$ or $\alpha_5\beta1$. The integrins localize at the basal side of polarized cells in contact with ECM. Therefore, the transmigrated gonococci might choose to re-enter the cell instead of being released into the medium.

3.2.4.2 FLCN delays gonococcal transmigration in an E-cadherin independent fashion

Aside from adherence and invasion, E-cadherin plays a role in transmigration. E-cadherin was cleaved through bacterial transmigration. In our study, we found that FLCN inhibits E-cadherin expression and polarization but does not affect that of ZO-1 (Figure 37). *Clostridium perfringens* produces a pore-forming delta toxin, which was found capable of reducing cell surface E-cadherin by enhancing ADAM-10 sheddase activity (Seike *et al*., 2018). The HtrA sheddase of *Helicobacter pylori* was found to open adherence junctions by cleaving E-cadherin and claudin-8 (Tegtmeyer *et al.*, 2017). In this study, we found that FLCN delays gonococcal transmigration (Figure 37B). Considering the important role of E-cadherin in transmigration as well as the negative control of FLCN on E-cadherin, we made the E-cadherin knockout cells in the background of FLCN negative cell UOK257. The transmigration assay showed that E-cadherin delayed gonococcal transmigration (Figure 38B). Our data indicates that opening the E-cadherin is critical for gonococcal transmigration. But FLCN might regulate other proteins, which are essential for bacterial transmigration in addition to E-cadherin.

In addition to E-cadherin, EGFR is critical for transmigration across polarized epithelial cells. In our study, we showed that EGFR distributes at the basolateral

surface of the polarized UOK cells. Apical gonococcal infection recruits EGFR from the basolateral surface to the apical side (Figure 39), which agrees with the data reported by Edwards *et al.* (2013). In addition to redistribution of EGFR, inoculation of *N. gonorrhoeae* leads to phosphorylation of EGFR as well (Edwards *et al*., 2013). Interestingly, Laviolette *et al.* (2017) showed that FLCN-/- cells have increased EGFR signaling upon EGF ligand activation, which indicated a negative role of the FLCN on EGFR signaling. Therefore, it is of high interest to explore the role of FLCN on EGFR activation and redistribution upon gonococcal infection to better understand the role of FLCN in transmigration process.

In conclusion, we revealed the important function of the FLCN-E-cadherin axis in *N. gonorrhoeae* infection, particularly related to the intracellular survival (Fig45) and transmigration (Fig46). This is also the first study that connects FLCN and bacterial infection.

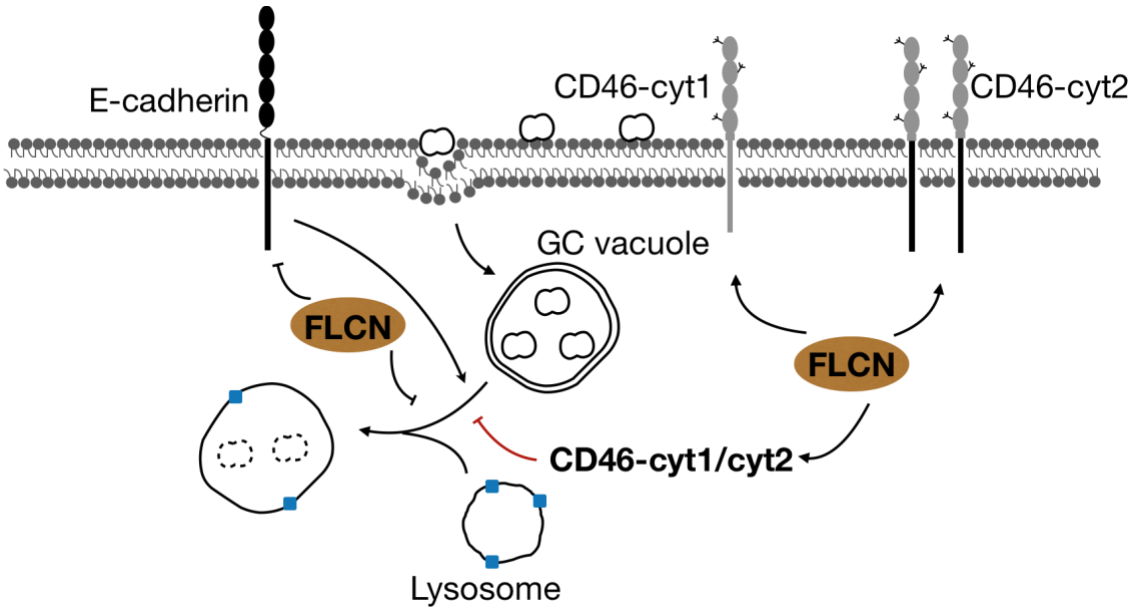

Figure 45: A schematic representation of the FLCN mediated protective effect on *N. gonorrhoeae* survival in the two-dimensional flat monolayer

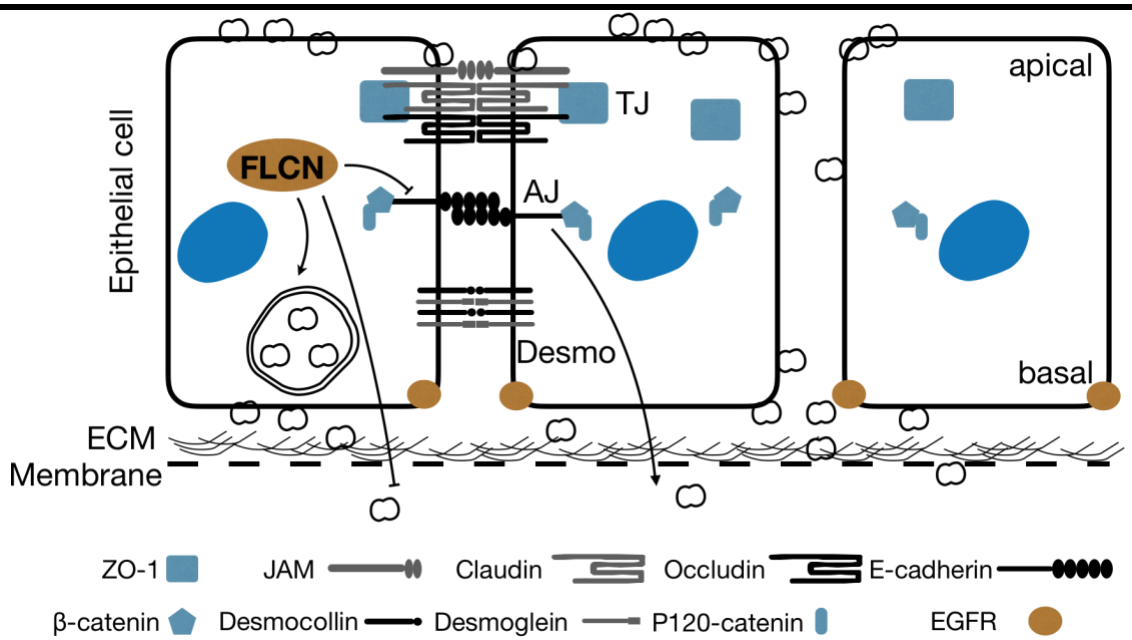

Figure 46: A schematic representation of the FLCN mediated protective effect of gonococcal survival and inhibition of gonococcal transcytosis in the three-dimensional polarized monolayer

3.3 Perspectives of the study

Through the course of this work, we explored functions of bacterial virulence factor NGFG_01605 and host factor FLCN to better understand the host-pathogen interactions. Further exploration to find its interacting proteins will give us a better understanding of its importance in *N. gonorrhoeae* pathogenesis. The host factor FLCN was identified to favor gonococcal survival by decreasing autophagy in this study. However, we have not established a pathway by which FLCN regulates autophagy. Our preliminary data showed that FLCN increases the CD46-cyt1/VD46-cyt2 ratio. CD46-cyt1 promotes autophagy upon *N. gonorrhoeae* infection, but CD46-cyt2 does not. In addition to CD46, we found FLCN regulates the peri-nuclear localization of LAMP1 upon infection, which has been reported in the case of starvation (Starling *et al*., 2016). *N. gonorrhoeae* infection cleaves LAMP1 and remodels the lysosome to better survive (Lin *et al*., 1997). Therefore, those data open up a pathway for determining the role of FLCN in regulating autophagy upon infection. Additionally, we determined in this study that FLCN decreased E-cadherin expression. E-cadherin inhibits gonococcal survival by increasing autophagy. However, the molecular bases by which FLCN interferes with E-cadherin have not been elucidated. FLCN has been reported to interact with P0071, which belongs to the armadillo repeat-containing protein family. P120-catenin, the E-cadherin associated protein, is a member of this family as well and acts as a “set-point” for cadherin levels (Hatzfeld *et al*., 2014;

Kowalczyk and Nanes, 2012). This cue highlights the way to explore the relationship between FLCN and E-cadherin in the future. While the traditional 2D cell culture gave us a lot of insight into the role of FLCN in gonococcal infection, we discovered that FLCN is essential for *Neisseria* survival in the 3D cell culture independently of regulating autophagy. Even though FLCN decreases the E-cadherin formed adherens junction, which blocks bacterial transmigration, FLCN delays gonococcal transmigration in our study. FLCN possibly regulates other factors which contribute to transmigration. Previous study showed that *N. gonorrhoeae* activates EGFR and recruits them to the apical infection site to facilitate transmigration (Edwards *et al.*, 2013). In this study, we found that the polarized EGFR at the basal cell surfaces migrates to the apical surface upon infection. Furthermore, previous study reported that FLCN negatively regulates EGFR signaling pathway (Laviolette *et al*., 2017), therefore, the FLCN-EGFR network opens up a door for us to explore the mechanism by which FLCN regulates gonococcal transmigration. Until now we did all the research in the epithelial cells. Gonococcal infection induces transcription of numerous cytokines and chemokines in epithelial cell lines, e.g TNFα and IL-1β, IL-6 (Maisey *et al*., 2003). Those cytokines attract immune cells to wipe out pathogens. Loss of FLCN or pharmacological activation of AMPK induces TFEB/TFE3-dependent pro-inflammatory cytokine expression (El-Houjeiri *et al*., 2019). FLCN might be a bridge between bacterial infection and the innate immune system. This study is the first one to inquire into the role of tumor suppressor FLCN in bacteria and mammalian cell interactions. In essence, we hope that this study will open up several new frontiers regarding the function of FLCN in bacterial pathogenesis.

4 Methods

4.1 Eukaryotic Cell Biology

4.1.1 Cell culture techniques

The mainly used cell lines in this study were UOK cells (UOK-FLCN and UOK257, kindly provided by Dr Laura Schmidt Richard Harbottle, Deutsches Krebsforschungszentrum (DKFZ), 293T cells, Hec-1-B cells, human dermal fibroblasts (HDFib), Chang cells, HeLa2000 cells, T84, and End1E6/E7 cells. UOK kidney epithelial cells, and 293T human kidney epithelial cells, and HEC-1-B human endometrial adenocarcinoma cell line (ATCC® HTB113™), and human dermal fibroblasts (HDFib), isolated according to the published protocol from foreskin biopsies of healthy donors(Pudlas *et al*., 2011), were cultured in Dulbecco's Modified Eagle Medium (DMEM). Chang human conjunctival epithelial cells and HeLa2000 epithelial cervical carcinoma cells, were maintained in RPMI 1640. T84 colorectal carcinoma cells (ATCC® CCL-248™) were cultured in DMEM/F12. END1 cervix epithelial cells (ATCC CRL-2615) were grown in DMEM including NEAA L-glutamine, pyruvate, 4500 mg/L glucose. All media were supplemented with 10% FBS and 1% Penicillin/Streptomycin.
To make cell stocks, Cells were grown in a 75 cm_2 flask to a confluency of about 80 %. The monolayer was washed once with DPBS and cells were detached by adding 1.5 ml Trypsin for 5 min at 37 °C. The cells were diluted in cell culture medium and centrifuged at 800 g for 5 min. The pellet was dissolved in a cell stocking medium composed of FBS with 10% DMSO, transferred into cryo tubes and stored at -80 °C in a cell freezing container to cool down the cells slowly. For longer storage, cells were stored in a liquid nitrogen tank.

4.1.2 shRNA knock-down cell line production

Constitutive knockdown lines were produced by virus transduction. The virus was produced in in 293T cells using the shRNA expression vector pLVTHM and two packaging plasmids pVSVG and psPAX, which were introduced into the cells by Ca-phosphate transfection. The oligonucleotides were annealed in a concentration of 1 mM in 48 µl annealing buffer. The mixture was heated at 94 °C for 4 min, at 70 °C for 10 min and cooled down for 1 h at room temperature. The annealed oligonucleotides were diluted 1:100 in H_2O. The annealed oligonucleotides were ligated into the pLVTHM vector cleaved with ClaI and MluI

and plasmids were amplified by transforming into *E. coli* DH5α. Plasmids were extracted from *E. coli* overnight cultures by the help of the PureYieldTM Plasmid Midiprep System.
293T cells were seeded in 6 well plates one day before the transfection. 2 µg of the plasmid pLVTHM and 1 µg of the plasmids pVSVG and psPAX were mixed with 225 µl ddH_2O and 25 µl 2.5 M $CaCl_2$. 250µl 2x HBS was added dropwise, while making bubbles with a Pasteur pipette. The mixture was incubated at room temperature for 15 min. Meanwhile, 1 µl/ml chloroquine was added to the cells. After the incubation time, the mixture was slowly added dropwise to the 293T cells. The infected 293T cells were incubated overnight and medium was changed after 24 h. Two days after the infection, the supernatant of the 293T cells containing the viruses was taken off and sterile filtered with 40 µm nitrocellulose filters. The medium of the target cell lines was removed and the virus-supernatant together with 10 µg/ ml polybrene were added to the cells. Western blotting and FACS analysis were followed to select for the positive clones.

4.1.3 Gentamicin protection assay

Cells were grown to 80% confluency. Medium was changed for different infection purposes. When the infection medium is different from the culture medium, the cells should be washed at least three times to reduce the effects of old medium and incubate for 30 min before infection. Bacteria were suspended in HEPES medium and added to cells at the MOI50. To synchronize infections, infected monolayers were centrifuged for 3 min at 600 g. Infected cells were cultured at 37°C in 5% CO2 for different time periods and infections were stopped by washing the cells several times with the infection medium.
To quantify total cell associated bacteria, cells were lysed with 1% saponin in infection for 7 min. After vigorous pipetting, a series of dilutions were plated on GC agar plates and CFU were determined 24 h later. For quantification of intracellular viable bacteria, extracellular bacteria were selectively killed by addition of 50 µg/ml gentamicin in infection medium for further 2 h incubation at 37 °C and 5% CO_2, prior to lysis in 1% saponin and plating. Experiments were conducted in triplicate wells.

4.1.4 Differential staining assay and FIJI quantification

To differentiate intracellular from extracellular bacteria, the differential staining method was used. Cells were seeded on coverslips and grown to a confluency of 80%. Cells were infected with the respective gonococcal strains at MOI 10. The

infection was stopped by intensive washing with an infection medium. The following process was performed at room temperature (RT). Infected cells were fixed with 4% PFA for 15 min. After blocking with 1% BSA in PBS for 30 min, extracellular bacteria were detected with a 1:100 dilution of the primary antibody, polyclonal rabbit anti-*N. gonorrhoeae* in 1% bovine serum albumin in PBS, for 1 h followed by three washes with PBS. Then, the coverslips were incubated for 1 h with a Cy5 conjugated secondary anti-rabbit antibody (1:100). After intensive washing, cells were permeabilized with 0.1% Triton-X-100 in PBS for 15 min. Blocking and staining of the extracellular and intracellular bacteria were subsequently performed as described above using a Cy2 conjugated secondary anti-rabbit antibody. The coverslips were then embedded in Mowiol on microscope slides and analyzed by confocal microscopy. The extracellular bacteria were stained twice, and the intracellular bacteria were only stained once. The numbers of bacteria were quantified by FIJI with three independent experiments with counting 100 cells per each.

4.1.5 Establishing and characterization 3D cell culture

For the monolayer transwell system,6.5 mm diameter, 3 µm pore size polyester Transwell inserts (Corning, Lowell, MA, USA) were seeded with 100 000 epithelial cells on the apical side. The effect of coated rat tail collagen type I was tested. Models were grown 10 days under submerged static conditions at 37 °C / 5% CO_2. The medium was exchanged every 2 days.
For the SIS scaffold models, preparation of porcine small intestinal submucosa (SIS) scaffold and decellularization were done according to the established protocol (Schweinlin *et al*., 2016). Pieces of SIS scaffold were mounted on the plastic 8 mm diameter cell crowns and 100,000 fibroblasts were seeded on the apical side of cell crown. After 48 h, 300,000 epithelial cells were seeded on the apical side of the model. In cases where different mediums were required for fibroblasts and epithelial cells, the models were cultured in the medium consisting of 50:50 fibroblast/epithelial cell medium. Models were grown 10 days under submerged static conditions at 37 °C / 5% CO_2. The medium was exchanged every 2 days.

4.1.6 Barrier integrity assay

The integrity of the monolayer was assessed using 4 kDa FITC-dextran permeability assay after 10 days of cultivation. To this purpose, 0.25 mg/ml FITC-dextran was dissolved in cell culture medium and filtered. The medium was

removed from both the apical and basal sides of the cell crown or Transwell®. One milliliter of fresh medium was added to the basal side, and 300 µl of FITC-dextran-containing medium to the apical side. After 30 min of incubation, 200 µl from the lower compartment were collected into a 96 well plate and fluorescence was analyzed using a TECAN reader (absorption 490 nm, emission 525 nm). The results were normalized to the sample with an empty SIS scaffold or Transwell® membrane.

4.1.7 Immunofluorescence staining of the whole 3D models

All the steps were performed at RT. Four percentage paraformaldehyde were used to fix the tissue models for 2 h on cell crowns and 1 h on transwell membrane. The tissue models were then intensively washed with PBS, and permeated using 1% Saponin for 30min, blocked with 1% BSA in PBS for 1 h and decorated with primary antibodies (1:100) overnight. This was followed by decoration with fluorophore-coupled secondary antibodies (1:100), Phalloidin-555 (1:300), DAPI (1:100) for 1 h, and mounting using Dako. Z-stacks of images were obtained through 25 µm from the top of the monolayer using Leica SP5 and processed by FIJI.

4.1.8 Immuno-histological staining

Tissue samples were fixed with 4% PFA for 1 h at 4 °C, processed for embedding in paraffin, and sectioned with a thickness of 5 mm on a microtome. Tissue slices were first deparaffinized with xylene and rehydrated in a graded series of ethanol according to standard protocols. Tissue and scaffold sections were stained with hematoxylin and eosin according to standard protocols for general morphological investigation. Further characterization of the models was done by immunofluorescence staining. Briefly, antigen retrieval was done by heat pretreatment at 100C for 20 min in pH 6 citrate buffer. After blocking with PBS plus 0.3% Triton, 5% BSA for 30 min, slices were incubated with primary antibodies at 4C overnight. After washing, secondary antibodies were added at a dilution of 1:100 in PBS for 1 h at room temperature. Samples were covered using Mowiol with DAPI for staining of the nucleus.

4.2 Bacteria cell biology

4.2.1 Culture of *N. gonorrhoeae*

N. gonorrhoeae was grown on GC agar plates supplemented with 1 % vitamin mix. The bacteria culture for infection should be around 16 - 18 h growth at 37 °C/ 5 % CO2. The selection for pili-positive or Opa-positive colonies was done using a binocular microscope.

4.2.2 *N. gonorrhoeae* stocks

Neisseria strains grown on GC agar plate for 16–18 h were suspended in 1 mL PPM medium. The bacterial cultures were then mixed with 350 µL 100% glycerol to a final concentration of 25% (v/v) and transferred to a 2 mL cryo tube. The stocks were stored in -80°C.

4.2.3 Growth curve of *N. gonorrhoeae*

Growth curves were performed with non-piliated *Neisseria* to prevent bacterial aggregation. 16 - 18 hours old gonococci were collected in 1 ml PPM medium supplemented with 1 % vitamin mix and 0.042 % $NaHCO_3$. A bacterial pre-culture with an OD550 of 0.15 was incubated at 100 - 120 rpm and 37 °C for 2 – 3 hours until they reached an OD550 0.5 – 0.6. The growth curves were started by synchronizing the *Neisseria* culture to an OD550 of 0.1 in PPM medium in a 50 ml glass flask. The bacteria were incubated at 100 - 120 rpm and 37 °C and their optical density was measured every hour for a total of 5 hours of incubation.

4.2.4 Complement plasmid construction

The plasmid PLASpilEmcherry were digested with FseI and PacI respectively to remove the mcherry fragment together with pilE promoter. Meanwhile, the coding sequence of NGFG_01605 together with 100 bp upstream sequence were amplified by PCR from the gonococcal genomic DNA. FseI (GGCCGGCC) and PacI (TTAATTAA) were added to the 5’ ends of the primers for amplification. The PCR products were digested with FseI and PacI respectively as well and then ligated to the linearized vector PLASpilEmcherry.

4.2.5 *N. gonorrhoeae* transformation

Piliated *Neisseria gonorrhoeae* transformation. *N. gonorrhoeae* are natural competent bacteria and the transformation of PCR fragments requires a DNA uptake sequence (GCCGTCTGAA) (Goodman & Scocca, 1988, Elkins et al., 1991). Pilus positive gonococci was taken from the GC agar plate and was

resuspended in PPM medium. 50 µl of an OD_{550} 0.32 bacterial suspension were mixed with 10 ng of a PCR or 100 ng plasmid product and were dropped in a non-selection GC agar plate. The plate was incubated at 37 °C for 6 h. The grown bacteria were taken up in PPM medium, centrifuged for 5 min at 5 000 x g and plated on an appropriate selective GC agar plate. The screening for successfully transformed colonies was done by colony PCR.

4.2.6 *Neisseria* transmigration assay

Infections of cells grown on Transwell inserts were performed in DMEM plus 10% FBS at a MOI of 50. To determine the transmigration of bacteria across the polarized monolayer after different time points of infection, 25 µl of medium were plated on GC-agar plate or the medium was centrifuged shortly at 100 x g and the pellet resuspended in 25 µl of medium, was plated on GC agar. To determine adherent bacteria, the infected tissues were incubated for 30 min with 1% saponin and series dilution were plated for counting. To quantify intracellular survival, infection samples were treated with 50 µM gentamicin for another 4 h and the procedure described above to release the intracellular surviving bacteria was repeated. Infected or non-infected samples were fixed with 4% PFA at RT for 30 min and decorated with anti-E-cad and anti-ZO-1 (Proteintech, Manchester, United Kingdom) to observe cell junction proteins and polarization. Z-stack images were taken under a SP5 confocal microscope and reconstructed by FIJI.

4.2.7 Recombination NGFG_01605 purification

E. coli SoluBL21strain with plasmid pET28b-NGFG_01605 made by Xian (2014) was selected on LB agar plates with kanamycin. Single colonies were picked into 5 mL LB medium containing kanamycin and incubated overnight (200 rpm, 37 °C). Overnight bacterial cultures were diluted at 1:20 and transferred to fresh kanamycin containing LB medium. They were incubated at 250 rpm at 37 °C until on OD 600 of 0.4–0.6 was reached. The cultures were induced by addition of 0.25 mM IPTG and were incubated at 25 °C and 200 rpm for 4 h. Afterwards, the bacterial pellet was collected by centrifugation at 4,000 rpm and 4 °C for 15 min. The pellet was either used directly for purification or stored at −20 °C.
The pellet was thawed for 15 min on ice and resuspended in 4 ml per gram wet weight lysis buffer (table 16). After addition of 1 mg/ml lysozyme and incubation for 30 min on ice the pellet was sonicated using 10 sec bursts with a 10 sec cooling period. 10 µg/ml ribonuclease A and 5 µg/ml desoxyribonuclease I were

added to and incubated on ice for 15 min. The lysate was centrifuged at 10 000 x g for 20 min. 7 ml of the supernatant were mixed in a column with 1.75 ml 50 %

Ni-NTA slurry and incubated for 1 h at 4 °C on a rotary shaker. the column was washed twice with the wash buffer (table 16) and eluted with 2 ml elution buffer (table 16).

4.2.8 NGFG_01605 immunoprecipitation

The bacteria pellets were resuspended in pre-cooled lysis buffer containing 1 mg/mL lysozyme and incubated on ice for 30 min. Afterwards, the bacterial suspension was sonicated on ice for 10 min (Branson Sonifier 250; 50% duty cycle, output 4). Then the lysate centrifuged at 10,000 g and 4 °C for 30 min. The supernatant was used for CO-IP. The Flag-tagged protein was followed by protocol of ANTI-FLAG M2 Affinity Gel (Sigma-aldrich) and the His-tagged protein was followed by protocol of Ni-NTA Aragose (Sigma-aldrich).

4.2.9. Acetone precipitation of secreted protein

N. gonorrhoeae were seeded with an OD550=0.1 and harvested at OD600=0.6 via 5,200 rpm for 12 min at 4°C. Supernatant was sterile filtered (0.45 µm) and proteins were precipitated with acetone. For the precipitation of proteins from bacterial supernatants, the supernatant was mixed with 4x the volume ice-cold acetone in order to precipitate secreted proteins. Precipitation was performed overnight at -20°C followed by centrifugation for 60 min at 6,000 rpm at 4°C. Precipitated proteins were washed once with ice cold acetone, air-dried and resuspended in an appropriate amount of PBS. Proteins were stored at -20°C.

4.2.10 *E. coli* cultivation and stock preparation

E. coli were grown on LB agar plates or shaken at 190 rpm in LB medium at 37 °C overnight. Bacteria were grown on agar plates or in medium supplemented with the appropriate antibiotic if selection was required. For preparation of a bacteria stock 0.5 ml of an overnight culture were mixed with 0.5 ml of stocking solution and was frozen at - 80 °C.

4.2.11 Chemo-competent *E. coli* DH5α generation

Overnight bacteria culture was inoculated into fresh LB medium with a dilution factor of 1:50 and grown until OD_{600} 0.6. The culture was incubated for 15 min on ice and centrifuged at 4 000 rpm for 10 min at 4 °C. The pellet was resuspended in 20 ml cold 0.1 M $CaCl_2$ and incubated on ice for 30 min. Another centrifugation

step followed and the pellet was resuspended in 10 ml 0.1 M $CaCl_2$ and 20 % glycerol.

4.2.12 Chemo-competent *E. coli* DH5α transformation

100 µl competent E. coli DH5α were thawed on ice for a few minutes. They were mixed with 15 µl of the ligation and incubated on ice for 30 min. The heat-shock was achieved by incubating the bacteria for 90 sec at 42 °C followed by 2 min on ice. 1 ml of LB medium was added and the bacteria were shaken for 45 min at 37 °C. Lastly, the bacteria were plated on selective LB agar plates and incubated overnight at 37 °C.

4.3 Molecular and biochemical biology

4.3.1Total RNA extraction

Cells were trypsinized, centrifuged at 800 g for 4 min. DPBS resuspension and centrifuge to wash the cells twice. Afterward, the pellet was resuspended in 1 ml of TRI Reagent® and incubated at room temperature for 5 min. The solution was transferred to a Phase Lock GelTM tube and 200 µl of chloroform was added and mixed thoroughly. After 7 min incubation at RT the samples centrifuged at 12000 g and 4°C for 15 min. The aqueous phase was transferred carefully to a fresh tube. To precipitate RNA, 500 µl of isopropanol was added, the sample was mixed gently and incubated at room temperature for 8 min. Afterwards the sample was centrifuged at 14000 g for 15 min and the supernatant was discarded. To wash, 1 ml of 75% ethanol was added and the samples were centrifuged at 7500 g for 5 min. After removal of the supernatant the pellet was air dried. RNA was diluted in H_2O and stored at -80°C.

4.3.2 Generation of cDNA by reverse transcription

RNA was reverse transcribed into cDNA using the RevertAidTM First Strand cDNA Synthesis Kit. 2 µg RNA was added to the reaction mix containing oligo(dT)18 primer. Reverse transcription into cDNA was performed in a

thermocycler with the following temperature profile: 60 min at 42°C and 5 min at 70°C. Samples were stored at -20°C until further use.

4.3.3 Quantification of mRNAs by qPCR

The relatively quantification of gene expression based on the cDNA was carried out in a Step One Plus RT-PCR system using PerfeCta SYBR Green FastMix. 0.2 µl of cDNA was mixed with 10 µl qRT-PCR mix, 100 nM of each primer and H_2O to a final volume of 20 µl. Each sample was analyzed in triplicates.

4.3.4 Plasmid isolation

Plasmids extractions from *E. coli* overnight cultures supplemented with the appropriate antibiotic were performed using the AxyPrepTM Plasmid Minipret Kit or the PureYieldTM Plasmid Midiprep System.

4.3.5 Polymerase Chain Reaction (PCR)

PCR reactions were performed in a 50 µl reaction mix using 100 ng template DNA, 1 U Taq- Polymerase or 1 U Phusion polymerase, 1x Polymerase buffer, 1 µl of 0.5 mM dNTP-mix, 0.2 pmol forward and reverse primer. The volume could be scale down accordingly. After an initiation step of 10 min at 95°C, 30 cycles at 98°C for 30 s, 56-62°C (depending on the melting temperatures of the primers) for 20 s, and a 72°C step in a time appropriate to the template length [30 s/1 kb (Phusion); 1 min/1 kb (Taq)] followed. PCR products were analyzed on agarose gels, visualized under UV-light by ethidium bromide staining and purified using a PCR purification kit for further experiments.

4.3.6 DNA digestion and ligation

Restriction enzymes as well as T4 DNA ligase reactions were performed according to manufacturer's protocol. The vector/insert ratio to obtain efficient ligation of vector and insert was calculated with the Cranenburgh's formula (Cranenburgh, 2004). Recombinant DNA constructs were verified by sequencing (Seqlab, Göttingen, Germany).

4.3.7 SDS-PAGE

The proteins were separated on the basis of mass by electrophoresis using a vertical SDS-polyacrylamide gel electrophoresis (SDS-PAGE). Suspension cells were centrifuged for 5 min at 1000 g, resuspended in 100 µl Laemmli sample buffer (2 x). Adhered cells on the 6 -well plates were digested with 100 µl Laemmli sample buffer (2 x) directly after intensive washes with PBS. The

proteins were denatured by heating for 10 min at 95 °C. 20 µl of the samples were loaded into wells in the 10 – 12% SDS-PAGE and run for 1.5 h at 120 V.

4.3.8 Coomassie staining and silver staining

Colloidal coomassie G-250 was used for Coomassie. Gels were fixed for 1 h in fixing solution before staining overnight in colloidal staining solution. Staining solution was prepared freshly by mixing 400 ml of Staining A, 10 ml of Staining B and 100 ml of methanol. Gels were incubated afterwards for 5 min in neutralizing solution, washed for 15 min in washing solution and until destaining was sufficient in dH_2O.
Silver staining were used to detect the protein of small amount. Gels were fixed for 1 h in fixing solution, washed twice for 20 min in washing solution and incubated for 1 min in the sensitizer. The gel was washed three times for 20 sec with dH_2O before silver staining solution was added for 20 min. After staining the gel was washed twice for 20 sec with dH_2O before the developing solution was added. The gel was incubated until the strength of the staining was sufficient and developing was stopped by incubating the gel for 2 min in stop solution. The gel was afterwards washed with dH_2O.

4.3.9 Semi-dry Western Blot

PVDF membranes were activated in 100 % methanol and washed with a transfer buffer. Proteins of the gel were transferred to the membrane in a semi-dry apparatus for 2 h at 1 mA/cm. After transferring, membranes were blocked for 1 h in 5 % milk/TBS and incubated overnight in the primary antibody diluted in 3 % BSA in TBS. Membranes were washed 3 times for 10 min in TBS-T and stained in the secondary antibody diluted 1:3000 in 5 % milk powder in TBS for 1 h. Membranes were again washed 3 times for 10 min in TBS-T and ECL reagent was added. Chemiluminescence was detected by a chemiluminescence imager system.

5 Materials

5.1 Bacterial strains and medium

Table1 *N. gonorrhoeae* strains used in this study

Strain Identifier	Phenotype	Genotype/Plasmid	Source
MS11	$PorB_{IB}$	PorB	Our lab
N00130	$PorB_{IB}$	MS11-mcherry	This study
N2009	$PorB_{IA}$	MS11, PorB::PorA	Sprenger, 2010
N00125	$PorB_{IA}$	N2009, NGFG_01605 ::Kan_R, cl5	Ebert, 2016
N00126	$PorB_{IA}$	N2009, NGFG_01605 ::Kan_R, cl7	Ebert, 2016
N00127	$PorB_{IA}$	N2009 Δ01605, cat<NGFG_01605< >SpecC. cl2	This study
N00128	$PorB_{IA}$	N2009 Δ01605, cat<NGFG_01605< >SpecC. cl3	This study
N2013	$pili^{+}$, $PorB_{IA}$	$recA_I$, cat<$PorB_{IA}$< >ermC	Faulstich, 2012
N924	$pili^{-}$,$PorB_{IB}$,Opa^{-}	Δ$pilE_{I/2}$, cat<$PorB_{IB}$<>ermC	Bauer, 1997
N927	$pili^{-}$,$PorB_{IA}$,Opa^{-}	Δ$pilE_{I/2}$, cat<$PorB_{IA}$<>ermC	Bauer, 1997
N931	N219, Opa_{50}	N219, pTH6a (Opa_{50})	Kupsch et al., 1993
N313	N219, Opa_{57}	N219, pTH6a (Opa_{57})	Kupsch et al., 1993

Table 2 Bacteria culture medium and buffers

Medium and buffers	ingredients
Lysogeny broth (LB) medium	10 g/l tryptone, 5 g/l yeast extract, 10 g/l NaCl
LB agar	11 g/l tryptone, 5 g/l yeast extract, 10 g/l NaCl, 15 g agar
Proteose Peptone Medium	15 g proteose peptone, 5 g NaCl, 0.5 g soluble starch, 1g

(PPM)	KH_2PO_4, 4 g K_2HPO_4 in 1 l H_2O. Adjust to pH 7.2. Sterilize by sterile filtration
Neisseria growth medium	PPM, 1 % vitamin mixture, 0.042 % $NaHCO_3$ (8.4 %)
Neisseria transformation medium	PPM, 1 % vitamin mixture, 10 mM $MgCl_2$, 0.042 % (v/v) $NaHCO_3$ (8.4 %)
GC Agar	36.23 g GC Agar base (Oxoid) in 1 l ddH_2O, after autoclaving 1 % vitamin mixture is added
Neisseria freezing mix	PPM, 10 % glycerol
E. coli freezing mix	LB medium, 50 % glycerol, 2.9 % NaCl
Vitamin mix	Combine solution I and II, add H_2O to 2 l and sterile filter
Vitamin mix solution I	200 g D(+)-glucose, 20 g L-glutamine, 52 g L-cysteine-hydrochloride-monohydrate, 0.2 g cocarboxylase, 0.04 g iron-(III)-nitrate-nonahydrate, 0.006 g thiamine hydrochloride (vitamin B1), 0.026 g 4-aminobenzoic acid, 0.5 g NAD, 0.02 g vitamin B12. Add 1 l H_2O
Vitamin mix solution II	2.2 g L-cystine, 2 g adenine-hemisulfate, 0.06 g guanine-hydrochloride, 0.3 g L-arginine-monohydrochloride, 1 g uracil, add 600 ml dest. H_2O, 30 ml 32 % HCl
HEPES Medium	50 ml solution I, 10 ml solution II, 200 µl solution III, 3 ml solution IV/V, 5 ml solution VI, 50 ml solution VII, 50 ml solution VIII, in distilled water up to 500 ml, pH 7.3, sterilize by filtration
HEPES-solution I	0.1 % (w/v) L-alanine, 0.15 % (w/v) L-arginine, 0.025 % (w/v), L-asparagine, 0.025 % (w/v) glycine, 0.018 % (w/v) L-histidine, 0.05 % (w/v) L-lysine, 0.015 % (w/v) L-methionine, 0.05 % (w/v) proline, 0.05 % (w/v) L-serine, 0.05 % (w/v) L-threonine, 0.061 % (w/v) L-cysteine, 0.036% (w/v) L-cystine, 0.05 % (w/v) L-glutamine, 0.046% (w/v) GSH, 0.0032 % (w/v) hypoxanthine, 0.008 % (w/v) uracil, 0.004 % (w/v) D-biotin, in 18 % 1 N NaOH and 82 % ddH_2O, pH 7.2
HEPES-solution II	37.5 % (w/v) glucose
HEPES-solution III	1 % (w/v) $Fe(NO_3)_3$ x $9H_2O$
HEPES-solution IV/V	0.33 % (w/v) NAD, 0.33 % (w/v) cocarboxylase, 0.33 % (w/v) thiamine, 0.33 % (w/v) calcium pantothenate,

	0.188 % (w/v) $CaCl_2$ x $2H_2O$, 4.17 % (w/v) sodium lactate, 15.33 % (w/v) glycerol, 3.33 % (w/v) oxaloacetate
HEPES solution VI	5 % (w/v) $MgCl_2$ x $7H_2O$
HEPES solution VII	5 % (w/v) NaCl, 3.4 % (w/v) sodium acetate
HEPES solution VIII	2.38 % (w/v) Hepes

5.2 Cell lines and medium

Table 3 Cell lines used in the study

Cell line	Properties	Media	Source
UOK-FLCN	Kidney epithelial cells	DMEM	Dr Richard Harbottle, DKFZ
UOK257	Kidney epithelial cells	DMEM	Dr Richard Harbottle, DKFZ
293T	Kidney epithelial cells	DMEM	ATCC CRL-11268
Hec-1-B	Uterus epithelial cells	DMEM	ATCC® HTB-113™
HDFib	Dermal fibroblast	DMEM	This study
Chang	Conjunctival epithelial cells	RPMI1640	ATCC CCL-20.2
HeLa2000	Cervix epithelial cells	RPMI1640	ATCC CCL2.1
T84	Colon epithelial cells	DMEM/F12	ATCC® CCL-248TM
End1	Cervix epithelial cells	DMEM	ATCC CRL-2615

Table 4 Cell culture medium and buffers

Medium and buffers	Manufacturer/ ingredients
RPMI 1640	GIBCO
DMEM	GIBCO
DPBS	GIBCO
F12	GIBCO

DMEM/F12	GIBCO
FBS	Sigma/Merck
Cell stocking medium	FBS, 10 % dimethyl sulfoxide (DMSO) (v/v)
2 x HBS	50 mM Hepes pH 7.05, 140 mM NaCl, 1.5 mM Na_2HPO_4
Chloroquine	25 mM in PBS

5.3 Oligonucleotides

Table 5 Primers used for shRNA knockdown

Primer	Sequence (5’ to 3’)
FLCN_shR_For	CGCGTCCCCTCAGTATGCAGTCGCAATAACTTCAAGAGAG TTATTGCGACTGCATACTGATTTTTGGAAAT
FLCN_shR_Rev	CGATTTCCAAAAATCAGTATGCAGTCGCAATAACTCTCTTG AAGTTAT TGCGACTGCATACTGAGGGGA
E-cad_shR1_For	CGCGTCCCCGGACGTGGAAGATGTGAATTTCAAGAGAATT CACATCTT CCACGTCCTTTTTGGAAA
E-cad_shR1_Rev	CGATTTCCAAAAAGGACGTGGAAGATGTGAATTCTCTTGAA ATTCACATCTTCCACGTCCGGGGA
E-cad_shR2_For	CGCGTCCCCGTCTAACAGGGACAAAGAATTCAAGAGATTCT TTGTCCCTGTTAGACTTTTTGGAAAT
E-cad_shR2_Rev	CGATTTCCAAAAAGTCTAACAGGGACAAAGAATCTCTTGAAT TCTTTGTCCCTGTTAGACGGGGA

Table 6 primers used for qPCR

Primer	Sequence (5’-3’)
FLCN_qrt_For	GCCAGTCTTCAAGTCCCTCC
FLCN_qrt_Rev	TGTATGGGATGATGCGGACG
E-Cad-qPCR-For	CCCGCCTTATGATTCTCTGCTCGTG
E-Cad-qPCR-Rev	TCCGTACATGTCAGCCAGCTTCTTG
CD46-cyt1-qFOR	CTAACTGATGAGACCCACAGAGAAGT
CD46-cyt1-qRev	TCAGCTCCACCATCTGCTTTC

CD46-cyt2-qFOR	GAAGAAAGGGAAAGCAGATGGT
CD46-cyt2-qRev	CCTCTCTGCTCTGCTGGAGTG

Table 7 Primers used for FLCN overexpression

Primer	Sequence (5'-3')
FLCN_over_For	CTGATGAATGCCATCGTGGCTCTCTG
FLCN_over_Rev	TCGGTTCCGAGACTCCGAGGCTG

Table 8 Primers used for NGFG_01605 complementation

Primer	Sequence (5'-3')
NGFG01605-For	TAATAGGCCGGCCCGCCGTTTTCACGGAAGG
NGFG01605-Rev	GCGAGTTAATTAATCAGGGGTTCAACACGCG
PLAS-fseI-for	CCATAGCCCACACAACTAACC
PLAS-pacI-Rev	CGTACCTGCTCGACATGTTCA
NGFG01605-mid-Rev	GCTGCAAATGCCGTCTGAAG

5.4 Plasmids

Table 9 Plasmids used in the study

Plasmid	Description	Source
plvthm	Amp_R , shRNA expression vector	Wiznerowicz and Trono, 2003
plvthm-FLCN-shRNA	Amp_R, shRNA expression vector, FLCN	This study
plvthm-E-cadherin-shRNA	Amp_R, shRNA expression vector, E-cadherin	This study
plvthm-LAMP1-yGFP	Integrating LAMP1-yGFP into genomic DNA	Kerstin Paprotka
pCDNA3	Expression vector for fusing a C-terminal FLAG tag to a protein	Dr. V. Kozak- Pavlovic
pCDNA3-FLCN	Expression vector for fusing a C-terminal FLAG tag to FLCN	This study

pLAS:pilEmCherry	Sm_R, Neo /Kan mCherry	Darowski, thesis
pLASpilEmCherry:: NGFG_01605	Sm_R, Neo /Kan NGFG_01605	This study
pET28b	Expression vector, mutation in 244-239 from GGCAGC to GGATCC	Dr. Rosalia Deeken, Wuerzburg University
pET28b-NGFG-01605	ORF of NGFG_01605 cloned in pET28b (BamHI/HindIII)	(Xian 2014)

5.5 Antibodies

Table 10 Primary antibodies

Antibody	Origin	Dilution	Supplier
Anti-FLCN	Rabbit polyclonal	1:100 for IF/1:500 for WB	Cell signaling
Anti-E-cadherin	Rabbit polyclonal	1:100 for IF	Proteintech
Anti-ZO-1	Rabbit polyclonal	1:100 for IF	Proteintech
Anti-actin	Mouse monoclonal	1:3000 for WB	Sigma Aldrich
Anti-LC3	Rabbit polyclonal	1:500 for WB	Cells signaling
Anti-PARP-1	Rabbit polyclonal	1:500 for WB	Santa cruz
Anti-*N.gonorrhoeae*	Rabbit polyclonal	1:100 for IF	US Biological
Anti-Opa	Mouse monoclonal	1:50 for WB	Custom made
Anti-$PorB_{IA}$	Rabbit polyclonal	1:1000 for WB	Davids Biotechnology (self-made)
Anti-Omp85	Rabbit polyclonal	1:1000 for WB	Davids Biotechnology (self-made)

Table 11 Secondary antibody

Antibody	Origin	Dilution	Source

ECL anti-mouse IgG HRP linked	goat	1:3000 for WB	Santa Cruz
ECL anti-rabbit IgG HRP linked	goat	1:3000 for WB	Santa Cruz
Anti-rabbit IgG cy2 linked	goat	1:100 for IF	Dianova
Anti-rabbit IgG cy5 linked	goat	1:100 for IF	Dianova
Anti-mouse IgG cy5 linked	goat	1:100 for IF	Dianova

5.6 Commercial kits

Table 12 Commercial kits

Kit	Manufacture
GeneJETTM Gel Extraction Kit	Thermo Scientific
Wizard® SV Gel and PCR Clean-Up System	Promega
PureYieldTM Plasmid Midiprep System	Promega
AxyPrepTM Plasmid Miniprep Kit	Axygen
RNeasy® Mini Kit Qiagen	Qiagen
RevertAid First Strand cDNA Synthesis Kit Thermo Scientific	Thermo Scientific
ANTI-FLAG® M2 Affinity Gel	Merck
Ni-NTA His•Bind Resin	Merck

5.7 Enzymes

Table 13 Enzymes used in this study

Enzymes	Manufacturer
iProofTM High-Fidelity DNA Polymerase	Bio-rad
Phusion High-Fidelity DNA polymerase	Thermo Scientific

Taq DNA polymerase	Genaxxon Bioscience
FastAP Thermosensitive Alkaline	Thermo Scientific
Dnase I	Thermo Scientific
Rnase A	Thermo Scientific
T4 DNA Ligase	Thermo Scientific
ClaI	Thermo Scientific
FseI	New England BioLabs
MluI	Thermo Scientific
PacI	Thermo Scientific
Revert Aid Reverse Transcriptase	Thermo Scientific
Ribolock RNase Inhibitor	Thermo Scientific

5.8 Buffers and solutions for biochemical assays

Table 14 Buffers for agarose gel electrophoresis, SDS-PAGE and WB

Buffer	Ingredients
1 x TAE buffer	2 M Tris, 0.05 M EDTA, 1 M acetic acid (pH 8.5)
2 x Laemmli buffer	4 % SDS, 20 % glycerol, 120 mM Tris pH 6.8, 0.4 - 2 % β-mercaptoethanol, 0.02 g bromphenolblau
12.5 % SDS gel solution	6.9 ml Acrylamide/bis (30/0.8), 3.5 ml 1.875 M Tris pH 8.8, 0.1 % (w/v) SDS, 6.3 ml dH_2O, 100 µl 10 % (w/v) ammonium persulfate (APS), 10 µl tetramethylethylenediamine (TEMED)
SDS running buffer	25 mM Tris, 0.191 M glycine, 1 % (w/v) SDS
SDS stacking gel solution	0.83 ml Acrylamide/bis (30/0.8), 0.5 ml 0.8 M Tris pH 6.8, 50 µl 10 % (w/v) SDS, 3.55 ml dH_2O, 50 µl 10 % (w/v) APS, 10 µl TEMED
10 x (tris buffered saline) TBS buffer	1.5 M NaCl, 200 mM Tris/HCl, pH 7.5

10 x transfer buffer	20 mM Tris, 150 mM glycine, 0.02 % SDS; for 1 x transfer buffer add 20 % methanol
Blocking buffer for WB	1 x TBS, 5 % non-fatty milk powder
ECL solution I	2.5 mM Luminol, 0.4 mM p-coumaric acid
ECL solution II	100 mM Tris/HCl pH 8.5, 0.02 % H_2O_2
Coomassie staining solution	40 % ethanol, 7 % acetic acid, 0.2 % (w/v) coomassie R-250
Coomassie destaining solution	30 % ethanol, 10 % acetic acid
Colloidal fixation solution	7 % acetic acid, 40 % methanol
Colloidal staining solution A	2.375 % phosphoric acid, 10 % (w/v) ammonium sulfate
Colloidal staining solution B	5 % (w/v) coomassie G-250
Colloidal neutralization solution	1.2 % (w/v) Tris, pH 6.5 adjust with phosphoric acid
Colloidal washing solution	25 % methanol
Silver staining fixation solution	50% (v/v) ethanol, 12% (v/v) acetic acid, 0.5 ml/L formaldehyde (37%)
Silver staining washing solution	50% (v/v) ethanol
Silver staining sensitizing solution	0.2 g/l $Na_2S_2O_3$ x 5 H_2O
Silver staining solution	2 g/l $AgNO_3$, 0.750 ml/l formaldehyde (37%)
Silver staining developer	60 g/l Na_2CO_3, 4 mg/l $Na_2S_2O_3$ x 5H_2O, 0.5 ml/l formaldehyde (37%)
Silver staining stop solution	1% (v/v) glycine

Table 15 Buffers for immunofluorescence and immunohistochemical staining

Materials

Buffer	Ingredients
Fixation solution	4% PFA
Blocking solution	1 x PBS, 1 % (w/v) bovine serum albumin (BSA)
Permeabilization solution	1 x PBS, 0.1 % or 0.2 % (v/v) Triton X-100
Mowiol	35 g glycerol, 12 g Mowiol, 30 ml dH_2O, 60 ml 0.2 M Tris/HCl pH 8.5
Citrate buffer	10 mM citric acid, 0.05% Tween 20, pH 6.0

Table 16 Buffers for recombinant protein purification

Buffer	Ingredients
Lysis buffer	20 mM Hepes, 150 mM NaCl, PH 7.5
Wash buffer	25 mM Hepes, 300 mM NaCl PH 7.5
Elution buffer	25 mM Hepes, 300 mM NaCl, imidazole 500 mM PH 7.5
Hitrap Q purification buffer	100 mM to 1000 mM NaCl, PH 7.5
Gel filtration buffer	50 mM sodium phosphate, 0.15 M NaCl, pH 7.5

Table 17 Buffers for immunoprecipitation

Buffer	Ingredients
Lysis buffer	50 mM Tris HCl PH=7,4, 150 mM NaCl, 1 mM EDTA, 0.2% triton X 100, 1 X complete protease inhibitor
TBS (washing)	50 mM Tris HCl, with 150 mM NaCl, pH 7.4
Elution buffer 1	0.1 M glycine HCl, pH 3.5
Elution buffer 2	125 mM Tris HCl, pH 6.8, with 4% SDS, 20% (v/v) glycerol, and 0.004% bromophenol blue

Table 18 Annealing buffer for shRNA annealing and knockdown cell production

Buffer	Ingredients
Annealing buffer	100 mM potassium acetate, 30 mM Hepes KOH (pH 7.4), 2 mM magnesium acetate
Calcium chloride	2.5 M $CaCl_2$
Ca-phosphate buffer	50 mM Hepes (pH7.05), 140 mM NaCl, 1.5 mM Na_2HPO_4

5.9 Technical equipment

Table 20 Technical Equipment

Devices	Manufacturer
TCS SP5 confocal microscope	Leica
FACSaria III	BD
StepOnePlusTM Real-Time PCR	Thermo Scientific
2720 Thermal Cycler	Applied Biosciences
Hera Cell 240i incubator	Thermo
Hera Safe sterile bench	Thermo
Spectrophotometer Ultrospec 3100 pro	Amersham
UV transilluminator	Biostep
PerfectBlueTM 'Semi-Dry'-Electro-blotter	Peqlab
Plate reader infinite 200	TECAN
NanoDrop 1000 spectrophotometer	Peqlab Biotechnology
Äkta pure	GE healthcare
Anion exchanger column (Source Q)	GE healthcare
Superdex 200 10/300 GL	GE healthcare
Amicon® Ultra Centrifugal Filters	Merck Millipore

Cold centrifuge CT15RE	Himac

5.10 Software

Table 21 Software used in the study

Software	Purpose
FIJI	Image analysis
Affinity design	Figure preparation
R	Figure preparation, Statistical Analysis
GraphPad-Prism6	Statistical Analysis
Zotero	Reference bibliography
Serial Cloner 2.5	Sequence analysis; primer design
Mafft	Sequence alignment
Tree of life	phylogeny
StepOneTM software v2.3 (Thermo Scientific)	qRT-PCR data acquisition and analysis
Google docs	Utilities
Word	Utilities

6 References

Andrade WA, Agarwal S, Mo S, Shaffer SA, Dillard JP, Schmidt T, Hornung V, Fitzgerald KA, Kurt-Jones EA, Golenbock DT. 2016. Type I interferon induction by *Neisseria gonorrhoeae*: dual requirement of cyclic GMP-AMP synthase and Toll-like receptor 4. *Cell Rep* **15**: 2438–2448.

Apicella MA, Ketterer M, Lee FKN, Zhou D, Rice PA, Blake MS. 1996. The pathogenesis of gonococcal urethritis in men: confocal and immunoelectron microscopic analysis of urethral exudates from men infected with *Neisseria gonorrhoeae*. *J Infec Dis* **173**: 636–646.

Ashida H, Mimuro H, Ogawa M, Kobayashi T, Sanada T, Kim M, Sasakawa C. 2011. Cell death and infection: A double-edged sword for host and pathogen survival. *J Cell Biol* **195**: 931–942.

Baba M, Furihata M, Hong S-B, Tessarollo L, Haines DC, Southon E, Patel V, Igarashi P, Alvord WG, Leighty R, Yao M, Bernardo M, Ileva L, Choyke P, Warren MB, Zbar B, Linehan WM, Schmidt LS. 2008. Kidney-targeted Birt-Hogg-Dube gene Inactivation in a mouse model: Erk1/2 and Akt-mTOR activation, cell hyperproliferation, and polycystic kidneys. *JNCI* **100**: 140–154.

Bals R. 2000. Epithelial antimicrobial peptides in host defense against infection. *Respir Res* **1**: 5.

Barrila J, Crabbé A, Yang J, Franco K, Nydam SD, Forsyth RJ, Davis RR, Gangaraju S, Ott CM, Coyne CB, Bissell MJ, Nickerson CA. 2018. Modeling host-pathogen interactions in the context of the microenvironment: three-dimensional cell culture comes of age. *Infect Immun* **86**: e00282-18.

Bauer, FJ, 1997. Herstellung von PorB-Mutanten und Untersuchungen zur möglichen Rolle von PorB als Virulenzfaktor von *Neisseria gonorrhoeae*. Dissertation, Eberhard Karls Tübingen University.

Bennett JS, Jolley KA, Earle SG, Corton C, Bentley SD, Parkhill J, Maiden MCJ. 2012. A genomic approach to bacterial taxonomy: an examination and proposed reclassification of species within the genus *Neisseria*. *Microbiology* **158**:1570–1580.

Bhatia SN, Ingber DE. 2014. Microfluidic Organs-On-Chips. *Nat Biotechnol* **32**: 760-772.

Binnicker MJ, Williams RD, Apicella MA. 2003. Infection of human urethral epithelium with *Neisseria gonorrhoeae* elicits an upregulation of host anti-apoptotic factors and protects cells from staurosporine-induced apoptosis. *Cell Microbiol* **5**: 549–560.

Boettcher JP, Kirchner M, Churin Y, Kaushansky A, Pompaiah M, Thorn H, Brinkmann

V, MacBeath G, Meyer TF. 2010. Tyrosine-phosphorylated caveolin-1 blocks bacterial uptake by inducing Vav2-RhoA-mediated cytoskeletal rearrangements. *PLoS Biol* **8**: e1000457.

Boulton IC, Gray-Owen SD. 2002. *Neisserial* binding to CEACAM1 arrests the activation and proliferation of CD4+ T lymphocytes. *Nat Immunol* **3**:229–236.

Cannon JG, Buchanan TM, Sparling PF. 1983. Confirmation of association of protein I serotype of Neisseria gonorrhoeae with ability to cause disseminated infection. *Infect Immun* **40**: 816–819.

Cash TP, Gruber JJ, Hartman TR, Henske EP, Simon MC. 2011. Loss of the Birt–Hogg–Dubé tumor suppressor results in apoptotic resistance due to aberrant TGFβ-mediated transcription. *Oncogene* **30**: 2534–2546.

Chaitanya G, Alexander JS, Babu P. 2010. PARP-1 cleavage fragments: signatures of cell-death proteases in neurodegeneration. *Cell Commun Signal* **8**: 31.

Chen J, Futami K, Petillo D, Peng J, Wang P, Knol J, Li Y, Khoo S-K, Huang D, Qian C-N, Zhao P, Dykyma K, Zhang R, Cao B, Yang XJ, Furge K, Williams BO, Teh BT. 2008. Deficiency of FLCN in mouse kidney led to development of polycystic kidneys and renal neoplasia. *PLoS ONE* **3**: e3581.

Chen T, Belland RJ, Wilson J, Swanson J. 1995. Adherence of pilus- Opa+ gonococci to epithelial cells in vitro involves heparan sulfate. *J Exp Med* **182**: 511–517.

Cheng X-T, Xie Y-X, Zhou B, Huang N, Farfel-Becker T, Sheng Z-H. 2018. Revisiting LAMP1 as a marker for degradative autophagy-lysosomal organelles in the nervous system. *Autophagy* **14**: 1472–1474.

Collins JC, Paietta E, Green R, Morell AG, Stockert RJ. 1988. Biotin-dependent expression of the asialoglycoprotein receptor in HepG2. *J Biol Chem* **263**: 11280-11283.

Craig L, Forest KT, Maier B. 2019. Type IV pili: dynamics, biophysics and functional consequences. *Nat Rev Microbiol* **17**: 429–440.

Danaher RJ, Levin JC, Arking D, Burch CL, Sandlin R, Stein DC. 1995. Genetic basis of *Neisseria gonorrhoeae* lipooligosaccharide antigenic variation. *J bacteriol* **177**: 7275–7279.

Dehio M, Gómez-Duarte OG, Dehio C, Meyer TF. 1998. Vitronectin-dependent invasion of epithelial cells by *Neisseria gonorrhoeae* involves α_v integrin receptors. *FEBS Letters* **424**: 84–88.

Derk R, Davidson DC, Manke A, Stueckle TA, Rojanasakul Y, Wang L. 2015. Potential Devaux CA, Mezouar S, Mege J-L. 2019. The E-Cadherin cleavage associated to pathogenic bacteria infections can favor bacterial invasion and transmigration, dysregulation of the immune response and cancer induction in humans. *Front Microbiol* **10**: 2598.

de Tomasi JB, Opata MM, Mowa CN. 2019. Immunity in the cervix: interphase between

immune and cervical epithelial cells. *J Immunol* **219**: 1-13.

Diallo K, MacLennan J, Harrison OB, Msefula C, Sow SO, Daugla DM, Johnson E, Trotter C, MacLennan CA, Parkhill J, Borrow R, Greenwood BM, Maiden MCJ. 2019. Genomic characterization of novel *Neisseria* species. *Sci Rep* **9**: 13742

Duensing TD, van Putten JP. 1997. Vitronectin mediates internalization of *Neisseria gonorrhoeae* by Chinese hamster ovary cells. *Infect immun* **65**: 964–970.

Edwards JL, Apicella MA. 2002. The role of lipooligosaccharide in *Neisseria gonorrhoeae* pathogenesis of cervical epithelia: lipid A serves as a C3 acceptor molecule. *Cell Microbiol* **4**: 585–598.

Dunlop E, Seifan S, Claessens T, Behrends C, Kamps MAF, Rozycka E, Kemp AJ, Nookala RK, Blenis J, Coull BJ, Murray JT, van Steensel MM, Wilkinson S, Tee AR. 2014. FLCN, a novel autophagy component, interacts with GABARAP and is regulated by ULK1 phosphorylation. *Autophagy* **10**: 1749-1760.

Ebert, J 2016. *Neisserial* factors important for low phosphate- dependent invasion and for survival in neutrophils. Dissertation, Würzburg University.

Edwards JL, Brown EJ, Ault KA, Apicella MA. 2001. The role of complement receptor 3 (CR3) in *Neisseria gonorrhoeae* infection of human cervical epithelia. *Cell Microbiol* **3**: 611–622.

Edwards JL, Brown EJ, Uk-Nham S, Cannon JG, Blake MS, Apicella MA. 2002. A co-operative interaction between *Neisseria gonorrhoeae* and complement receptor 3 mediates infection of primary cervical epithelial cells. *Cell Microbiol* **4**: 571–584.

Edwards JL, Jennings MP, Seib KL. 2018. Neisseria gonorrhoeae vaccine development: hope on the horizon? *Curr Opin Infect Dis* **31**: 246-250.

Edwards VL, Wang L-C, Dawson V, Stein DC, Song W. 2013. *Neisseria gonorrhoeae* breaches the apical junction of polarized epithelial cells for transmigration by activating EGFR: Gonococci breach the apical junction of epithelia. *Cell Microbiol* **15**: 1042–1057.

El-Houjeiri L, Possik E, Vijayaraghavan T, Paquette M, Martina JA, Kazan JM, Ma EH, Jones R, Blanchette P, Puertollano R, Pause A. 2019. The transcription factors TFEB and TFE3 link the FLCN-AMPK signalling axis to Innate Immune response and pathogen resistance. *Cell Rep* **26**: 3613-3628.e6.

Evans CM, Pratt CB, Matheson M, Vaughan TE, Findlow J, Borrow R, Gorringe AR, Read RC. 2011. Nasopharyngeal colonization *by Neisseria lactamica* and induction of protective immunity against *Neisseria meningitidis*. *Clin Infec Dis* **52**: 70–77.

Fatehullah A, Tan SH, Barker N. 2016. Organoids as an *in vitro* model of human development and disease. *Nat Cell Biol* **18**: 246–254.

Faulstich, M, 2012. From local to disseminated infection: Mechanism of the porin-dependent gonococcal invasion. Dissertation, Würzburg University.

References

Faulstich M, Böttcher J-P, Meyer TF, Fraunholz M, Rudel T. 2013. Pilus phase variation switches Gonococcal adherence to invasion by Caveolin-1-dependent host cell signalling. *PLoS Pathog* **9**: e1003373.

Fichorova RN, Desai PJ, Gibson FC, Genco CA. 2001. Distinct proinflammatory host responses to *Neisseria gonorrhoeae* infection in immortalized human cervical and vaginal epithelial cells. *Infect Immun* **69**: 5840–5848.

Fisette PL, Ram S, Andersen JM, Guo W, Ingalls RR. 2003. The Lip lipoprotein from *Neisseria gonorrhoeae* stimulates cytokine release and NF-κB activation in epithelial cells in a Toll-like receptor 2-dependent manner. *J Biol Chem* **278**: 46252–46260.

Freissler E, Meyer auf der Heyde A, David G, Meyer TF, Dehio C. 2000. Syndecan-1 and syndecan-4 can mediate the invasion of Opa$_{HSPG}$-expressing *Neisseria gonorrhoeae* into epithelial cells. *Cell Microbiol* **2**: 69–82.

Giardina PC, Williams R, Lubaroff D, Apicella MA. 1998. *Neisseria gonorrhoeae* Induces focal polymerization of actin in primary human urethral epithelium. *Infect Immunity* **66**: 3416–3419.

Gold R, Goldschneider I, Lepow ML, Draper TF, Randolph M. 1978. Carriage of *Neisseria meningitidis* and *Neisseria lactamica* in infants and children. *J Infect Dis* **137**:112–121.

Gómez-Duarte OG, Dehio M, Guzmán CA, Chhatwal GS, Dehio C, Meyer TF. 1997. Binding of vitronectin to Opa-expressing *Neisseria gonorrhoeae* mediates invasion of HeLa cells. *Infect immun* **65**: 3857–3866.

Goncharova EA, Goncharov DA, James ML, Atochina-Vasserman EN, Stepanova V, Hong S-B, Li H, Gonzales L, Baba M, Linehan WM, Gow AJ, Margulies S, Guttentag S, Schmidt LS, Krymskaya VP. 2014. Folliculin controls lung alveolar enlargement and epithelial cell survival through E-Cadherin, LKB1, and AMPK. *Cell Rep* **7**: 412–423.

Gorringe AR, Taylor S, Brookes C, Matheson M, Finney M, Kerr M, Hudson M, Findlow J, Borrow R, Andrews N, Kafatos G, Evans CM, Read RC. 2009. Phase I safety and immunogenicity study of a candidate meningococcal disease vaccine based on *Neisseria lactamica* outer membrane vesicles. *Clin Vaccine Immun* **16**: 1113–1120.

Grassmé H, Gulbins E, Brenner B, Ferlinz K, Sandhoff K, Harzer K, Lang F, Meyer TF. 1997. Acidic sphingomyelinase mediates entry of *N. gonorrhoeae* into nonphagocytic cells. *Cell* **91**: 605–615.

Gulati S, Beurskens FJ, de Kreuk B-J, Roza M, Zheng B, DeOliveira RB, Shaughnessy J, Nowak NA, Taylor RP, Botto M, He X, Ingalls RR, Woodruff TM, Song W-C, Schuurman J, Rice PA, Ram S. 2019. Complement alone drives efficacy of a chimeric antigonococcal monoclonal antibody. *PLoS Biol* **17**: e3000323.

References

Gulati S, McQuillen DP, Sharon J, Rice PA. 1996. Experimental immunization with a monoclonal anti-idiotope antibody that mimics the *Neisseria gonorrhoeae* lipooligosaccharide epitope 2C7. *J Infect Dis* **174**: 1238–1248.

Guo P, Weinstein AM, Weinbaum S. 2000. A hydrodynamic mechanosensory hypothesis for brush border microvilli. *Am J Physiol-Renal* **279**: F698–F712.

Häcker G. 2018. Apoptosis in infection. *Microbes Infect* **20**: 552-559.

Hafes ES, Kenyans P. 1982. Atlas of human reproduction: by scanning electron microscopy. Springer.

Harrison WO, Hooper RR, Wiesner PJ, Campbell AF, Karneval WW, Reynolds GH, Jones OG, Holmes KK. 1979. A trial of minocycline given after exposure to prevent gonorrhea. *N Engl J Med* **300**: 1074-1078.

Harvey HA, Jennings MP, Campbell CA, Williams R, Apicella MA. 2008. Receptor-mediated endocytosis of *Neisseria gonorrhoeae* into primary human urethral epithelial cells: the role of the asialoglycoprotein receptor: Endocytosis of gonococci into urethral epithelial cells. *Mol Microbiology* **42**: 659–672.

Harvey HA, Ketterer MR, Preston A, Lubaroff D, Williams R, Apicella MA. 1997. Ultrastructural analysis of primary human urethral epithelial cell cultures infected with *Neisseria gonorrhoeae*. *Infect immun* **65**: 2420–2427.

Hatzfeld M, Wolf A, Keil R. 2014. Plakophilins in desmosomal adhesion and signaling. *Cell Commun Adhes* **21**: 25–42.

Hedges SR, Mayo MS, Mestecky J, Hook EW, Russell MW. 1999. Limited local and systemic antibody responses to *Neisseria gonorrhoeae* during uncomplicated genital infections. *Infect Immun* **67**: 3937–3946.

Hennig B, Wang Y, Ramasamy S, McClain CJ. 1992. Zinc deficiency alters barrier function of cultured porcine endothelial cells. *Nutr J* **122**:1242–1247.

Heydarian M, Yang T, Schweinlin M, Steinke M, Walles H, Rudel T, Kozjak-Pavlovic V. 2019. Biomimetic human tissue model for long-term study of *Neisseria gonorrhoeae* infection. *Front Microbiol* **10**:1740.

Hill SA, Masters TL, Wachter J. 2016. Gonorrhea – an evolving disease of the new millennium. *MIC* **3**: 371–389.

Hong S-B, Oh H, Valera VA, Baba M, Schmidt LS, Linehan WM. 2010a. Inactivation of the FLCN tumor suppressor gene induces TFE3 transcriptional activity by increasing its nuclear localization. *PLoS ONE* **5**: e15793.

Hong S-B, Oh H, Valera VA, Stull J, Ngo D-T, Baba M, Merino MJ, Linehan WM, Schmidt LS. 2010b. Tumor suppressor FLCN inhibits tumorigenesis of a FLCN-null renal cancer cell line and regulates expression of key molecules in TGF-β signaling. *Mol Cancer* **9**: 160.

Howie HL, Glogauer M, So M. 2005. The *N. gonorrhoeae* type IV pilus stimulates

mechanosensitive pathways and cytoprotection through a pilT-dependent mechanism. *PLoS Biol* **3**: e100.

Janeway CA, Travers P, Walport M. 2001. Immunobiology: the immune system in health and disease. 5th edition. Garland Science.

Jeong E, Brady OA, Martina JA, Pirooznia M, Tunc I, Puertollano R. 2018. The transcription factors TFE3 and TFEB amplify p53 dependent transcriptional programs in response to DNA damage. *eLife* **7**: e40856.

Johnson MB, Criss AK. 2011. Resistance of *Neisseria gonorrhoeae* to Neutrophils. *Front Microbio* **2**: 1-12.

Jolley KA, Bliss CM, Bennett JS, Bratcher HB, Brehony C, Colles FM, Wimalarathna H, Harrison OB, Sheppard SK, Cody AJ, Maiden MCJ. 2012. Ribosomal multilocus sequence typing: universal characterization of bacteria from domain to strain. *Microbiology* **158**: 1005–1015.

Jones RT, Talley RS. 1977. Simplified complete medium for the growth of *Neisseria gonorrhoeae*. *J Clin Microbiol* **5**: 6.

Kallstrom H, Blackmer Gill D, Albiger B, Liszewski MK, Atkinson JP, Jonsson A-B. 2001. Attachment of *Neisseria gonorrhoeae* to the cellular pilus receptor CD46: identification of domains important for bacterial adherence. *Cell Microbiol* **3**: 133–143.

Kato T, Takahashi N, Kuramitsu HK. 1992. Sequence analysis and characterization of the *Porphyromonas gingivalis* prtC gene, which expresses a novel collagenase activity. *J Bacteriol* **174**: 3889–3895.

Kawai M, Uchiyama I, Kobayashi I. 2005. Genome comparison in silico in *Neisseria* suggests integration of filamentous bacteriophages by their own transposase. *DNA Res* **12**: 389–401.

Kepp O, Gottschalk K, Churin Y, Rajalingam K, Brinkmann V, Machuy N, Kroemer G, Rudel T. 2009. Bim and Bmf synergize to induce apoptosis in *Neisseria gonorrhoeae* infection. *PLoS Pathog* **5**: e1000348.

Kim WJ, Mai A, Weyand NJ, Rendón MA, Van Doorslaer K, So M. 2019. *Neisseria gonorrhoeae* evades autophagic killing by downregulating CD46-cyt1 and remodeling lysosomes. *PLoS Pathog* **15**: e1007495.

Kirchner M, Heuer D, Meyer TF. 2005. CD46-Independent binding of *Neisserial* type IV pili and the major pilus adhesin, pilC, to human epithelial cells. *Infect Immun* **73**:3072–3082.

Kowalczyk AP, Nanes BA. 2012. Adherens junction turnover: regulating adhesion through cadherin endocytosis, degradation, and recycling in: Harris T, editor. Adherens junctions: from molecular mechanisms to tissue development and disease, subcellular biochemistry. Dordrecht: Springer Netherlands. pp. 197–222.

References

Kraus SJ, Perkins GH, Geller RC. 1970. Lymphocyte transformation in repeated gonococcal urethritis. *Infect Immun* **2**: 655–658.

Kuhlewein C, Rechner C, Meyer TF, Rudel T. 2006. Low-phosphate-dependent invasion resembles a general way for *Neisseria gonorrhoeae* to enter host cells. *Infect Immun* **74**: 4266–4273.

Kupsch EM, Knepper B, Kuroki T, Heuer I, Meyer TF, 1993. Variable opacity (Opa) outer membrane proteins account for the cell tropisms displayed by *Neisseria gonorrhoeae* for human leukocytes and epithelial cells. *EMBO J* **12**: 641-650.

Łaniewski P, Gomez A, Hire G, So M, Herbst-Kralovetz MM. 2017. Human three-dimensional endometrial epithelial cell model to study host interactions with vaginal bacteria and *Neisseria gonorrhoeae*. *Infect Immun* **85**: e01049-16.

Laviolette LA, Mermoud J, Calvo IA, Olson N, Boukhali M, Steinlein OK, Roider E, Sattler EC, Huang D, Teh BT, Motamedi M, Haas W, Iliopoulos O. 2017. Negative regulation of EGFR signalling by the human folliculin tumour suppressor protein. *Nat Commun* **8**: 15866.

Lee SW, Bonnah RA, Higashi DL, Atkinson JP, Milgram SL, So M. 2002. CD46 is phosphorylated at tyrosine 354 upon infection of epithelial cells by *Neisseria gonorrhoeae*. *J Cell Biol* **156**: 951–957.

Lenz JD, Dillard JP. 2018. Pathogenesis of *Neisseria gonorrhoeae* and the host defense in ascending infections of human fallopian tube. *Front Immunol* **9**: 2710.

Lin L, Ayala P, Larson J, Mulks M, Fukuda M, Carlsson SR, Enns C, So M. 1997. The *Neisseria* type 2 IgA1 protease cleaves LAMP1 and promotes survival of bacteria within epithelial cells. *Mol Microbiol* **24**: 1083–1094.

Li R, Hatcher JD. 2020. Gonococcal arthritis. StatPearls.

Liu G, Tang CM, Exley RM. 2015. Non-pathogenic *Neisseria*: members of an abundant, multi-habitat, diverse genus. *Microbiology* **161**:1297–1312.

Los M, van de Craen M, Penning LC, Schenk H, Westendorp M, Baeuerle PA, Dröge W, Krammer PH, Fiers W, Schulze-Osthoff K. 1995. Requirement of an ICE/CED-3 protease for Fas/APO-1-mediated apoptosis. *Nature* **375**: 81-83.

Lu P, Wang S, Lu Y, Neculai D, Sun Q, van der Veen S. 2018. A subpopulation of intracellular *Neisseria gonorrhoeae* escapes autophagy-mediated killing inside epithelial cells. *J Infect Dis*. **219**: 133-144.

Meyer TF.1977. Ecology and infection mechanisms of pathogenie *Neisseria* species.

Maiden MCJ, Bygraves JA, Feil E, Morelli G, Russell JE, Urwin R, Zhang Q, Zhou J, Zurth K, Caugant DA, Feavers IM, Achtman M, Spratt BG. 1998. Multilocus sequence typing: A portable approach to the identification of clones within populations of pathogenic microorganisms. *PNAS* **95**: 3140–3145.

Maisey K, Nardocci G, Imarai M, Cardenas H, Rios M, Croxatto HB, Heckels JE,

References

Christodoulides M, Velasquez LA. 2003. Expression of proinflammatory cytokines and receptors by human fallopian tubes in organ culture following challenge with *Neisseria gonorrhoeae*. *Infect Immun* **71**: 527–532.

Marri PR, Paniscus M, Weyand NJ, Rendón MA, Calton CM, Hernández DR, Higashi DL, Sodergren E, Weinstock GM, Rounsley SD, So M. 2010. Genome sequencing reveals widespread virulence gene exchange among human *Neisseria* Species. *PLoS ONE* **5**: e11835.

Massari P, Ram S, Macleod H, Wetzler LM. 2003. The role of porins in neisserial pathogenesis and immunity. *Trends Microbiol* **11**: 87–93.

McCormack WilliamM, Johnson K, Stumacher RussellJ, Donner A, Rychwalski R. 1977. Clinical spectrum of gonococcal infection in women. *The Lancet* **309**:1182–1185.

McGee ZA, Stephens DS, Hoffman LH, Schlech WF, Horn RG. 1983. Mechanisms of mucosal invasion by pathogenic *Neisseria*. *Clin Infect Dis* **5**: S708–S714.

McSheffrey GG, Gray-Owen SD. 2015. *Neisseria gonorrhoeae*. Molecular Medical Microbiology (Second Edition).

Medvetz DA, Khabibullin D, Hariharan V, Ongusaha PP, Goncharova EA, Schlechter T, Darling TN, Hofmann I, Krymskaya VP, Liao JK, Huang H, Henske EP. 2012. Folliculin, the product of the Birt-Hogg-Dube tumor suppressor gene, interacts with the adherens junction protein p0071 to regulate cell-cell adhesion. *PLoS ONE* **7**: e47842.

Meiffren G, Joubert P-E, Grégoire IP, Codogno P, Rabourdin-Combe C, Faure M. 2010. Pathogen recognition by the cell surface receptor CD46 induces autophagy. *Autophagy* **6**: 299–300.

Miller KE. 2006. Diagnosis and treatment of *Neisseria gonorrhoeae* infections **73**:6.

Mizushima N. 2007. Autophagy: process and function. *Gene Dev* **21**: 2861–2873.

Morales P, Reyes P, Vargas M, Rios M, Imarai M, Cardenas H, Croxatto H, Orihuela P, Vargas R, Fuhrer J, Heckels JE, Christodoulides M, Velasquez L. 2006. Infection of human fallopian tube epithelial cells with *Neisseria gonorrhoeae* protects cells from tumor necrosis factor alpha-induced apoptosis. *Infect Immun* **74**: 3643–3650.

Muller A. 1999. Neisserial porin (PorB) causes rapid calcium influx in target cells and induces apoptosis by the activation of cysteine proteases. *EMBO J* **18**: 339–352.

Murakami Y, Matsumoto H, Roh M, Giani A, Kataoka K, Morizane Y, Kayama M, Thanos A, Nakatake S, Notomi S, Hisatomi T, Ikeda Y, Ishibashi T, Connor KM, Miller JW, Vavvas DG. 2014. Programmed necrosis, not apoptosis, is a key mediator of cell loss and DAMP-mediated inflammation in dsRNA-induced retinal degeneration. *Cell Death Differ* **21**: 270–277.

Newman L, Rowley J, Vander Hoorn S, Wijesooriya NS, Unemo M, Low N, Stevens G,

References

Gottlieb S, Kiarie J, Temmerman M. 2015. Global estimates of the prevalence and incidence of four curable sexually transmitted infections in 2012 based on systematic review and global reporting. *PLoS ONE* **10**: e0143304.

Nighot P, Ma T. 2016. Role of autophagy in the regulation of epithelial cell junctions. *Tissue Barriers* **4**: e1171284.

Nookala RK, Langemeyer L, Pacitto A, Ochoa-Montaño B, Donaldson JC, Blaszczyk BK, Chirgadze DY, Barr FA, Bazan JF, Blundell TL. 2012. Crystal structure of folliculin reveals a hidDENN function in genetically inherited renal cancer. *Open Biol* **2**: 120071.

Noren NK, Niessen CM, Gumbiner BM, Burridge K. 2001. Cadherin engagement regulates Rho family GTPases. *J Biol Chem* **276**: 33305–33308.

Nudel K, Massari P, Genco CA. 2015. *Neisseria gonorrhoeae* modulates cell death in human endocervical epithelial cells through export of exosome-associated cIAP2. *Infect Immun* **83**: 3410–3417

Ogou SI, Yoshida-Noro C, Takeichi M. 1983. Calcium-dependent cell-cell adhesion molecules common to hepatocytes and teratocarcinoma stem cells. *J Cell Biol* **97**: 944–948.

Ortega FE, Rengarajan M, Chavez N, Radhakrishnan P, Gloerich M, Bianchini J, Siemers K, Luckett WS, Lauer P, Nelson WJ, Theriot JA. 2017. Adhesion to the host cell surface is sufficient to mediate *Listeria monocytogenes* entry into epithelial cells. *MBoC* **28**: 2945–2957.

Pacitto A, Ascher DB, Wong LH, Blaszczyk BK, Nookala RK, Zhang N, Dokudovskaya S, Levine TP, Blundell TL. 2015. Lst4, the yeast Fnip1/2 orthologue, is a DENN-family protein. *Open Biol* **5**: 150174.

Pantelic M, Kim Y-J, Bolland S, Chen I, Shively J, Chen T. 2005. *Neisseria gonorrhoeae* kills carcinoembryonic antigen-related cellular adhesion molecule 1 (CD66a)-expressing human B Cells and inhibits antibody production. *Infect Immun* **73**: 4171–4179.

Porat N, Apicella MA, Blake MS. 1995. *Neisseria gonorrhoeae* utilizes and enhances the biosynthesis of the asialoglycoprotein receptor expressed on the surface of the hepatic HepG2 cell line. *Infect immun* **63**:1498–1506.

Possik E, Jalali Z, Nouët Y, Yan M, Gingras M-C, Schmeisser K, Panaite L, Dupuy F, Kharitidi D, Chotard L, Jones RG, Hall DH, Pause A. 2014. Folliculin regulates Ampk-dependent autophagy and metabolic stress survival. *PLoS Genet* **10**: e1004273.

Pudlas M, Koch S, Bolwien C, Thude S, Jenne N, Hirth T, Walles H, Schenke-Lavland K. 2011. Raman spectroscopy: a noninvasive analysis tool for the discrimination of human skin cells. *Tissue Eng Part C Methods* **17**: 1027-1040.

Quayle AJ. 2002. The innate and early immune response to pathogen challenge in the

female genital tract and the pivotal role of epithelial cells. *J Reprod Immunol* **57**: 61–79.

Quillin SJ, Seifert HS. 2018. *Neisseria gonorrhoeae* host adaptation and pathogenesis. *Nat Rev Microbiol* **16**: 226–240.

Rajić J, Inic-Kanada A, Stein E, Dinić S, Schuerer N, Uskoković A, Ghasemian E, Mihailović M, Vidaković M, Grdović N, Barisani-Asenbauer T. 2017. *Chlamydia trachomatis* infection is associated with E-Cadherin promoter methylation, downregulation of E-Cadherin expression, and increased expression of fibronectin and α-SMA—implications for epithelial-mesenchymal transition. *Front Cell Infect Microbiol* **7**: 253.

Ram S, Gulati S, Lewis LA, Chakraborti S, Zheng B, DeOliveira RB, Reed GW, Cox AD, Li J, Michael FS, Stupak J, Su X-H, Saha S, Landig CS, Varki A, Rice PA. 2018. A novel sialylation site on *Neisseria gonorrhoeae* lipooligosaccharide links heptose II lactose expression with pathogenicity. *Infect Immun* **86**: 16.

Ram S, McQuillen DP, Gulati S, Elkins C, Pangburn MK, Rice PA. 1998. Binding of complement factor H to loop 5 of porin protein 1A: a molecular mechanism of serum resistance of nonsialylated *Neisseria gonorrhoeae*. *J Exp Med* **4**: 671-680

Ram S, Sharma AK, Simpson SD, Gulati S, McQuillen DP, Pangburn MK, Rice PA. 1998. A aovel sialic acid binding site on factor H mediates serum resistance of sialylated *Neisseria gonorrhoeae*. *J Exp Med* **187**: 743–752.

Rechner C, Kühlewein C, Müller A, Schild H, Rudel T. 2007. Host glycoprotein Gp96 and scavenger receptor SREC interact with PorB of disseminating *Neisseria gonorrhoeae* in an epithelial invasion pathway. *Cell Host Microbe* **2**: 393–403.

Ritter JL, Genco CA. 2018. *Neisseria gonorrhoeae* – induced inflammatory pyroptosis in human macrophages is dependent on intracellular gonococci and lipooligosaccharide. *J Cell Death* **11**: 1-12.

Rotman E, Seifert HS. 2014. The genetics of *Neisseria* species. *Annu Rev Genet* **48**: 405–431.

Rotman E, Webber DM, Seifert HS. 2016. Analyzing *Neisseria gonorrhoeae* pilin antigenic variation using 454 sequencing technology. *J Bacteriol* **198**: 2470–2482.

Rubinstein MR, Wang X, Liu W, Hao Y, Cai G, Han YW. 2013. Fusobacterium. nucleatum promotes colorectal carcinogenesis by modulating E-cadherin/β-catenin signaling via its FadA adhesin. *Cell Host Microbe* **14**: 195–206

Sadarangani M, Pollard AJ, Gray-Owen SD. 2011. Opa proteins and CEACAMs: pathways of immune engagement for pathogenic *Neisseria*. *FEMS Microbiol Rev* **35**: 498–514.

Sakai K, Yamauchi T, Nakasu F, Ohe T. 1996. Biodegradation of cellulose acetate by *Neisseria sicca*. *Biosci, Biotech, Bioch* **60**: 1617–1622.

References

Saunders NJ, Snyder LAS. 2006. The majority of genes in the pathogenic *Neisseria* species are present in non-pathogenic *Neisseria lactamica*, including those designated as 'virulence genes'. *BMC Genomics* **7**: 128.

Schork S, Schlüter A, Blom J, Schneiker-Bekel S, Pühler A, Goesmann A, Frosch M, Schoen C. 2012. Genome sequence of a *Neisseria meningitidis* capsule null locus strain from the clonal complex of sequence type 198. *J Bacteriol* **194**: 5144–5145.

Schweinlin M, Wilhelm S, Schwedhelm I, Hausmann J, Rietschel R, Jurowich C, Walles H, Metzger M. 2016. Development of an advanced primary human in vitro model of the small intestine. *Tissue Eng Part C Methods* **22**: 873-883.

Sebbagh M, Santoni M-J, Hall B, Borg J-P, Schwartz MA. 2009. Regulation of LKB1/STRAD localization and function by E-cadherin. *Curr Biol* **19**: 37–42.

Seike S, Takehara M, Takagishi T, Miyamoto K, Kobayashi K, Nagahama M. 2018. Delta-toxin from *Clostridium perfringens* perturbs intestinal epithelial barrier function in Caco-2 cell monolayers. *BBA - Biomembranes* **1860**: 428–433.

Shah B 2016. Comprehensive approach to infections in dermatology. *Indian Dermatol Online J* **7**: 230.

Shapiro L, Fannont AM, Kwong PD, Thompson A. 1995. Structural basis of cell-cell adhesion by cadherins *Nature* **374**: 11.

Singh R, Letai A, Sarosiek K. 2019. Regulation of apoptosis in health and disease: the balancing act of BCL-2 family proteins. *Nat Rev Mol Cell Biol* **20**:175–193.

Song W, Condron S, Mocca BT, Veit SJ, Hill D, Abbas A, Jerse AE. 2008. Local and humoral immune responses against primary and repeat *Neisseria gonorrhoeae* genital tract infections of 17β-estradiol-treated mice. *Vaccine* **26**: 5741–5751.

Sparling PF, Yobs AR. 1967. Colonial morphology of *Neisseria gonorrhoeae* isolated from males and females. *J Bacteriol* **93**: 513.

Sprenger J, 2010. Faktoren von *Neisseria gonorrhoeae* für die disseminierende Infektion von Epithelzellen. Dissertation, Würzburg University.

Starling GP, Yip YY, Sanger A, Morton PE, Eden ER, Dodding MP. 2016. Folliculin directs the formation of a Rab34– RILP complex to control the nutrient-dependent dynamic distribution of lysosomes. *EMBO Rep* **17**: 823–841.

Stein DC, LeVan A, Hardy B, Wang L-C, Zimmerman L, Song W. 2015. Expression of opacity proteins interferes with the transmigration of *Neisseria gonorrhoeae* across polarized epithelial cells. *PLoS ONE* **10**: e0134342.

Stern A, Brown M, Nickel P, Meyer TF. 1986. Opacity genes in *Neisseria gonorrhoeae*: control of phase and antigenic variation. *Cell* **47**: 61–71.

Stohl EA, Seifert HS. 2001. The recX gene potentiates homologous recombination in *Neisseria gonorrhoeae*. *Mol Microbiol* **40**: 1301–1310.

Swanson J, Robbins K, Barrera O, Corwin D, Boslego J, Ciak J, Blake M, Koomey JM.

1987. Gonococcal pilin variants in experimental gonorrhea. *J Exp Med* **165**: 1344–1357.

Tanida I, Ueno T, Kominami E. 2008. LC3 and Autophagy. *Methods Mol Biol* **445**: 77-78.

Tegtmeyer N, Wessler S, Necchi V, Rohde M, Harrer A, Rau TT, Asche CI, Boehm M, Loessner H, Figueiredo C, Naumann M, Palmisano R, Solcia E, Ricci V, Backert S. 2017. *Helicobacter pylori* employs a unique basolateral type IV secretion mechanism for CagA delivery. *Cell Host Microbe* **22**: 552-560.

Thurston TLM, Ryzhakov G, Bloor S, von Muhlinen N, Randow F. 2009. The TBK1 adaptor and autophagy receptor NDP52 restricts the proliferation of ubiquitin-coated bacteria. *Nat Immunol* **10**: 1215–1221.

Thurston TLM, Wandel MP, von Muhlinen N, Foeglein Á, Randow F. 2012. Galectin 8 targets damaged vesicles for autophagy to defend cells against bacterial invasion. *Nature* **482**: 414–418.

Tobiason DM, Seifert HS. 2010. Genomic content of *Neisseria* species. *J Bacteriol* **192**: 2160–2168.

Tobiason DM, Seifert HS. 2006. The obligate human pathogen, *Neisseria gonorrhoeae*, is polyploid. *PLoS Biol* **4**: e185.

Tronel H, Chaudemanche H, Pechier N, Doutrelant L, Hoen B. 2001. Endocarditis due to *Neisseria mucosa* after tongue piercing. *Clin Microbiol Infect* **7**: 275–276.

Tsun Z-Y, Bar-Peled L, Chantranupong L, Zoncu R, Wang T, Kim C, Spooner E, Sabatini DM. 2013. The Folliculin tumor suppressor Is a GAP for the RagC/D GTPases that signal amino acid levels to mTORC1. *Mol Cell* **52**: 495–505.

Tzeng Y-L, Thomas J, Stephens DS. 2015. Regulation of capsule in *Neisseria meningitidis*. *Crit Rev Microbiol* **42**: 1–14.

van Putten JP, Paul SM. 1995. Binding of syndecan-like cell surface proteoglycan receptors is required for *Neisseria gonorrhoeae* entry into human mucosal cells. *EMBO J* **14**: 2144–2154.

van Putten JPM, Duensing TD, Carlson J. 1998. Gonococcal invasion of epithelial cells driven by P.IA, a bacterial ion channel with GTP binding properties. *J Exp Med* **188**: 941–952.

Vandenabeele P, Galluzzi L, Vanden Berghe T, Kroemer G. 2010. Molecular mechanisms of necroptosis: an ordered cellular explosion. *Nat Rev Mol Cell Biol* **11**: 700–714.

Vaughan TE, Skipp PJ, O'Connor CD, Hudson MJ, Vipond R, Elmore MJ, Gorringe AR. 2006. Proteomic analysis of *Neisseria lactamica* and *N eisseria* meningitidis outer membrane vesicle vaccine antigens. *Vaccine* **24**: 5277–5293.

Vieira OV, Botelho RJ, Grinstein S. 2002. Phagosome maturation: aging gracefully. *Bioche J* **366**: 689–704.

References

Virji M, Evans D, Hadfield A, Grunert F, Teixeira AM, Watt SM. 1999. Critical determinants of host receptor targeting by *Neisseria meningitidis* and *Neisseria gonorrhoeae*: identification of Opa adhesiotopes on the N-domain of CD66 molecules. *Mol Microbiol* **34**: 538–551.

Wang L-C, Yu Q, Edwards V, Lin B, Qiu J, Turner JR, Stein DC, Song W. 2017. *Neisseria gonorrhoeae* infects the human endocervix by activating non-muscle myosin II-mediated epithelial exfoliation. *PLoS Pathog* **13**: e1006269.

Weyand NJ, Calton CM, Higashi DL, Kanack KJ, So M. 2010. Presenilin/γ-secretase cleaves CD46 in response to *Neisseria* infection. *J Immunol* **184**: 694–701.

Winkler AC. 2015. Identification of human host cell factors involved in *Staphylococcus aureus* 6850 infection. PhD thesis. Wuerzburg University.

Wong S-P, Harbottle RP. 2013. Genetic modification of dividing cells using episomally maintained S/MAR DNA vectors. *Mol Ther Nucleic Acids* **2**: ve115.

Wyle FA, Rowlett C, Blumenthal T. 1977. Cell-mediated immune response in gonococcal infections. *Sex Transm Infec* **53**: 353–359.

Xian YB. 2014. Identification of essential genes and novel virulence factors of *Neisseria gonorrhoeae* by transposon mutagenesis. PhD thesis. Wuerzburg University.

Yu Q, Chow EMC, McCaw SE, Hu N, Byrd D, Amet T, Hu S, Ostrowski MA, Gray-Owen SD. 2013. Association of *Neisseria gonorrhoeae* OpaCEA with dendritic cells suppresses their ability to elicit an HIV-1-specific T cell memory response. *PLoS ONE* **8**: e56705.

Yu Q, Wang L-C, Di Benigno S, Gray-Owen SD, Stein DC, Song W. 2019. *Neisseria gonorrhoeae* infects the heterogeneous epithelia of the human cervix using distinct mechanisms. *PLoS Pathog* **15**: e1008136.

Zemirli N, Boukhalfa A, Dupont N, Botti J, Codogno P, Morel E. 2019. The primary cilium protein folliculin is part of the autophagy signaling pathway to regulate epithelial cell size in response to fluid flow. *CST* **3**:100–109.

Zeth K, Kozjak-Pavlovic V, Faulstich M, Fraunholz M, Hurwitz R, Kepp O, Rudel T. 2013. Structure and function of the PorB porin from disseminating *Neisseria gonorrhoeae*. *Biochem J* **449**: 631–642.

Zhang Y-Z, Ran L-Y, Li C-Y, Chen X-L. 2015. Diversity, structures, and collagen-degrading mechanisms of bacterial collagenolytic proteases. *Appl Environ Microbiol* **81**: 6098–6107

Zhu W, Ventevogel MS, Knilans KJ, Anderson JE, Oldach LM, McKinnon KP, Hobbs MM, Sempowski GD, Duncan JA. 2012. *Neisseria gonorrhoeae* suppresses dendritic cell-induced, antigen-dependent CD4 T cell proliferation. *PLoS ONE* **7**: e41260.

7. Appendix

7.1 Abbreviations

2D	two-dimensional
3D	three-dimensional
ACEs	alveolar epithelial cells
AMPK	AMP-activated kinase
ASGP-R	asialoglycoprotein receptors
ASM	acid sphingomyelinase
ATP	adenosine triphosphate
BafA1	Bafilomycin A1
BHD	Birt-Hogg-Dubé syndrome
ble	bleomycin
C4BP	c4b-binding protein
CD46	membrane cofactor protein
CDC	Centers for Disease Control and Prevention
CEACAM	carcinoembryonic antigen family
CFU	colony forming units
cGAS	cyclic-GMP-AMP synthase
cgMLST	core genome multi locus sequence typing
CHO	Chinese hamster ovary
cIAP2	cellular inhibitor of apoptosis-2
CR	coding repeat
CR3	a CD11b/CD18 integrin heterodimer
DAMPs	damage-associated molecular patterns
DCs	dendritic cells
DMEM	Dulbecco's Modified Eagle Medium
DMSO	dimethyl sulfoxide
DNA	deoxyribonucleic acid
dRS3	duplicated repeat sequence 3

DUS	DNA uptake sequences
EC	extracellular cadherin
ECM	extracellular matrix
EGFR	epidermal growth factor receptor
FBS	fetal bovine serum
FLCN	Folliculin
GAS	Group A *Streptococcus*
GC	*Neisseria gonorrhoeae*
GOPC	Golgi-associated PDZ and coiled-coil motif-containing
HEK	human embryonic kidney
HGT	horizontal gene transfer
hiFBS	Heat inactivated FBS
HSPG	heparan sulfate proteoglycan
IE	inside end
InlA	internalin A
IPTG	Isopropyl β- d-1-thiogalactopyranoside
kan	kanamycin
LAMP1	lysosomal associated membrane protein 1
LC3	microtubule-associated protein 1A/1B-light chain 3
LC3-I	a cytosolic form of LC3
LC3-II	LC3-phosphatidylethanolamine conjugate
LOS	lipopolysaccharide
mAb	monoclonal antibody
MDMs	monocyte-derived macrophages
MDCK	Madin-Darby canine kidney
MLST	multi locus sequence typing
mTOR	mammalian target of rapamycin
NDP52	nuclear dot protein 52 kDa
N. meningitidis	*Neisseria meningitidis*
N. gonorrhoeae	*Neisseria gonorrhoeae*
Opa	opacity-associated proteins
OMV	outer membrane vesicle

Appendix

PC-PLC	phosphatidylcholine-specific phospholipase C
P. gingivalis	*Porphyromonas gingivalis*
phospho-S6	phosphorylated ribosomal protein S6
pilS	silent copies of pili
RIP3	receptor-interacting protein 3
rMLST	ribosomal multi locus sequence typing
OE	outside end
RNA	ribonucleic acid
RNAi	RNA interference
ROS	reactive oxygen species
RPMI	Roswell Park Memorial Institute
RWV	rotating wall vessel
shRNA	short hairpin RNA
SCV	*salmonella*-containing vacuole
SQSTM1/p62	the autophagic marker sequestosome 1/p62
str	streptomycin
STS	Staurosporine
TEF3	transcription enhancer factor 3
TEFB	transcription elongation factor B
TGF-β	transforming growth factor β
TLR	toll-like receptors
TZ	transformation zone
VPS34	class III PI 3-kinase
ZO-1	Zonula occludens-1

7.2 Publications and presentations

Publications

Tao Yang, Vera Kozjak-Pavlovic, Thomas Rudel. Folliculin controls the intracellular survival and trans-epithelial passage of *Neisseria gonorrhoeae*. (Frontiers in cellular and infection microbiology, to be published), 2020.

Motaharehsadat Heydarian, **Tao Yang**, Matthias Schweinlin, Maria Steinke, Heike Walles, Thomas Rudel, Vera Kozjak-Pavlovic. Biomimetic Human Tissue Model for Long-Term Study of *Neisseria gonorrhoeae* Infection. Frontiers in Microbiolgy. 2019.

Presentations

05-07 Apr 2019, 3D Tissue Infection Symposium organized by the GRK2157 "3D Tissue Models for Studying Microbial Infections by Human Pathogens", Wuerzburg, Germany.
Poster prensentation: “Characterization the role of FLCN in *Neisseria gonorrhoeae* adherence, invasion and survival”

10-13 Jul 2019, EMBO | EMBL Symposium: New Approaches and Concepts in Microbiology, Heidelberg, Germany
Poster prensentation: “Functional insights into the role of FLCN in *Neisseria gonorrhoeae* infection”

09-10 Oct 2019, Eureka, 14th international GSLS student symposium, Wuerzburg, Germany.
Poster prensentation: “Functional insights into the role of FLCN in *Neisseria gonorrhoeae* infection”

7.3 Acknowledgements

I would like to thank the supervisors of this project, Prof. Dr. Thomas Rudel and PD Dr. Vera Kozjak-Pavlovic, for the supervision, mentorship and inspirational discussion.

I would like to thank the members of my thesis committee, Prof. Dr. Alexandra Schubert-Unkmeir and Dr. Brandon Kim for their helpful input during our meetings.

I would like to thank Elke, Kerstin, Susanne and Heike for the amazing technical supports and cares. Thanks to Dr. Martin Fraunholz and Prof. Dr. Dagmar Beier for the safety training. Thanks to Prof. Dr. Jürgen Kreft for picking me up and showing me how to register in the city hall at the first days of my arrival in Wuerzburg.

Thanks to all my colleagues in the department for the lovely atmosphere and supports. Thanks to Mota, Tobias, Franziska, Marie, Michaela, Pargev, David Ke, David Kr, Pargev, Sophie, Nadine, Adriana, Qi and Yongxia for discussion and help during all phases of my thesis and also for the nice time after work. Thanks to my friends in the GRK program, Sara G, Manli and Marie.

Thanks to Dr Richard Harbottle for the UOK cell lines. Thanks to Dr Matthias Schweinlin for the training of 3D models setup and analysis.

Thanks to Graduate School of Life Sciences (GSLS), especially Gabriele and Katrin for being helpful and supportive.

Thanks for the DGF (GRK2157) and DAAD-STIBET fellowship for funding.

Last, I would like to express my thankfulness to my parents, my brother and my husband Xiaoguang Xue for their support, encouragement, motivation and love.

Appendix

7.4 Curriculum Vitae

Appendix

7.5 Affidavit

Affidavit

I hereby confirm that my thesis entitled Functional insights into the role of a bacterial virulence factor and a host factor in Neisseria gonorrhoeae infection is the result of my own work. I did not receive any help or support from commercial consultants. All sources and / or materials applied are listed and specified in the thesis.

Furthermore, I confirm that this thesis has not yet been submitted as part of another examination process neither in identical nor in similar form.

Place, Date Signature

Eidesstattliche Erklärung

Hiermit erkläre ich an Eides statt, die Dissertation Funktionelle Einblicke in die Rolle eines bakteriellen Virulenzfaktors und eines Wirtsfaktors bei der Infektion mit Neisseria gonorrhoeae eigenständig, d.h. insbesondere selbständig und ohne Hilfe eines kommerziellen Promotionsberaters, angefertigt und keine anderen als die von mir angegebenen Quellen und Hilfsmittel verwendet zu haben.

Ich erkläre außerdem, dass die Dissertation weder in gleicher noch in ähnlicher Form bereits in einem anderen Prüfungsverfahren vorgelegen hat.

Ort, Datum Unterschrift